Journal of the
OPTICAL SOCIETY *of* AMERICA

VOLUME 31 FEBRUARY, 1941 NUMBER 2

Editorial Comment

EMERITUS MEMBERS

A RECENTLY created new class of membership in the Optical Society will be of interest particularly to those who have reached the retiring age and desire to be relieved of the financial requirements of ordinary membership, yet wish to maintain their connection with the Society.

At the Rochester meeting in October, the Board of Directors voted to amend the by-laws by creating a new "Emeritus Membership." The amendment which was adopted provides that any person who has retired from active work, has reached the age of sixty-five years, and has been a member of the Society for at least twenty years, is eligible for emeritus membership. Any eligible member may, at his own request, be transferred to emeritus membership by the Secretary.

Although an emeritus member need pay no dues, he will retain all privileges of his former membership status except a subscription to the Journal. For example, he will continue to receive announcements of meetings and other routine communications from the Secretary. In short, he may continue to regard himself in all respects as an active member of the Society.

Though it is sometimes said that the United States is destined eventually to become a nation of old people, this is far from the case at present. Certainly the Optical Society is not a society of old people. Even apart from the affiliation of the applied spectroscopists, announced in the November issue, young and enthusiastic workers in optical science are joining the Society at a rate which appears never to have been exceeded. The Optical Society is young, active, and growing. Such growth brings profit, and one such profit is the newly achieved opportunity to honor those entering the grade of emeritus membership.

The Board of Directors, by placing acceptance of emeritus membership on a voluntary basis, very wisely recognizes the fact that there are many who never grow old. Thus members who have retired from their professional duties, and can meet the other requirements of emeritus membership, may instead elect to continue in full touch with the affairs of the Society and the field of science which it serves, through the pages of the Journal.

BOSTON UNIVERSITY
COLLEGE OF LIBERAL ARTS
LIBRARY

Photographic Analysis of Some Unexplored Visual Phenomena*

WILLIAM A. GARDNER
Columbia University, New York, New York
(Received November 13, 1940)

IF an observer fixate a stationary point along the line of transit of a rapidly moving automobile, he will apparently be able to see the spokes of the rotating wheels. This visibility is in the form of a sudden flash of sharply defined criss-crossing lines which seem themselves to be standing still. The effect is best seen in direct sunlight, while watching an automobile with bright yellow wooden spokes. Given adequate illumination and suitable spokes, the effect is independent of the velocity of the car.

The direction and velocity of spoke motion preclude the possibility of the eye being able to follow such motion, even for a brief period of time. Furthermore (as will be shown below) one of the essential conditions for seeing this effect is that the eye be held motionless during the observation.

It therefore seemed logical to ask (as did Gaehr,[1] Packard,[2] and Ferree,[3] who first noted this effect) whether such apparent spoke visibility might not be due to stroboscopic vision. Other observers suggested that more intricate, subjective factors were involved. Guilford,[4] for example, described the effect as involving an "alternate stopping and starting of Time. We literally 'freeze' a portion of Time into a stationary mass."

In an attempt to see whether the effect had an objective counterpart that could be photographed, a camera was set up, and a suitable automobile driven past this camera at velocities varying from 10 to 40 miles per hour. Photographs were then taken in each case, at camera speeds varying from 1/20 to 1/500 second.

In those cases where the camera speed was slow, relative to the velocity of the car (e.g. 1/40 second shutter speed and 40 miles per hour car velocity) there appeared—instead of the expected total blur—a well defined pattern of criss-crossing lines. This photographic pattern exactly duplicated the visual effect, and showed thereby that the latter was due to objective factors (Fig. 1).

For laboratory duplication and study of this effect, an inclined plane was set up at an angle of 10° with the horizontal. A cylinder was prepared, with a diameter of 10″, and a black base marked out with eight white adhesive tape "spokes," each 1″ wide, extending from center to periphery. The cylinder was then allowed to roll down the incline. Observations were made (with direct current electric light) at varying distances and angles, during the descent of the cylinder. If the eye rigidly fixated a stationary point along the line of descent, a sharp pattern of interlacing lines became visible, just as the cylinder passed the point of ocular fixation (Fig. 2). This pattern was immediately lost, however, if the eye made any attempt to follow the track of the descending cylinder. Introspection further showed that apparent spoke visibility was invariably limited to the lower hemisphere. The effect was equally well seen with very dim light (one candle at 18 feet) with white spokes on a black background, and again with brilliant illumination (four 500-watt lamps at 4 feet) with bright yellow spokes on a bright blue ground. This result indicated that the effect was not a property of rod or cone vision as such. The effect was likewise seen through polarizing lenses, irrespective of the axis of polarization. Monocular vision did not modify the effect, nor did changes in the orientation of the head. A mirror placed in the plane of the incline yielded the expected inverted image of the lower hemisphere spoke pattern and the upper hemisphere blur.

Further observations showed that fixation of gaze and limitation of the effect to the lower hemisphere were likewise the essential factors in the apparent visibility of automobile wheel spokes.

With the inclined plane and the experimental cylinder and slow shutter speeds (e.g. 1/10 second), a camera reproduced the effect precisely as seen by the eye, again demonstrating that

* Publication assisted by the Ernest Kempton Adams Fund for Physical Research of Columbia University.
[1] P. F. Gaehr, Science **68**, 567 (1928).
[2] R. M. Packard, Science **68**, 567–568 (1928).
[3] C. E. Ferree, Science **68**, 645–646 (1928).
[4] J. P. Guilford, J. Exp. Psych. **12**, 259–266 (1929).

FIG. 1. The cycloid effect. Automobile with twelve yellow wooden spokes driven past camera at forty miles per hour. Shutter speed, 1/40 sec. An example of the pattern of spoke visibility as seen by both eye and camera.

apparent spoke visibility was due to external causes; and further, that stroboscopy was not involved (Fig. 2).

Photographs of eye movements were then made while the eye was observing the apparent spoke visibility. (These photographs were made with the kind assistance of Professor Harold Fisher, at the New York Eye and Ear Infirmary.) These photographs confirmed the verdict of introspection: that fixation of gaze corresponded with subjective appreciation of the effect. Conversely, with a record showing eye movements while attempting to follow the descent of the cylinder, the observer reported only a total blur. The eye in fixed position resembled the camera with rigid orientation.

FIG. 2. The cycloid effect. The cylinder base is marked out with eight white adhesive tape "spokes," and the cylinder allowed to roll down the inclined plane. This photograph (taken with an exposure of 1/10 sec. at the time when the cylinder had reached the end of the incline) reproduces the effect approximately as the eye sees it. Diagram shows pattern of cylinder base. Motion is from right to left, with counterclockwise rotation.

It seemed at first very curious that the fixed eye and the slow shutter speed camera did not record a total blur during the transit of the experimental wheel. The conditions of the experiment were therefore simplified, in order to find out the mechanism at work. The 8 adhesive tape spokes were removed from the cylinder base, and 4 white spots were pasted on, along one radial line. One spot was put at the periphery, one at the center, and the two others in intermediate positions. The cylinder was then allowed to roll down the incline. A camera was set up on a tripod, and the shutter left wide open during the entire descent of the cylinder. The film recorded the trajectory of each white spot during the descent. Examination of the photographs (Fig. 3) showed that the peripheral spot described a series of cycloids, created by the combined rotation and translation of the cylinder. The central spot described a straight line, parallel with the edge of the inclined plane. The intermediate spots described prolate cycloids. Above the straight line described by the central spot there was no overlap of the various individual trajectories, but at and below this line the trajectories formed a series of specific overlaps. The loci of maximum overlap of trajectories constituted loci of maximum brightness. Their spacing formed the mechanical and optical basis for an apparent "spoke."

A single radius was now marked out along the radial line of spots on the cylinder base. The cylinder was again allowed to roll down the

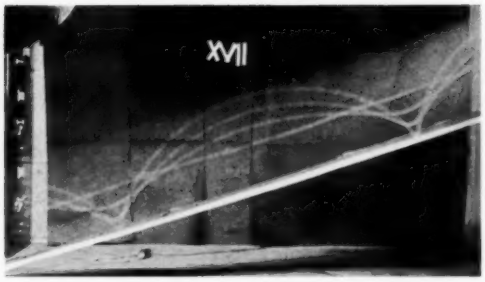

FIG. 3. Creation of the cycloid effect through mechanical and optical overlap. Cylinder base black, with four white spots along one radial line. Background black. Cylinder allowed to roll down inclined plane. The camera with shutter open records the trajectory of the spots: (1) The central spot describes a straight line. (2) The peripheral spot describes a cycloid. (3) The intermediate spots describe prolate cycloids. It is noted that in the upper hemisphere there is no overlap of the trajectories, whereas in the lower hemisphere these trajectories form a repetitive pattern of overlap. The loci of maximum overlap become loci of maximum brightness, and their summation forms the basis of the apparent "spokes."

inclined plane, and photographed by the fixed camera, with shutter wide open during the entire time of transit. In the photograph, there appeared a series of apparent curved and paired "spokes." Each "spoke," however, was in reality only the locus of maximum overlap (and therefore of maximum brightness) of successive positions of the radius. This locus of maximum overlap was the smooth curve connecting the loci of maximum overlap of the single-spot trajectories in the previous experiment. This smooth curve was a half-cycloid to which the actual radius was at each successive point tangent.

Additional radii were then laid out on the cylinder base, and the cylinder descent photographed at each step with the camera shutter wide open. With each added radius there appeared on the film additional cycloids. Each cycloid represented in turn the pattern created by the overlapping of each new radius, in its combined motion of rotation and translation.

When the full complement of 8 spokes was marked out on the cylinder base, and photographed in the same manner, the resultant pattern was seen to be a series of interlacing cycloids. This pattern constituted a sort of frieze, the length of which depended only on the length of the exposure time. The portion of this total pattern which was seen by the eye at any given fixation point constituted a small fragment of the whole, and could be approximated by exposure times of the order of 1/10 to 1/20 second (Fig. 2).

It was noted that it was not the radii themselves which became visible (or were photographed), but the cycloids to which their combined rotation and translation gave rise.

The same mechanism holds for the apparent visibility of automobile wheel spokes, though here only the central, criss-crossing portion of the total cycloid pattern is visible, since the spokes fail of being complete radii owing to tire and hub cap. Radial markings on tires become visible in the same manner, since they are, in effect, the distal portions of radii.

This cycloid pattern was now mechanically reproduced, by using a stencil replica of the 8 radius cylinder base (Fig. 4). The stencil was placed flat on a sheet of paper, and made to rotate along a base line through successive 1/2″ arcs. A tracing of the stencil was made in each position. The summation of these tracings gave rise to a series of cycloids, exactly duplicating the photographic and subjective effects. Again the cycloids were seen to be the loci of maximum overlap.

The experimental conditions were now changed. A stationary wheel was set up, with a pattern of 8 white radii on a black background, identical with the cylinder base. The camera—with shutter wide open—was held in the hand, and swept across the field horizontally, from left to right. The photographic result was a total blur, save for

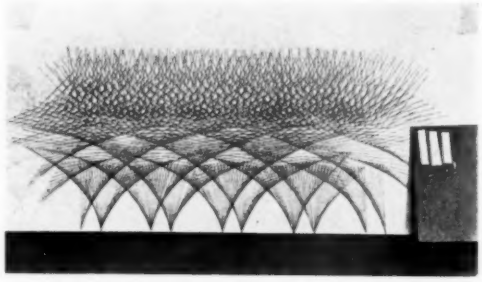

FIG. 4. The cycloid effect produced mechanically by stencil replica of cylinder base. Stencil rotated through successive ½″ arcs, along base line, and tracings made at each position. Photograph shows summation of tracings made during one-half of a complete revolution of the stencil. The loci of maximum overlap are cycloids, which give rise to the illusion of "spokes."

the apparent elongation of the horizontal diameter. When, however, the same wheel was made to rotate on a stationary axis and the camera swept horizontally across the field in the same manner, a spread-out of interlacing cycloids was registered on the film (Fig. 5). The eye saw this same effect when made to move rapidly past the fixed rotating wheel. The resultant pattern (retinal or photographic) was identical with that produced when lateral and rotatory motion were combined in the cylinder itself as it rolled down the incline.

This internal cycloid spread-out is probably an example of the "unexplained visual phenomenon" described by Gradle,[5] who reported moving airplane propellor visibility, "as the visual axis was turned laterally."

It is therefore seen that the apparent visibility of the spokes of rapidly moving automobile wheels, and the occasional apparent visibility of the spokes of stationary wheels both depend upon the mechanical creation of a cycloidal pattern—progressively brought into existence by the component rotation and translation. (These component motions may be united in the wheel itself, or divided between the wheel and the eye.) This pattern glides across the sentient retina, or the sensitive film. The well-known persistence of the retinal image allows the eye to summate a variable fraction of the total pattern. Similarly, the photographic film registers a variable fraction of the total pattern, depending upon the exposure time.

FIG. 5. The cycloid effect, as seen when the eye is made to move rapidly past a stationary rotating wheel. (The resultant pattern is identical with that produced when lateral and rotatory motion are combined in the cylinder itself as it rotated down the inclined plane.) When the camera, with wide open shutter, is held in the hand, and swept past the stationary rotating wheel, the same pattern of interlacing cycloids is created. This effect is probably an example of the "unexplained visual phenomenon" described by Gradle, who reported moving airplane propellor visibility "as the visual axis was turned laterally."

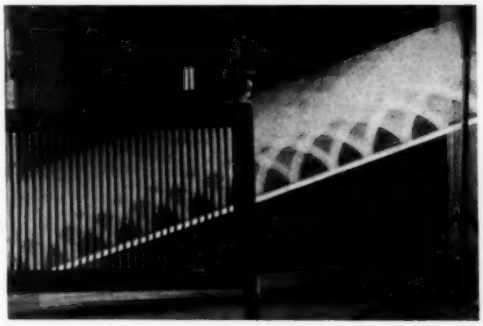

FIG. 6. The cycloid effect is not modified by the interposition of a stationary grid. Cylinder base marked out with eight white adhesive tape radii, and cylinder allowed to roll down inclined plane. The apparent curvature of rapidly rolling carriage wheels, when viewed through a series of slits, as described by "J.M." in 1821, is therefore seen as an example of and anticipation of the cycloid effect.

Far from demanding a stroboscopic theory of vision, this "cycloid effect" favors a theory of continuity of vision, analogous to the continuous sensitivity of the camera film with wide open shutter.

In 1821, a certain "J. M.,"[6] writing in the *Quarterly Journal of Science, Literature, and the Arts*, described an effect whereby the spokes of a rapidly rolling carriage wheel, when viewed through a series of stationary slits, appeared curved. In an attempt to duplicate his observations, a stationary grid, composed of alternate 1/4″ vertical slits and bars, was set up in front of the familiar inclined plane. The cylinder with 8 white spokes marked out on its black base was now once more allowed to roll down the incline, and viewed through the grid. Both introspection and photography recorded the familiar cycloidal pattern (Fig. 6). The only difference was that the presence of the slits made it easier for the eye to see the cycloids as such, by making it harder to follow the track of the descending cylinder. It

[5] H. S. Gradle, Science **68**, 404 (1928).

[6] "J. M.," Quarterly J. Sci. Lit. Arts **10**, 282 (1821.)

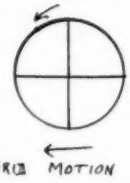

FIG. 7. The Roget effect, as seen by the eye, and as recorded by the camera with wide-open shutter. Stationary rotating wheel with four white adhesive tape radii on black background. Rotation counterclockwise. Grid composed of alternate vertical $\frac{1}{4}''$ slits and bars moved slowly from right to left between wheel and camera.

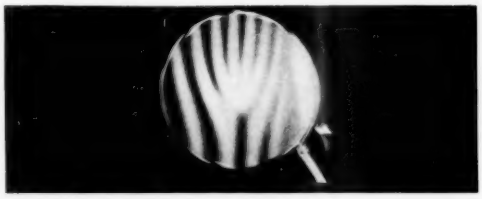

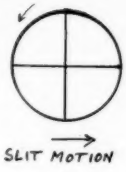

FIG. 8. The Roget effect, as seen by the eye, and as recorded by the camera with wide-open shutter. Stationary rotating wheel with four white adhesive tape radii on black background. Rotation counterclockwise. Grid composed of single $\frac{1}{4}''$ vertical slit, moved slowly from left to right between wheel and camera. The pattern itself is static. The eye sees the same effect as here recorded.

seems likely, therefore, that "J. M." was really seeing and describing the "cycloid effect."

In 1824, Roget, speaking before the Royal Society of London,[7] referred to the observations of "J. M.," and himself described an independent illusion. He set up a stationary rotating wheel, and viewed it through a transversely moving system of slits. He described the resultant effect as "irresistible and exceedingly striking." He made careful drawings of the effect as seen by the eye, and explained the illusion as due to the retinal summation of the separate images created "from the combination of a rotary, with a progressive motion of the spokes, in relation to the apertures through which they are viewed."

In order to duplicate the conditions as described by Roget, the stationary rotating wheel with 8 white radii on a black background was again set up. The grid composed of alternate 1/4" vertical slits and bars (as used in the previous experiment) was placed between the stationary wheel and the observing eye. This grid was now moved slowly across the line of vision between wheel and eye. The resultant distortion of the spokes was a startling fixed pattern of variably curved vertical lines, in the form of a candelabra (Figs. 7 and 8). This candelabra appeared upright or inverted according to the relative directions of wheel rotation and slit translation. (An identical effect was observed, with both the rotating wheel and the grid in fixed positions, by turning the eyes rapidly from side to side.)

A fixed camera with wide open shutter produced in each case an image identical with that seen by the eye (Figs. 7 and 8). This fact demonstrated the truth of the hypothesis advanced by Roget, that the effect depended on purely mechanical considerations.

Variations in the number of radii on the face of the stationary rotating wheel did not alter the fundamental candelabra pattern as recorded by both eye and camera. Similarly, reducing the width or the number of slits caused no essential change. Variations in the velocity of the lateral motion of the grid did result in changes in the subjective pattern (as described by Roget). The photographs here reproduced were made with relatively slow grid motions. (No pictures have yet been made using faster grid velocities.)

This curious visual phenomenon—apparently neglected for the past 120 years—provides a second example of the manner in which both eye and camera build up, by a summation of mechanically produced images, a retinal—or optical—pattern, which has wholly objective causality, but wholly subjective—or photographic—existence. Both the "cycloid effect" and the "Roget effect" are made possible not by stroboscopy, but by the temporary persistence of the retinal image. The photographs are, in each case, proof of the external, as opposed to the internal origin of the illusion.

[7] P. M. Roget, Phil. Trans. Roy. Soc. London, **1**, 131 (1825) (cited by Helmholtz, *Physiological Optics* (Optical Society of America) Vol. II, p. 223).

The Interferometer Method of Determining the Amplitudes of Small Mechanical Vibrations

W. JAY KENNEDY
Trinity University, Waxahachie, Texas*
(Received December 2, 1940)

INTERFEROMETER methods of determining the amplitudes of small mechanical vibrations have been reported by Thomas and Warren,[1] H. Osterberg,[2] S. H. Cortez[3] and others. H. Osterberg has given a mathematical theory of the method when monochromatic fringes are used and one of the returning mirrors vibrates normally with sinusoidal motion, and also when either the first or second overtone is imposed on the fundamental. This article presents an experimental verification of Osterberg's analysis when only the fundamental is present.

If both returning surfaces are at rest and uniformly illuminated, and the two interfering beams are of equal intensity, the brightness of the fringes is given by the expression

$$I_0 = K\left[1+\cos\frac{2\pi x}{h}\right],$$

where K is a constant, h is the fringe width, and x is the distance measured perpendicularly across the fringes.

With one of the mirrors set into vibration sinusoidally, a simple harmonic motion is imparted to the fringe system. Osterberg has shown theoretically that under this condition the brightness of the fringes is

$$I = K\left[1+J_0\left(\frac{4\pi\xi}{\lambda}\right)\cos\frac{2\pi x}{h}\right],$$

where ξ is the amplitude of vibration of the mirror, λ is the wave-length of the light and $J_0(4\pi\xi/\lambda)$ is the Bessel function of zero order.

An examination of this expression shows that for $J_0(4\pi\xi/\lambda)=0$, $I=K$, and the fringes disappear; i.e., the field appears uniformly illuminated. That is, for all values of ξ which give $J_0(4\pi\xi/\lambda)=0$, the fringes disappear. This disappearance is quite sharp.

In Table I is given the number of the zero with the corresponding roots of $J_0(x)$ in columns 1 and 2, while column 3 contains the appropriate value of ξ/λ. The corresponding values of ξ are given in column 4, when $\lambda=5.461\times10^{-5}$ cm, the Hg green line, is used to produce interference fringes. The ratios of ξ producing the nth disappearance of fringes to that producing the first disappearance is included in column 5.

Essentially the work described below consists of showing that the first disappearance of fringes occurs at $\xi/\lambda=0.191$ and that the ratios ξ_n/ξ_1 have the values predicted by theory.

THE APPARATUS

The cone and voice coil of a loudspeaker were replaced by a driving coil with an aluminum head on the front of the coil form. The oscillating mirror is secured to this head. A brass wire was also attached to the rear of the driving head and extended through a hole drilled in the center pole. The other end of this brass wire carries a small "search" coil so that one side is suspended between the poles of a permanent magnet, Fig. 1. The small e.m.f. generated in this search coil when the moving system is set into oscillation is amplified and read on the meter I, Fig. 2.

EXPERIMENTAL PROCEDURE

With S in position 1 the output of the oscillator is applied to the driving coil and adjusted until

TABLE I. *Comparison between theoretical and experimental values of* ξ_n/ξ_1

No. of Zero*	Root of $J_0(x)$*	ξ/λ	ξ cm $\times10^5$	ξ_n/ξ_1	c.v.	$\frac{(c.v.)_n}{(c.v.)_1}$
1	2.40	0.191	1.04		2.29	
2	5.52	0.439	2.40	2.30	5.27	2.30
3	8.65	0.688	3.76	3.60	8.25	3.60
4	11.80	0.938	5.12	4.91	11.23	4.90
5	14.90	1.190	6.48	6.21	14.21	6.21

* Gray, Matthews and MacRoberts, *Bessel Functions* (1922), Appendix.

* The work reported here was completed at the University of Texas.

[1] H. A. Thomas and G. W. Warren, Phil. Mag. **5**, 1125 (1928).

[2] H. Osterberg, J. Opt. Soc. Am. **22**, 19 (1932).

[3] S. H. Cortez, J. Opt. Soc. Am. **24**, 127 (1934).

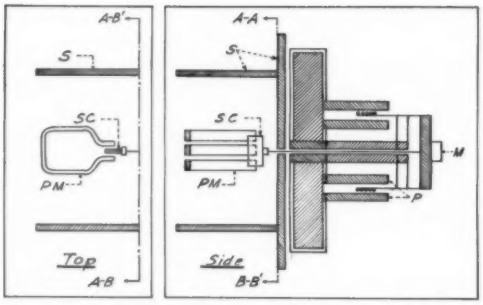

FIG. 1. Apparatus for oscillating one mirror of a parallel plate interferometer. *M*—vibrating mirror, *P*—poles, *S*—search coil shields, *SC*—search coil, *PM*—permanent magnet.

the fringes disappear. The reading of I is noted. Then S is placed in position 2 so that the oscillator output is applied across A, and adjusted until I indicates the previous value. If the input impedance of the pre-amplifier is sufficiently high, the voltage across the three-ohm resistor may be considered as having the same value as that generated in the search coil. The voltage across A is read on the vacuum tube voltmeter and recorded as the "comparison voltage," or c.v. It is unnecessary to actually compute the e.m.f. generated in the search coil since it is proportional to the comparison voltage.

In subsequent work in making certain acoustical measurements it was desired to determine the amplitude of vibration from the value of the amplified output of the search coil as indicated by I. In order to do this the instrument was calibrated at several frequencies between 50 and 1000 cycles. The calibration constant for each frequency consists of the ratio of ξ to the corresponding comparison voltage.

RESULTS

At 50 cycles the instrument was calibrated by the interferometer method and also by observing the double amplitude of vibration with a microscope under stroboscopic illumination. The results are shown below.

Interferometer method (first disappearance)
$\xi_1 = 1.043 \times 10^{-5}$ cm
Comparison voltage, c.v. = 0.280 volt
Constant at 50 cycles = 3.73×10^{-5} cm/volt

Microscope method
Double amplitude = 0.01025 cm
$\xi = 0.00513$ cm
Comparison volts, c.v. = 138 volts
Constant at 50 cycles = 3.72×10^{-5} cm/volt
Difference = 0.01×10^{-5} cm/volt
= 0.26 percent.

This shows definitely that the first disappearance of the fringes occurs at that amplitude predicted by theory, namely, $\xi_1 = 0.191\lambda$.

It should be noted at this point that for a given amplitude of the oscillating mirror the e.m.f. generated in the search coil, and, therefore, the comparison voltage, is proportional to the frequency. This relationship is shown graphically in Fig. 3, and is seen to be linear within the limits of experimental accuracy. The moving system must be symmetrical about its longi-

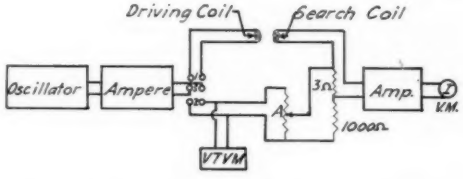

FIG. 2. Circuit diagram showing the arrangement for obtaining the comparison voltage.

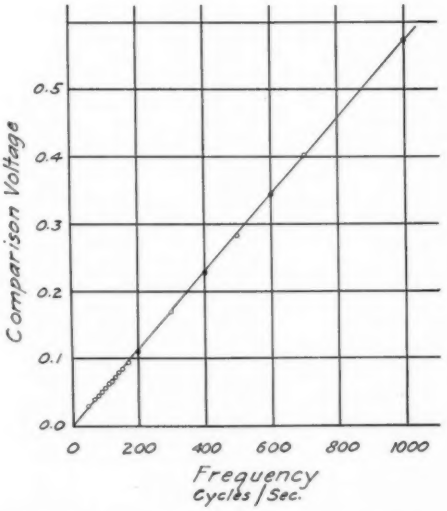

FIG. 3. The linear relationship between comparison voltage and frequency with a given amplitude of vibration, 0.191λ.

tudinal axis in order to obtain this degree of linearity.

It remains to be shown that the higher orders of fringe disappearance occur at those values of amplitude predicted by theory. Since the higher order disappearances are difficult to observe accurately at the lower frequencies where the microscope can be used most effectively, because of larger amplitudes, the comparison voltages were obtained for the first five disappearances at 400 cycles. These values are listed in order in column 6, Table I, while the ratios $(\text{c.v.})_n/(\text{c.v.})_1$ are listed in column 7.

A comparison of column 7 with column 5 shows that

$$\frac{(\text{c.v.})_n}{(\text{c.v.})_1} = \frac{\xi_n}{\xi_1}$$

within the limits of experimental accuracy. As many as three orders of fringe disappearances were observed at several other frequencies with the same result.

Therefore it can be said that the theory of the interferometer method of measuring the amplitudes of small mechanical vibrations has been verified for amplitudes sufficient to produce fifth-order fringe disappearances, and it is perfectly reasonable to assume that it holds for larger amplitudes.

The writer wishes to thank Dr. C. P. Boner, under whose guidance this work was done, Dr. M. Y. Colby and Dr. J. M. Kuehne, who offered timely suggestions and Mr. Jim Parks, mechanic, all in the Department of Physics of the University of Texas.

The Effect of the Size of the Particle on the Intensity of Fluorescence of a Phosphor

M. S. OLDHAM AND WILLIAM KUNERTH
Iowa State College, Ames, Iowa
(Received November 19, 1940)

The authors have used various sized particles of phosphors and have found that within the range of sizes used, the smaller the size the greater is the intensity of fluorescence. The graph bears out this relation. The phenomenon of fluorescence seems to be a surface phenomenon.

THE use of fluorescent powders in artificial illumination has become of great commercial importance. Because one of the many factors affecting the illuminating efficiency is the particle size of the fluorescent powder, an investigation to determine the variation of the intensity of fluorescence as the size of the particles of powder is varied has been undertaken.

The phosphor used in this investigation was synthetic willemite or $ZnBeSiO_3$, which fluoresces with a yellow light. This was furnished by the Nela Park Laboratory. The spectral emission curves for this phosphor have been determined[1] to a maximum value at about 6000A with an intensity spread of about 4000A. The total emission reaches a maximum when the wave-length of the exciting radiation is approximately 2600A.

The diameter of the particles of powder was found to vary up to one-sixteenth of an inch. Subsequent separation into various size ranges showed that there was a fairly uniform distribution of particles among the different ranges. The particles when viewed under a microscope appeared to be quite irregular in shape, but there were relatively few particles extremely different from spherical or cubical shape. Furthermore, after the separating process, the particles seemed to be more nearly spherical than before, a condition probably caused by the grinding action of the screening process.

Figure 1 is a diagram of the apparatus which was used for obtaining photographs of the spectrum emitted from the phosphor. The source of exciting radiation was a quartz mercury vapor arc which emits radiation very rich in ultra-violet light. The visible light emitted by this arc was cut out by the use of a Gaertner constant deviation quartz monochromator with a Wadsworth prism reflector system with the exit slit so arranged as to allow only the resonance line of mercury at twenty-five hundred and thirty-seven angstroms to pass through. By using slits especially constructed to allow most advantageous arrangement in the apparatus, and with a width of about three millimeters, a very intense beam of the desired wave-length was obtained. To determine the greatest efficiency, the wave-length of the exciting radiation was adjusted while the fluorescence of the phosphor was being viewed visually.

The light emitted by the phosphor upon excitation was photographed through a Gaertner monochromator with the telescope replaced by a spectroscopic camera attachment which showed spectral distribution as well as relative intensity of the fluorescent light. This instrument was of the constant deviation type with a Pellin-Broca prism. Both of these instruments were mounted in a vertical position to allow the layer of fluorescent powder to lie horizontal. Thus the need of an adhesive which might have affected the results was eliminated.

The photographic plates were compared with two microphotometers, one of which, ordinarily used in line spectroscopy, had a very small field and the other a very large field. The former was

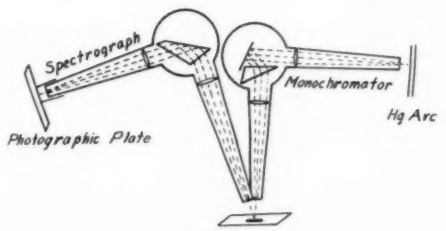

FIG. 1.

[1] R. N. Thayer and B. T. Barnes, "The basis for high efficiency in fluorescent lamps," J. Opt. Soc. Am. 29, 121–123 (1939).

used to compare the maximum intensities of the light emitted, the latter to compare the total intensity over a given region on the plate.

The photographic plates used were Wrattan and Wainright unbacked panchromatic dry plates made by the Eastman Kodak Company. The developer was Eastman formula D-19, a high contrast, rather slow developer which is used extensively in spectographic work.

The particles were separated into the various sizes (Table I) by a series of metal screens commonly used for the ordinary aggregate analysis of soils. The agitation was supplied by a Rototap shaking machine.

After the separation of the particles into size groups the particles were kept in a desiccator to prevent coalescing, except during the actual test. During the test, the particles were placed on a microscope slide to a thickness which allowed no ultraviolet light to completely penetrate the substance, a visual test being made by observing the glass from underneath the horizontally placed slides. If any visible light came through, or if the glass fluoresced, the thickness of the particle layer was increased.

TABLE I.

Size Ranges in Inches	Average Size	Mic. phot. gal. def.		Ratio = Opacity	Log $O=D$ $=\gamma$ log I*
		Clear Plate	Exposed		
0.0000–0.0018	0.0008†	22.5	5.2	4.32	0.62737
.0029– .0041	0.0035	"	5.55	4.06	0.60853
.0042– .0070	0.0055	"	5.8	3.88	0.58883
.0071– .0097	0.0083	"	6.1	3.69	0.56703
.0098– .0165	0.0131	"	6.6	3.41	0.53275
.0166– .0195	0.0180	"	7.2	3.14	0.49693
>0.0195	0.0270†	"	8.4	2.68	0.42813

* O =opacity, D =density, I =intensity, γ =gamma-factor of plate.
† Value taken from graph.

The mercury arc was operated for a sufficiently long time before the actual test to reach a temperature equilibrium with the surroundings, thus insuring a constant output of ultraviolet light. The metal housing of the arc was covered with black cloth in order to make the equilibrium temperature more independent of any variation in room temperature and to shut in the visible light. The room was kept as dark as possible during the tests so as to prevent any reflection of stray visible radiation from the white surface of the phosphor into the spectograph.

Attention was paid to obtaining equal exposure times for the different particle sizes. An independent test was run to determine the best exposure time and, for subsequent tests, the time of exposure was taken as one minute. A series of exposures of every particle size was made on each plate, along with a scale from which to plot the characteristic curve of the plate, in order to

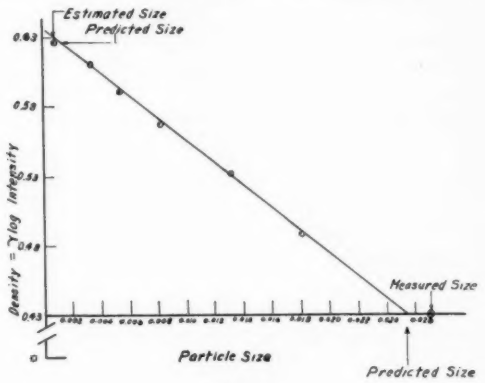

FIG. 2.

invalidate any variations in the plates and in the development times.

For all of the size ranges except the two extremes, the points on the graph (Fig. 2) define a straight line well within experimental error. The abscissa of the point on the curve which indicates the experimentally determined intensity for the two extreme size ranges should give the average size of those particles. In the case of the larger particles (those which are held back by the largest screen) this average size can be determined with the use of a traveling microscope. Many of these particles were measured for size with special care taken to obtain a random sample of particles. The particles which went through the smallest screen used were also tested in this manner. Their size could only be estimated with the use of the traveling microscope. The points which correspond to these measurements were found to lie very close to the points determined by the curve which was outlined by the other size ranges.

As a further check the larger particles were ground, screened and immediately tested. The

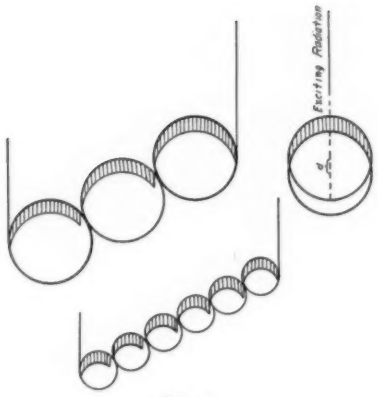

FIG. 3.

size variation of the intensity was compared with that of the original powder. Since no perceptible difference in results was obtained, it was concluded that the variation of the intensity with changing particle size is independent of the time which has elapsed between grinding and testing.

Various theories have been considered in an attempt to explain the results. Assuming that the intensity depends only on the surface exposed, the smaller particles should emit a more intense radiation than the larger ones because of the greater emitting surface per excited volume. For example, a particle with dimensions large compared to the depth of penetration of the exciting rays will emit light from only part of its surface, whereas a number of smaller particles with total volume equal to that of the larger particle will emit from a much larger surface (Fig. 3).

Because the particles are very irregular in shape, exact quantitative empirical relationships between particle size and intensity of fluorescence is difficult to obtain. If the assumption that the change in intensity with particle size is a surface phenomenon is valid, then the intensity should vary markedly as the particle size is changed.

The results of this investigation (Table I) indicate that there is a very real variation of intensity of fluorescence with changing particle size. Since the experimentally determined values fall on a straight line within experimental error, it is assumed that at least in the region of this experiment, a straight line best represents the data.

The consistency of the experimental evidence shows that if the foregoing procedure is followed for any given size of particle within the limits of size of the particles tested, the relative intensity of fluorescence may be obtained from the straight line graph.

The difficulty associated with an extension of this investigation to include other size ranges is very great, although it would be very helpful in obtaining the desired empirical relationship between intensity and particle size. However, the use of some other method of separation of the particle sizes, such as sedimentation, might possibly produce the needed data to extend the curve.

With the foregoing facts in mind the partial theory was advanced, that the variation of fluorescence depends on the surface exposed. This theory, coupled with the zone theory of solids as applied to luminescence[2] seems to allow and even predict the effect noticed, but as yet the correlation between the theory and the experiment, as in many other aspects of solid behavior, is largely of a qualitative nature.

[2] F. Seitz and R. P. Johnson, "Modern theory of solids," J. App. Phys. 8, 84–199, 246–260 (1937).

A Footcandle-Hour Integrator for Daylight

A. H. TAYLOR
Lighting Research Laboratory, General Electric Company, Nela Park, Cleveland, Ohio
(Received November 19, 1940)

IT is sometimes important to integrate exposures to daylight over a period of time, as, for example, in a recent research on the fading of colored textiles by daylight.[1] In that research we were interested in determining the exposures in footcandle-hours. Since no instrument for that purpose was available, the apparatus to be described was developed and used.

No photo-tube or other photoelectric device now available accurately reproduces the spectral sensitivity of the average eye, hence all are to some extent inaccurate for measuring the illumination from sources differing in spectral distribution. This is especially true with regard to daylight, since the blue, violet and near ultraviolet vary over a wide range with changes in atmospheric conditions.

In order to understand the principles upon which the integrator is based it is first necessary to consider the spectral energy distribution of daylight. Figure 1 shows data for several phases of daylight as measured in this laboratory.[2] These curves are plotted on a basis of *equal illumination* so that they are directly comparable at all wave-lengths. It will be seen that if practically monochromatic energy in a band centered at λ5600 is measured, its intensity will be directly proportional to the illumination within an error of only a few percent. The same is true with regard to tungsten filament lamps,[3] as will be seen from Fig. 2.

In 1935 Gibson[4] described a filter which transmits a very narrow spectral band centered at λ5600. Figure 3 shows a spectral transmission curve for one of these filters. It is composed of four separate filters cemented together, the individual filters being as follows: Corning No. 351, 4.55 mm; Corning didymium, 5.82 mm; Jena VG3, 1.99 mm; Jena BG18, 1.94 mm.

Since the filter serves to isolate the desired

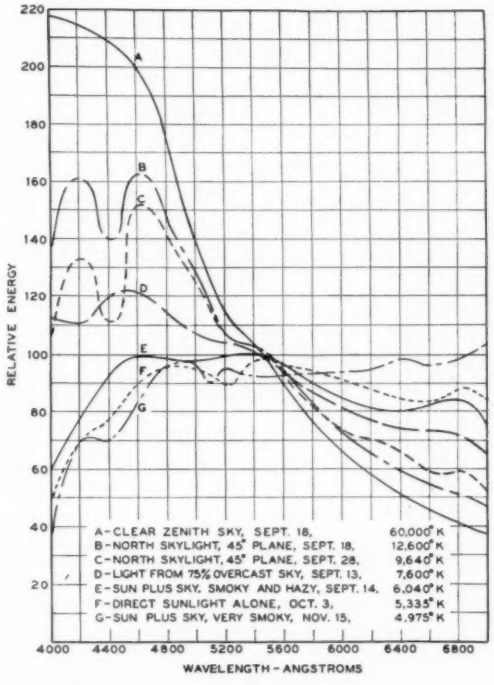
RELATIVE ENERGY
WAVELENGTH - ANGSTROMS
A-CLEAR ZENITH SKY, SEPT. 18, 60,000° K
B-NORTH SKYLIGHT, 45° PLANE, SEPT. 18, 12,600° K
C-NORTH SKYLIGHT, 45° PLANE, SEPT. 28, 9,640° K
D-LIGHT FROM 75% OVERCAST SKY, SEPT. 13, 7,600° K
E-SUN PLUS SKY, SMOKY AND HAZY, SEPT. 14, 6,040° K
F-DIRECT SUNLIGHT ALONE, OCT. 3, 5,335° K
G-SUN PLUS SKY, VERY SMOKY, NOV. 15, 4,975° K

FIG. 1. Spectral energy distribution of various phases of daylight, plotted on an *equal illumination* basis.

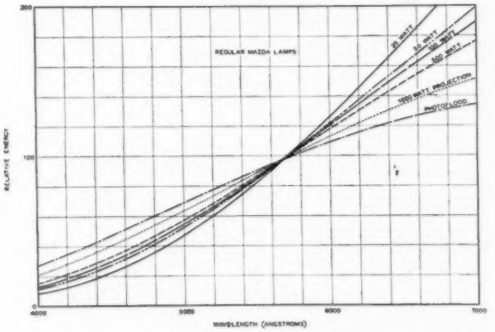

FIG. 2. Spectral energy distribution curves for various tungsten filament lamps, plotted on an *equal illumination* basis.

[1] M. Luckiesh and A. H. Taylor, "Factors affecting the fading of dyed textiles by radiant energy," Am. Dyestuff Rep., 543 (Oct. 14, 1940).

[2] A. H. Taylor, "The fluorescent Mazda daylight lamp," Light Mag. 8, No. 2 (1939).

[3] A. H. Taylor, "Spectral distribution of energy in common illuminants," Gen. Elec. Rev. 410 (Sept. 1934).

[4] K. S. Gibson, "A filter for obtaining light at 560mμ," J. Opt. Soc. Am. 25, 131 (1935).

spectral region, practically any type of photo-tube, or barrier-layer cell sensitive to this region can be used to measure the transmitted energy. In our work a General Electric vacuum type caesium photo-tube (PJ-14) was used.

The electronic integrator was of the same type as one which has been in use in our laboratory for six years to measure the ultraviolet in daylight.[5] The electrical circuit is shown in

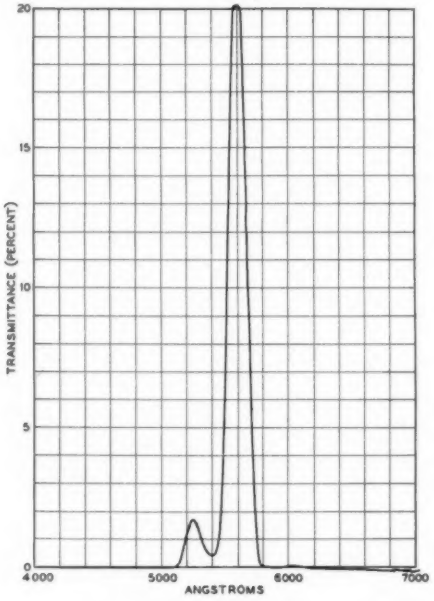

FIG. 3. Spectral transmission of Gibson type monochromatic filter.

[5] M. Luckiesh, A. H. Taylor and G. P. Kerr, "A four-year record of ultraviolet energy in daylight," J. Frank. Inst. **228**, 425 (1939).

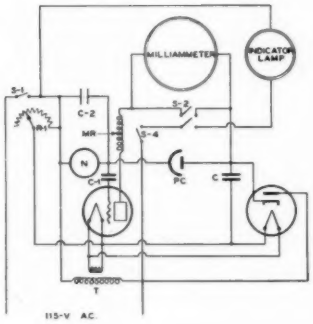

FIG. 4. Electrical circuit of electronic integrator.

Fig. 4. It utilizes a half-wave rectifier tube, Type 1-V, and 71A vacuum tube, a telephone message register *MR* being placed in the plate circuit. The current from the photo-tube *PC* charges condenser *C-2*. When its potential reaches a value of about 75 volts the small neon lamp *N* ($\frac{1}{4}$ watt) flashes and partially discharges *C-2*. This sudden flash momentarily changes the voltage of the grid of the 71A tube and causes a large drop in its plate current, with recovery very shortly thereafter, thus causing the message register *MR* to record the impulse. In such a circuit high insulation in the condenser *C-2* and neon lamp is essential for correct integration.

The filter and photo-tube were placed behind a sheet of opal glass, rough ground. For the most accurate integration of daylight it would be desirable to use an integrating sphere to receive the light. Our meter was calibrated by comparison with photometric measurements over a period of several hours.

A New Test for Convex Surfaces

EDWARD L. MCCARTHY
The Perkin-Elmer Corporation, New York, New York
(Received November 27, 1940)

THE speed and accuracy with which an optical surface may be produced in the hands of a genuinely skillful optician is principally limited by the suitability and precision of his test methods. Whenever the object or the image point of a reflecting surface is virtual, as in the case of a Cassegrain secondary mirror, testing is more of a problem than it is when both conjugates are real. Ideally, the test should permit a complete view of the surface at a convenient angular size; it should not involve large and expensive auxiliary pieces; it should not depend on slow measurement of zonal foci, but it should produce a simultaneous darkening over all parts of a perfect surface when a Foucault knife edge is introduced.

These conditions are reasonably well met by the system shown in Fig. 1. Light from an illuminated pinhole passes obliquely through two plane-parallel glass plates to a silvered spherical mirror. Reflected first from the sphere and then from the large plate, the light converges toward the virtual focus of the secondary mirror, which returns it through the plate to a real focus at the knife edge. These two foci of course represent the conjugates for which the secondary mirror is to be free of spherical aberration in actual use.

Since the large plate has a considerable thickness, it introduces serious aberration into the beams of light diverging and converging through it. It is the function of the two small plates to cancel the unsymmetrical aberrations such as lateral color and coma. To effect this compensation, all three plates are of the same thickness, and the small ones are set at the same angle to the axis as the large one, but in the sense which restores the displaced axis. The longitudinal aberrations, such as astigmatism and spherical aberration, are augmented by the small plates and must be removed in a different manner. If the pinhole is displaced from the center of curvature in a radial direction either toward or away from the spherical mirror, aberration is introduced of the proper sign to cancel the spherical aberration of the plates. Astigmatism is compensated by displacing the pinhole laterally with respect to an axis of the sphere, since the astigmatism in the field of a concave sphere is of the proper sign to cancel that of the plates.

Obviously the conditions will be different from one case to another, depending upon the character of the mirror to be tested, the thickness of the plates, and the axial obliquity through the plates. It is therefore desirable to calculate the correct arrangement for each case by ray tracing, and to place the pieces in accordance with this calculation. If the second conjugate distance is large compared to the aperture of

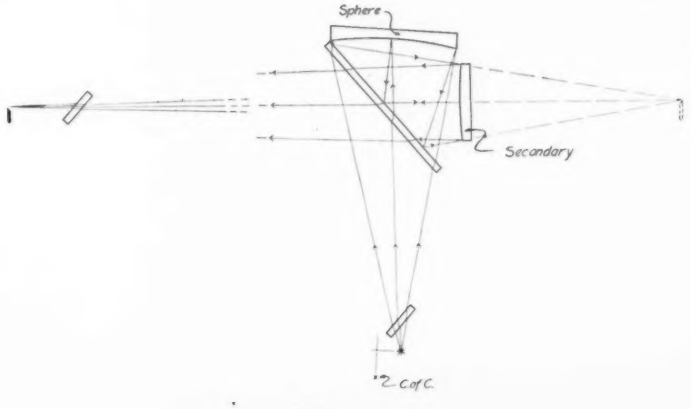

FIG. 1.

the test piece and the plate thickness, as it usually is in a Cassegrain, no calculation is necessary. Instead, the adjustments may be made by trial until the beam of convergent light reflected from the large plate is shown by the knife edge test to be homocentric. In such a case, of course, the secondary to be tested is temporarily removed in order not to interrupt the beam. This method of adjustment assumes that the final passage through the large plate will introduce no appreciable aberration, and it is justifiable in the case of a slender emergent beam. Whether it is good enough for a particular case may be tested by examining the effect of the final small plate. If its presence or absence makes no observable change in the character of the final image, other than a displacement, the indication is quite definite that the trial and error method of adjustment is suited to the particular case, inasmuch as the aberrations of a plane-parallel plate are constant, no matter where it happens to be along the axis.

An illustration is provided by two Cassegrain secondaries made for the McMath-Hulbert 24-inch telescope. Primary and secondary mirrors were made by Mr. Halley Mogey, who also introduced improvements over the original idea of the test. The primary is $f:4$ with a central hole 4.5 inches in diameter. The secondaries are 3.5 and 5.5 inches in diameter, and give magnifications of 12.5 and 6.5, respectively. The combination of large central hole, high magnification, and large unvignetted field made it impossible to see any error on the secondary mirrors when tested by the Ritchey method, even before any figuring at all had been done.

The test pieces, also made by Mr. Mogey, were a spherical mirror of 9 inches aperture and 24 inches radius of curvature, a plane-parallel plate of 12 inches diameter and 0.5 inch thickness, and two small plates 0.5 inch thick. The figure of the spherical mirror is required to be excellent; both sides of the large plate may depart from flatness by several waves, but should be parallel within a few minutes of arc; the small plates do not need a good figure. There are two unsilvered reflections, so that a fairly bright light source is necessary. Either a mercury or a ribbon-filament incandescent lamp has been quite satisfactory.

To make a Cassegrain secondary accurate to one-tenth of a wave-length does not require tenth-wave flatness in the large plate. If its figure is roughly spherical, of very long radius, the astigmatism introduced by oblique reflection and transmission may be compensated in the manner already described for the normal astigmatism arising from oblique passage through a plane-parallel plate. If the figure is generally flat with residual zonal errors, such errors are readily separated from those occurring on the secondary mirror, since the former appear elliptical and the latter circular.

In the present case, the first small plate was placed 1.5 inches from the pinhole and at an angle of 45 degrees to the direction chosen as the optical axis. Elimination of astigmatism required an angle of 8.76 degrees between the axial directions before and after reflection from the spherical mirror. A longitudinal separation of 2.0 inches between the center of curvature and the pinhole removed the slight spherical aberration. It was found that the last small plate was not required for either of these secondaries.

In testing larger Cassegrain mirrors, some economies could be introduced. For instance, in the case just described, the test equipment is large enough to show the complete secondary. An arrangement permitting an unsymmetrical view of about two-thirds of the surface would involve test pieces scarcely larger than the secondary itself.

The Distribution of Radiant Energy (Light) in a Group of Lattices*

STEPHAN T. SERGHIESCO
Columbia University, New York, New York
(Received October 18, 1940)

INTRODUCTION

IN previous communications,[1] I have made a special study of the mechanics of the corpuscle of light starting from the theorem of equivalence of mass and energy of Einstein and continuing its extension in order to examine the possibility of a real physical interpretation of certain phenomena in the theory of light. I demonstrated there the law of refraction from a corpuscular point of view (independently of the quanta idea) and also the coefficient of Fresnel, which was derived without introducing the relativistic kinematics. The corpuscular interpretation of this coefficient was one of the first achievements of the relativity theory.[2]

Since the next step in a theory of light would be the phenomenon of "fringes," which has been completely identified with the existence of wave phenomenon, I am analyzing here the possibility of demonstrating the formation of certain of these fringes without being compelled to invoke the wave hypothesis.

I. THE DISTRIBUTION OF THE INTENSITY OF LIGHT IN A DIHEDRAL ANGLE FORMED BY TWO CORPUSCULAR PLANES IMBEDDED IN A TRANSPARENT MASS

Let us assume the existence of two corpuscular planes A and B, making an angle α (extremely small), imbedded in an absorbing *transparent* mass. The corpuscular layers A and B are very thin and possess the property of transmitting and reflecting light. If Q and R represent, respectively, the fractional parts of the intensity of light transmitted and reflected at each of these surfaces, the value of Q is supposed to be here conveniently chosen in order to facilitate determination of the theoretical transparency of the whole system.

If i represents the angle of incidence of a beam of light falling upon this system (Fig. 1), let us assume that the rays of this beam are parallel to a plane perpendicular to the edge $\overline{SS'}$. If we count the angle i from $\overline{nN}$ to the left or to the right, there will be in general three regions $\angle AnP$; $\angle PnN$ and $\angle NnO$ to be discussed separately.

Let us first take the case $i>\alpha$ (region PnA): since the rays under the incidence i are making with the interior normal to the plane OA angles of magnitudes $(i-2\alpha)$, $(i-4\alpha)$, $(i-6\alpha)\cdots(i-2p\alpha)\cdots$ (Fig. 2) all the rays of incidence i which will ultimately pass through a point m after being reflected by OB can be constructed geometrically and the magnitudes of their segments: $\rho_{1,1}\rho_{1,2}$; $\rho_{2,1}\rho_{2,2}\rho_{2,3}\rho_{2,4}$; $\cdots$; $\rho_{p,1}\rho_{p,2}\cdots\rho_{p,2p}$ (Fig. 3) expressed trigonometrically (p being the maximum number of times the ray is reflected on OB before it rebounds through m). The intensity distribution of light as seen on the plane OA, viewed from above, and produced by the beam of light transmitted through A and reflected by OB (once or several times) can be obtained by evaluating the sum of the intensities of all the rays passing through a point m of this plane at a distance x from $\overline{SS'}$. (For the sake of simplicity we will, in the evaluation of this intensity, make abstraction from the intensity of reflected rays of light coming from points of $\overline{OA}$ situated between O and m.)

Now, if a beam of light of intensity I_0 is incident upon an absorbing mass, the intensity I of light after passing through a total thickness ρ is given by the general law of transmission as: $I=I_0\varepsilon^{-a\rho}$ (where $\varepsilon^{-a\rho}=\beta$ is the coefficient of transmission, its value changing with the nature of material, its

* Publication assisted by the Ernest Kempton Adams Fund for Physical Research of Columbia University.
[1] S. Serghiesco, Comptes rendus, **202**, 1563, 1761 (1936).
[2] Max Planck, *Lectures on Theoretical Physics Delivered at Columbia University in 1902* (Columbia Univ. Press, 1915).

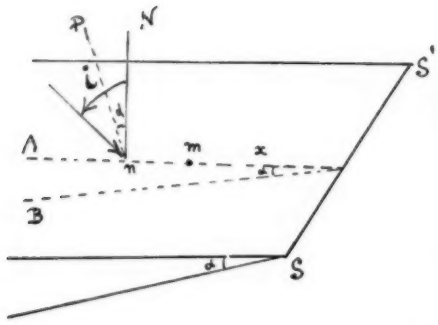

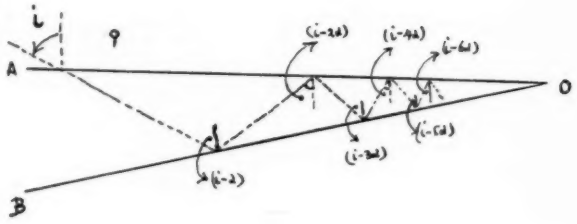

FIGS. 1 (left) and 2 (right).

concentration and with the nature of radiation). The intensity I at the point m will be:

$$I = I_0 Q^2 [R \exp [-a(\rho_{11}+\rho_{12})] + R^3 \exp [-a(\rho_{21}+\rho_{22}+\rho_{23}+\rho_{24})] + \cdots R^{2p-1} \exp [-a(\rho_{p,1}+\rho_{p,2}+\cdots+\rho_{p,2p})]]$$

or, after introducing the values of the different segments ρ, we will find that

$$I_m > I > I_M,$$

where

$$I_M = I_0 Q^2 R \exp\left[-2a\frac{\cos(i-2p\alpha)}{\cos i \cos(i-\alpha)}u_0'\right]\cdot\left[\frac{1-R^{2p}\exp\left[-2ap\frac{1}{\cos i}\frac{\cos(i-2p\alpha)}{\cos(i-\alpha)}u_0'\right]}{1-R^2\exp\left[-2a\frac{1}{\cos i}\frac{\cos(i-2p\alpha)}{\cos(i-\alpha)}u_0'\right]}\right]$$

and

$$I_m = I_0 Q^2 R \exp\left\{-2a\frac{1}{\cos[i-(2p-1)\alpha]}u_0'\right\}\cdot\left[\frac{1-R^{2p}\exp\left[-2ap\frac{1}{\cos(i-(2p-1)\alpha)}u_0'\right]}{1-R^2\exp\left[-2a\frac{1}{\cos i}\frac{\cos(i-2p\alpha)}{\cos(i-\alpha)}u_0'\right]}\right],$$

where $u_0' = x \sin \alpha$.

If x is supposed positive on the left (Fig. 4) as these two functions of x are decreasing with x from $x=0$ to $x=\infty$, the maximum of intensity will be concentrated on the edge of the dihedral angle AOB and if a is sufficiently great the descent of the curve of intensity will be more abrupt.

Similar results would have been obtained if we had calculated the intensity in a point of the OB. *The same result in the variation of intensity will be obtained for the regions NnO ($i>\alpha$) and PnN ($i\leq\alpha$)*

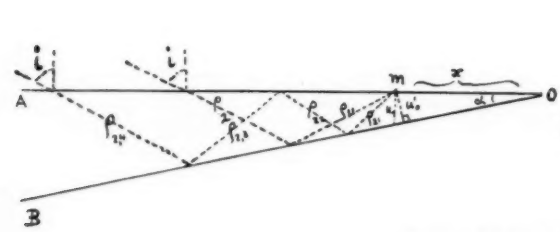

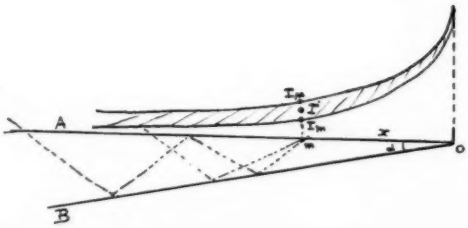

FIGS. 3 (left) and 4 (right).

and similar results will be obtained for whatever position the dihedral angle has with respect to the direction of the beam of light (its rays being always perpendicular to the edge).

The beam of light falling on this dihedral angle was supposed to have an initial uniform intensity I_0. We will obtain similar results if the beam of light of uniform intensity I_0 will fall first on a corpuscular plane AM (Fig. 5). The rays of this beam will not have the same intensity when they reach OA but the distribution of intensity on OA produced by this beam after oscillating between OA and OB will also show a maximum toward the point O.

II. The Distribution of Intensity of Light in a Film of Lattices and the Formation of Fringes under a Purely Corpuscular Aspect

Let us assume now the existence of a whole set of lattices formed by two sets of equidistant parallel planes intersecting at an angle extremely small and imbedded also in an absorbing transparent mass. These surfaces will intersect each other, and will form elementary prismatoidal surfaces of section *abcd* (Fig. 6(a) designates a section of this set of lattices produced by a plane perpendicular to the parallel sides of these prismatoidal surfaces.) The vertices a, b, c, d will form, as we notice, a net of points arranged in horizontal and vertical rows. If a beam of light is thrown upon this set of lattices, the light will undergo everywhere absorption, transmission and reflection but it will not spread uniformly in this medium. The intensity of light will be concentrated in the net of points forming horizontal and vertical rows as shown in Fig. 6(a) and in general the intensity, as viewed from above the set, will be maximum along the edges of the different dihedral angles. If we sum up the intensities of light in each point of this net of points along each edge as in a', b', $c' \cdots$ (Fig. 6(b)), the distribution of intensity will appear as a series of bright fringes alternating with dark fringes. If the distance between the parallel surfaces is very small the whole structure would appear as a *fibrous film of transparent absorbing mass of a very small thickness producing bright and dark linear fringes.*

Similar results will be obtained if instead of plane surfaces we consider also sets containing curved surfaces of very small curvature, as for instance, the structure composed of a set of concentric spherical surfaces intersecting a set of parallel planes, as in Fig. 6(c). There, in elements like *abcd*, the intensity of light will be maximum at the vertices a, b, c, and d while in elements like $a'b'c'$ the intensity will be maximum at a' and b' and minimum at c'. The distribution of intensity as viewed from above will *appear therefore, as a series of concentric circular bright and dark fringes.*

As we have demonstrated before[1] the law of refraction and the coefficient of Fresnel in a purely corpuscular way (and without even making use of the new idea of "quanta") we can conclude from the above study of the distribution of intensity of light in a film of lattices, that it is possible to admit the existence of *certain fringes* as a purely corpuscular phenomenon, independently of the introduction of the interference phenomenon and therefore of the wave idea.

III. On the Measurements of a Special Problem of Fringes under a Corpuscular Aspect

Let us consider again a set of lattices formed by two sets of equidistant parallel planes intersecting at an angle α (extremely small) and imbedded in an absorbing transparent mass (Fig. 7(a)) and let us suppose that the common distance between the parallel planes in both sets is $\delta/2$.

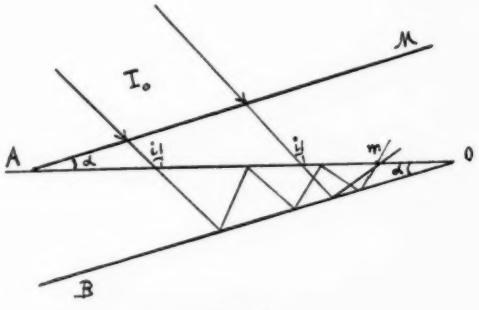

Fig. 5.

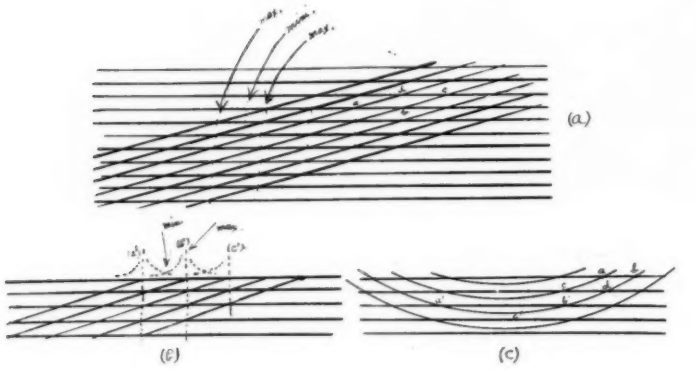

FIG. 6.

The distance between the bright fringes as viewed by an observer above OA will then be $\overline{mn}=\delta/2 \sin \alpha$ which would be the same as that between dark fringes.

Let us consider now a structure of lattices formed by a set of equidistant concentric spherical surfaces and a set of equidistant parallel planes with a common distance between the parallel surfaces of the both sets equal to $\delta/2$ (Fig. 7(b) and (c)). In elements like $abcd$ the intensity of light will be maximum at the points of intersections a, b, c, d and minimum at about half the common distance of the equidistant surfaces, while in elements like $y_1 e y_1' o$ the intensity will be maximum in y_1' and y_1 and minimum at e.

If the intersection of these sets of equidistant surfaces is such that the central points $o, e, f, g, \cdots$ correspond to a minimum like in the Fig. 7(b) where $e, f, g, \cdots$ are supposed to be (for the sake of simplicity) at half-distance between the parallel planes, the radii $\overline{oy}_1$, $\overline{oy}_2 \cdots \overline{oy}_n$ of the bright circular fringes will be given in general by the system:

$$x^2+y^2=\left[R+(2n+1)\frac{\delta}{4}\right]^2; \quad x=R$$

where R is the radius of the first spherical surface tangent to AB and therefore:

$$\overline{oy}_n=\left[(2n+1)R\frac{\delta}{2}+(2n+1)^2\frac{\delta^2}{16}\right]^{\frac{1}{2}}.$$

Since δ is almost an infinitesimal, $\delta^2/16$ can be neglected and the radius of the bright fringe of order n will then be

$$\overline{oy}_n=\left[(2n+1)R\frac{\delta}{2}\right]^{\frac{1}{2}}. \qquad \text{(I)}$$

Similarly the radius of a dark fringe of order n will be

$$\overline{oy}_n'=\left(2nR\frac{\delta}{2}\right)^{\frac{1}{2}}. \qquad \text{(II)}$$

The width of a fringe which can be taken by approximation as being represented algebraically by $\overline{oy}_n-\overline{oy}_{n-1}=R\delta/2\overline{oy}_n$ and which shows that it gets thinner and thinner toward the outside rings, can have here a real physical interpretation

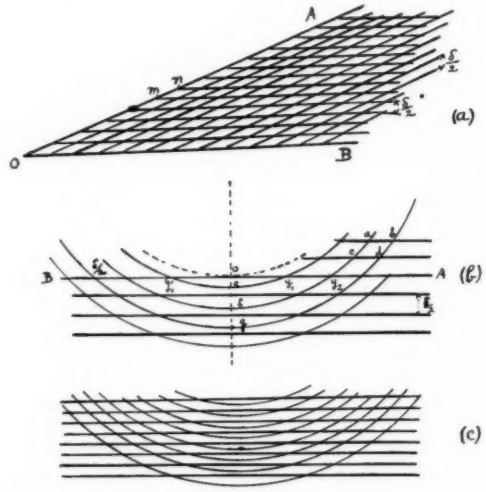

FIG. 7.

as we notice that the extreme vertices of elements *abcd* are nearer together as the rings are further away from the center.

Now, let us just notice (without entering into any new interpretation of the λ (wave-length) that if our $\delta=\lambda$, the first case of this paper $\overline{mn}=\delta/2 \sin \alpha$ becomes the distance between two bright or dark fringes given by O. Wiener[3] in calculating the stationary waves and the second case of this paper gives in (I) and (II) the radius of circular fringes in *Newton's rings*.

[3] O. Wiener, Ann. d. Physik u. Chemie **40**, 203 (1890).

Tenth Annual Meeting, Inter-Society Color Council

Washington, D. C., March 4 and 5, 1941

PROGRAM

Tuesday, March 4, 1941

9:30 A.M. *Discussion Session:* FORREST LEE DIMMICK, Chairman
At American Pharmaceutical Association Headquarters, 2215 Constitution Avenue

2:00 P.M. *Annual Business Session:* DEANE B. JUDD, Chairman

Reports of committees, and of chairmen of delegations from member bodies. (Reports should be in writing so that they may be included in the report of the meeting.)
At American Pharmaceutical Association Headquarters, 2215 Constitution Avenue

6:30 P.M. *Informal Dinner for Delegates and Members*

Wednesday, March 5, 1941

2:00 P.M. *Joint ASTM-ISCC Technical Session:* "Color—Its Specification and Use in Evaluating the Appearance of Materials": M. REA PAUL, Chairman

This meeting will be held at the Mayflower Hotel, which is to be ASTM Headquarters
Introduction to Color—DEANE B. JUDD
Color of Transparent Materials—FRANCIS SCOFIELD
Hiding Power and Opacity—R. H. SAWYER
Color Standards for Opaque Materials—I. H. GODLOVE
The Spectrophotometer in the Determination of the Color of Materials—A. E. PARKER
Photoelectric Colorimetry—RICHARD S. HUNTER

8:00 P.M. *Popular Session: Parade of Color:* WM. D. APPEL, Chairman

ASTM members will join the ISCC for this session. The meeting is to be held in the auditorium of the Potomac Electric Power Company, 10th and E Streets, N.W., the usual meeting place of the Washington-Baltimore branch of the Illuminating Engineering Society, who, with the Washington Colorists, are also joining the ISCC for this session.

Trends in Color Photography—an Indispensable Tool of the Scientist and Technician—EARL A. TRAGER, *manager of Washington Branch of Bell & Howell Company, formerly Chief Naturalist, National Park Service.*

Paint Styling Demonstration (will reveal interesting ways of creating color illusions on building interiors and exteriors)—NATIONAL PAINT, VARNISH & LACQUER ASSOCIATION, by prominent members of their Council on Paint Styling which keeps its finger on the color pulse of the nation.

Exploring the Magic World of Color (a spectacular and thrilling presentation by the "World's Greatest Color Magician")—HERBERT THOMPSON STRONG, *color consultant, Museum of Science and Industry, New York, New York.*

A Spectrophotometric Study of Glutathione

GLADYS A. ANSLOW AND ELISABETH REED LYMAN
Department of Physics, Smith College, Northampton, Massachusetts

(Received October 1, 1940)

The ultraviolet and visible absorption spectra of glutathione in aqueous, alcohol, and alkaline solutions show four regions of selective absorption at 500, 325, 280 and 252mμ, associated with absorption of energy in the α−β carbon bond of the glutamic acid radical, the −SH group of the cysteyl radical, the peptide linkage, and the S−S bond of oxidized glutathione, respectively. The peptide band at 280mμ consists of two components whose location, definition, and intensity depend upon the solvent. This band is shifted toward the visible in alkaline and alcohol solutions, as is the ultraviolet continuum. The location of the latter indicates that the energy absorbed in the peptide dissociates glutathione into its constituent amino acids. Oxidation follows the absorption of energy of wave-length about 325mμ; the subsequent reduction of the oxidized molecules is affected by energy of wave-length 252mμ. These conclusions are supported by freezing-point measurements of the van't Hoff dissociation factors of glutathione, glutamic acid, cysteine HCl, and glycine solutions before and after irradiation.

THE occurrence of glutathione in plant and animal tissue, the similarity of its tripeptide structure to that of the polypeptide proteins, and the physiological effects produced by radiant energy indicate the possible importance of a spectrophotometric investigation of the absorption of ultraviolet radiation by this molecule. Such a study should reveal the energy of the peptide linkage between the constituent amino acids and also that of the cystine bond, which is formed on the oxidation of the cysteine component of glutathione, whose probable formula is that of glutamyl-cysteyl-glycine,[1] $COOH \cdot CH(NH_2) \cdot CH_2 \cdot CONH \cdot CH(CH_2 \cdot SH) \cdot CONH \cdot CH_2 \cdot COOH$. Both the peptide, CO−NH, and the cystine, S−S, bonds are physiologically important, the former being that between the constituents of proteins and the latter playing a role in physiological oxidation, since cysteine-cystine is an auto-oxidable system.

The ultraviolet absorption associated with the peptide linkage has been studied in many proteins, the results of which are discussed in a separate paper dealing with similar proteins.[2] The spectra of numerous peptides have been previously reported by Allen and co-workers,[3] who noticed increased absorption in the region of 280mμ when a peptide linked molecule was substituted for a similar one without this linkage. An indirect investigation of the same problem has been reported by Rideal and Mitchell.[4] From studies of the hydrolysis of monolayers of stearic anilide they concluded that the energy absorbed in the aromatic groups is subsequently transferred along the molecule to adjacent peptide linkages, which are then broken. Their absorption spectra of stearic anilide in alcohol and in cyclohexane solutions exhibit strong bands characteristic of the benzene ring and in addition two weaker bands in the 280mμ region, which were not discussed by them.

The band associated with the cystine bond was identified in this laboratory at about 251mμ.[5] Since the sulfur group in glutathione is separated from the other absorbing groups by at least two carbon atoms, the spectrum of glutathione, if it is appreciably oxidized, should show this band in a nearly undisplaced position.

PROCEDURE

The analysis was made with a Hilger E3 quartz spectrograph and a rotating sector photometer, employing two quartz Baly cells, using as light source the hydrogen discharge tube mentioned in previous reports from this laboratory. The sectors were rotated at speeds of about 160

[1] F. G. Hopkins, J. Biol. Chem. **84**, 269, 321 (1929); E. C. Kendall, B. F. McKenzie and B. L. Mason, *ibid.* **84**, 657 (1929).
[2] G. A. Anslow and S. C. Nassar, J. Opt. Soc. Am. **31**, 118 (1941).
[3] A. C. Allen, R. E. Steiger, M. A. Maguill and R. A. Franklin, Biochem. J. **31**, 195 (1937).
[4] I. E. K. Rideal and J. S. Mitchell, Proc. Roy. Soc. **A159**, 206 (1937).
[5] G. A. Anslow and M. L. Foster, J. Biol. Chem. **97**, 37 (1932).

r.p.m.; thus the error due to intermittency of the beam was negligible.[6] The glutathione was obtained from the Eastman Kodak Company; solutions were made in conductivity water, absolute ethyl alcohol, and 0.5 normal NaOH. To avoid as much as possible the effects of photochemical action on the solutions, spectra were photographed promptly after forming solutions and short exposures were used. Since the absorption of energy changed the absorptivity of the solutions in the region of selective absorption, the Hilger quartz echelon, had it been available, would have been a more reliable tool than the sector photometer.

The absorption bands of glutathione are relatively weak, particularly in the water solution, the bands for the peptide and cystine bonds appearing only in fairly strong concentrations, about 0.1–0.05 *M*, weaker solutions, 0.001–0.000025 *M* being suitable for locating the ultraviolet continuum.

Results

The curves in Fig. 1 show the molecular absorption occurring in aqueous, alcohol and alkaline solutions. In all, bands with centers at 500, 325, 280 and 252mμ were identified and with one exception have the same locations in all solutions. In alcohol the bands are narrower and stronger than in the other solutions; in 0.5 normal NaOH solutions the absorption is very intense and the bands broad, making resolution difficult. The position and structure of the 280mμ band depends on the solvent; it has two components, which are just resolvable in aqueous solutions with maxima at 286 and 276mμ, which are well defined in alcohol solutions at 294 and 283mμ, and which are barely resolvable in alkaline solutions at 303 and 292mμ. In all, the long wave-length component is narrower than the other component and is particularly so in alcohol solutions.

The identification of the molecular bonds which are responsible for these bands is fairly direct. The band at 500mμ occurs in the same region as that found by Anslow and Foster[5] in the spectrum of glutamic acid. Since glutamic acid is freed by the hydrolysis of glutathione the 500mμ band may be thus identified.

[6] B. O'Brien, Phys. Rev. **37**, 471 (1931).

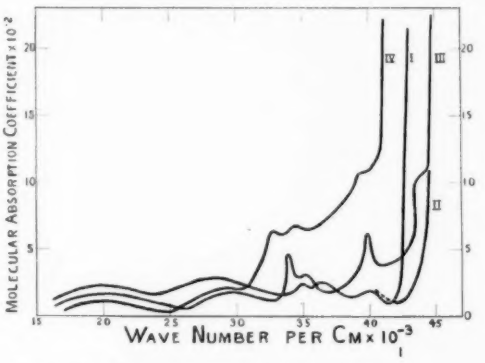

FIG. 1. Absorption curves of glutathione; I—aqueous solution; II—year-old specimen in aqueous solution; III—absolute EtOH solution; IV—0.5 normal NaOH solution.

In the absorption spectrum of cystine[5] the 251mμ band was explained as caused by the disruption of the S−S linkage about which axis the cystine molecule is arranged symmetrically. The similarly located band in the spectrum of glutathione indicates the presence in the solution of oxidized glutathione, containing S−S bonds produced from two molecules in the reduced form after the release of hydrogen from the −SH group.

The breaking of the C−N bonds of the peptide group apparently accounts for the two-component band at 280mμ in aqueous solutions, which is shifted to 294 and 283mμ in alcohol solutions and to 303 and 292mμ in 0.5 *N* NaOH solutions. It is reasonable that the energy required to affect this separation should depend upon the polarity of the solvent; the position of the ultraviolet continuum produced by the dissociation of the carboxyl group of amino acids is also affected by the solvent.[7] The positions of the bands indicate that the energy needed to break the peptide linkage is least in alkaline solution and less in alcohol than in aqueous solutions. Evidence for the assignment of these bands to this linkage also appears in the work of Allen and co-workers,[3] and more definitely in the two bands shown in the absorption curves of Rideal and Mitchell[4] for stearic anilide, appearing in a cyclohexane solution at 281 and 274mμ. Further discussion of these bands will appear in

[7] G. A. Anslow, M. L. Foster and C. Klingler, J. Biol. Chem. **103**, 81 (1933).

TABLE I. *Effects of irradiation of glutathione and its amino acid constituents on their degrees of dissociation.*

SAMPLE	FILTER NUMBER	ABSORBING GROUPS	HOURS OF IRRADIATION	VAN'T HOFF FACTOR, *i*		
				NON-IRRADIATED	IRRADIATED	Δi
0.1 *M* glutathione	none	all	2	0.96	1.36	+0.40
0.0725 *M* year-old glutathione	none	all	1	1.16	1.31	+0.15
0.08 *M* 7-year-old glutathione	none	all	2	1.32	2.71	+1.39
0.1 *M* glutathione	1	CONH, SH, $\alpha-\beta$C	3	1.01	0.91	−0.10
0.1 *M* glutathione irradiated through filter No. 1	2	S−S, CONH, SH, $\alpha-\beta$C	3	0.91	1.15	+0.24
0.1 *M* glycine	none	COOH	2	1.04	1.05	+0.01
0.1 *M* glycine in 0.1 *M* NaOH	none	COOH	2	2.31	2.52	+0.21
0.1 *M* glycine in 0.117 *M* HCl	none	COOH	2	1.99	1.89	−0.10
0.1 *M* cysteine HCl	none	COOH, SH	2	2.70	2.22	−0.58
0.1 *M* cysteine HCl	1	SH	3	2.68	1.82	−0.86
0.1 *M* cysteine HCl irradiated through filter No. 1	2	S−S, SH	3	1.82	2.12	+0.30
0.05 glutamic acid	none	COOH, $\alpha-\beta$C	1	1.13	0.90	−0.23

the following paper, which deals particularly with the peptide linkage.

The broad band with center at 325mμ is probably caused by the absorption of energy which disrupts the −SH group in the reduced form of glutathione. The published spectra of cysteine hydrochloride[3] indicate some slight absorption in this region and new plates taken with 0.5 *M* concentration in a 1.5-cm cell clearly indicate the band.

The long wave-length edge of the ultraviolet continuum obviously depends upon the state of the solution and its constituents. The frequency corresponding to the onset of the ultraviolet continua in aliphatic amino acids was found by Anslow and Foster[5] to be a linear function of the square root of the mass of the molecular ion. If a solution contains several amino acids the ultraviolet continuum of the heaviest constituent, if this be sufficiently abundant, will mask those of the lighter elements, since it will begin at longer wave-lengths. Consequently, if the solution contains a large percentage of undissociated glutathione, the ultraviolet continuum of an aqueous solution will start at about 254mμ; if it is dissociated into glutamic acid and cysteyl-glycine, the long wave-length limit will be that of cysteyl-glycine at approximately 232mμ; and if it is completely dissociated into glutamic acid, cysteine and glycine, the edge of the band is that of glutamic acid at 224mμ.

Spectra of a freshly prepared sample of glutathione in water solutions show the edge of the continuum at 232mμ approximately, indicating that the dissociation of the glutathione was not complete and that the dipeptide, cysteyl-glycine, was abundant in the irradiated solution. A few plates, for which long exposures were employed, and also those obtained from a sample of glutathione, which had been preserved for a year in a dark bottle in a desiccator, showed total absorption around 224mμ, indicating that either the state of the solution or the larger amount of irradiation, or both, completely dissociated the peptide linkage. In the alcohol solution of concentration 0.0001 *M* the continuum again indicated strong absorption at 232mμ, followed in a weaker solution, 0.000025 *M*, by stronger absorption at about 224mμ. The continuum obtained in the 0.5 normal NaOH solution was shifted toward the visible to 242mμ; if the interpretation given the alkaline solution shift occurring in glycine[7] is applied here, this indicates glutamic acid as the heaviest component existing after irradiation. In more dilute solutions the 232 and 242mμ band edges appear as a result of the action of the water in the solvent on the solute.

The effects produced by irradiation

The variations in the degree of dissociation of glutathione resulting in different positions for the

onset of the ultraviolet continuum appear to be the result of several causes, the accumulative dissociation into simple amino acids as a result of irradiation, the concentration of the solution, or the condition of the sample before irradiation. The year-old sample may have been partly dissociated before irradiation. Another sample similarly preserved for seven years did not show the 325, 280, or 252mμ bands in its spectrum, but was nearly identical with that of glutamic acid, its heaviest constituent.

After the molecules are dissociated by irradiation various associations apparently follow. Breakage of the peptide linkage permits recombinations of the amino acid constituents into glutathione or the formation of the possible dipeptides or of the amino acid constituents. Dissociation of the carboxyl group may be followed by reassociation or by polymerization of the zwitterions in the solute. The release of H ions from the −SH groups permits the association of pairs of glutathione ions into oxidized glutathione or of pairs of cysteine ions into cystine. Disruption of the $\alpha-\beta$ carbon bond of the glutamic acid radical may lead to association of the residues with ions of the solution into simple amino acids. All these processes of dissociation and association occur simultaneously during irradiation, as the spectra indicate.

To obtain other evidence of the degree of dissociation qualitative determinations of the van't Hoff factors of the various specimens of glutathione and of the constituent amino acids before and after irradiation, the effects of the unfiltered radiation and also of radiation filtered to eliminate one or more of the dissociations was studied. Filter No. 1 is a quartz cell containing a concentrated solution of phenylalanine in water, which absorbs wave-lengths shorter than 270mμ, but transmits continuously above this, eliminating the radiation which may dissociate the carboxyl and cystine groups, but passing that which breaks the peptide linkage and the cysteine group, as well as the $\alpha-\beta$ carbon bond of glutamic acid. Filter No. 2 is an Eastman No. 17 filter, which passes the same as above, the unimportant 300mμ and the 400–470mμ regions being lost, and also passes to a lesser extent the radiation which breaks the cystine bond. Glutathione and cysteine hydrochloride were irradiated using filter No. 1 and these irradiated solutions were later irradiated using filter No. 2. The results are given in Table I.

It is obvious that the fresh sample of glutathione was undissociated before irradiation, but that the samples which had been kept in the laboratory for some time had broken down at least partially. On all, irradiation has a net dissociation effect. The results for glycine are quoted,[7] those for NaOH and HCl solutions being included since cysteine is available in the HCl form only and comparisons with another HCl solution are desirable. Concentrations similar to the highest possible for glutathione were used in all the amino acid solutions. As previously discussed,[7] polymerization of glycine follows dissociation by irradiation, the net effect depending upon the concentration. Some association process apparently occurs in irradiated glutamic acid. The large decrease in the van't Hoff factor occurring in irradiated cysteine may be the result of the formation of cystine molecules from some of those dissociated. Since the use of filter No. 1 permits only the −SH dissociation, the very large decrease in i, −0.86, cannot be otherwise explained, for polymerization of released zwitterions cannot occur. The dissociation of some of these cystine molecules was then affected by irradiation through filter No. 2, as indicated by the increase in the van't Hoff factor.

Since irradiation of glutathione through filter No. 1 results in only a small decrease in the van't Hoff factor, the dissociation produced by breaking peptide linkages must nearly balance the cysteine-cystine and the glutamic acid association processes. That cystine is actually formed is obvious from the results of subsequent irradiation through filter No. 2 which indicate a resultant increase in the degree of dissociation caused by breakage of the cystine bond. Thus the oxidation and reduction processes must be produced in glutathione by the absorption of energy of wavelengths 325 and 252mμ, respectively, and it is clear that the role of sulfur in physiological processes is not confined to cysteine and cystine as free molecules, but also occurs in their compounds, the cystine components forming the cross-links in some large peptides.

The Absorption of Ultraviolet Energy by the Peptide Linkage

GLADYS A. ANSLOW AND SALWA C. NASSAR*
Smith College, Northampton, Massachusetts

(Received October 1, 1940)

The absorption spectra of the proteins, egg albumin, lactalbumin, and gelatin were studied and compared with those of related amino acids and simple peptides; the effect of various solvents on these compounds was investigated. A region of selective absorption at about 280 mμ, common to proteins and to simple peptides, indicates that the seat of absorption is the peptide linkage which is the main bond in such compounds. This region coincides with that characteristic of tryptophane and tyrosine. The band consists of two components, whose separation in proteins and amino acid peptides is approximately 1200 wave numbers and in anilides about 850 wave numbers. The breaking of the peptide linkage is the cause of denaturation; the energy required is about 4.4 electron volts and varies with the solvent.

INTRODUCTION

SPECTROPHOTOMETRIC studies of proteins have led to considerable information concerning the lethal effect of radiant energy on these molecules, by revealing the spectral region the energy of which is that necessary to break the peptide linkage between component amino acid groups. In order to obtain a fairly precise value of this energy, which is important for the determination of the relative efficiencies of various types of sources in breaking the peptide linkage, a detailed investigation of the absorption spectra of chosen proteins was undertaken. For the interpretation and confirmation of the results this study included the absorption spectra of the aromatic acids, important constituents of proteins and the spectrum of a dipeptide, acetanilide, comparisons being made with the available spectra of other peptides.

Various other observers have shown that proteins exhibit selective absorption with a maximum in the 280 and a minimum in the 252-mμ regions,[1–12] which has been interpreted as the maxima and minima caused by the constituent acids, tryptophane and tyrosine. In the proteins which contain a considerable percentage of phenylalanine the characteristic bands of the benzene ring appeared. Most of the absorption curves were smooth; however, definite structure in the maximum appeared in those of Lewis and of Spiegel-Adolf for serum albumin and in those of Lavin, Loring and Stanley for viruses. The appearance of the maxima in the region of the tryptophane and tyrosine bands led to the belief that the absorption of energy by these constituents was responsible for the activation and denaturation of protein molecules.

The simple peptides which have been previously studied or discussed in the preceding paper on glutathione[13] also show selective absorption in the 280-mμ region. Hence, the peptide linkage, which is common to these compounds and to proteins, may be a primary agent in the production of the band.

EXPERIMENTAL PROCEDURE

The proteins employed were egg albumin, prepared for this purpose by the method de-

* Now at the University of California, Berkeley, California.

[1] A. J. Lewis, Proc. Roy. Soc. **B89**, 327 (1925); Chem. Rev. **8**, 81 (1931).
[2] W. Stenstrom and M. Reinhard, J. Biol. Chem. **66**, 819 (1925).
[3] T. Svedberg and J. B. Nichols, J. Am. Chem. Soc. **48**, 3081 (1926).
[4] T. Svedberg and B. Sjogren, J. Am. Chem. Soc. **50**, 3318 (1928).
[5] M. Spiegel-Adolf, Archi. Path. **12**, 533 (1931).
[6] G. I. Lavin, J. N. Northrop and H. S. Taylor, J. Am. Chem. Soc. **55**, 3497 (1933).
[7] M. Spiegel-Adolf and O. Krumpel, Biochem. Zeits. **190**, 28 (1927).
[8] M. B. Duggar, *Biological Effects of Radiation* (McGraw-Hill, N.Y. and London, 1936), Vol. I, Chap. VII and VIII.
[9] K. Feraud, M. S. Dunn and J. Kaplan, J. Biol. Chem. **112**, 323 (1935).
[10] E. R. Holiday, Biochem. J. **30**, 1795 (1936).
[11] J. S. Fruton and G. I. Lavin, J. Biol. Chem. **130**, 375 (1939).
[12] G. I. Lavin and W. M. Stanley, J. Biol. Chem. **118**, 269 (1937); G. I. Lavin, H. S. Loring and W. M. Stanley, *ibid.* **130**, 259 (1939).
[13] G. A. Anslow and E. R. Lyman, J. Opt. Soc. Am. **31**, 114 (1941).

scribed by Clark[14] and preserved at 0°C, and lactalbumin and gelatin obtained from the Harris Laboratories. The amino acids were purchased from the Eastman Kodak Company and the acetanilide was furnished by Dr. Pauline Burt of the Department of Chemistry of Smith College. Aqueous solutions of egg albumin, gelatin, acetanilide and the amino acids were studied. The *p*H values of the proteins and of acetanilide in the solutions which yielded the absorption bands, all about 4.5, indicated similar degrees of acidity. Because of the insolubility of lactalbumin in water it was studied in alkaline solutions, as also were egg albumin, gelatin, and acetanilide. Alcohol and cyclohexane solutions of acetanilide were examined.

The spectrophotometric apparatus employed was the same as that used in previous investigations in this laboratory,[13] except for the plates, the cells, and a cooling jacket, which kept the protein solutions at 0°C. Eastman Kodak Superpanchro Press plates were employed, making extremely short exposures possible. The cells, of the Brode[15] type, were of adjustable length with Pyrex walls and quartz end plates. When the cooling jacket was employed it was impossible to align the cells for use with the sector photometer because of the close proximity of the apertures and the two half-lenses of the instrument. Hence the photometer had to be removed and a substitute method devised. It is known that during several days of operation the current in the discharge tube remains constant. This justifies the taking of exposures through the solvent and the solution alternately, using a constant time interval for the former and suitable time intervals, from one to thirty seconds, for the latter to permit the calculation of molecular coefficients according to the equation

$$\log I_0/I = \log t_2/t_1 = kCd,$$

where t_1 and t_2 are exposure times for the solvent and solution, respectively, and the other symbols have their usual meaning. For verification of the structure obtained by the above-mentioned methods some of the absorption curves were also analyzed by a photoelectric densitometer.

[14] J. H. Clark, Am. J. Physiol. **73**, 649 (1925).
[15] W. R. Brode, Bur. Stand. J. Research **2**, 501 (1929).

Results and Discussion

The spectra

The amino acids, phenylalanine, tryptophane and tyrosine, are known to exhibit selective absorption in the 290–220-mμ region, the absorption being attributed to vibrational and electronic energy changes in the aromatic groups. In order to compare the positions of their bands with those of the proteins studied, the absorption

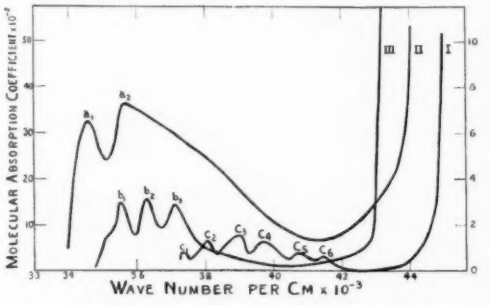

FIG. 1. Absorption curves of I—phenylalanine; II—tryptophane; III—tyrosine. The scale used in plotting the absorption coefficients of phenylalanine is five times that of tryptophane and tyrosine.

curves showing these bands and the ultraviolet continua are reproduced in Fig. 1. The positions of the bands agree fairly well with those of Feraud, Dunn and Kaplan,[9,16] except for the absence of the seventh band found in phenylalanine by these investigators at 235 mμ.

The ultraviolet continua began at wave-lengths 221.4, 229.3 and 223.0 mμ, respectively. An attempt was made to test the agreement of the wave numbers of the latter with the Anslow-Foster relation[17] for the ultraviolet continua of aliphatic amino acids in acidic solutions. The frequency at which continuous absorption of tyrosine begins agrees well with that relation, which ascribes the carboxyl group as the seat of the energy absorption. The corresponding values for phenylalanine and tryptophane, both in aqueous and acidic solutions, indicated that, if the relation holds for aromatic acids, the particles in the solution during irradiation must have smaller molecular weights than their normal

[16] K. Feraud, M. S. Dunn and J. Kaplan, J. Biol. Chem. **114**, 665 (1936).
[17] G. A. Anslow and M. L. Foster, J. Biol. Chem. **97**, 37 (1932).

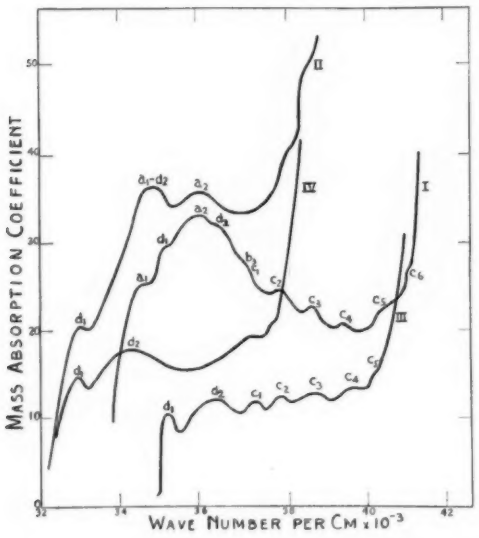

FIG. 2. Absorption curves of I—egg albumin in aqueous solution; II—lactalbumin in alkaline solution; III—gelatin in aqueous solution; IV—gelatin in alkaline solution.

values. Since this is improbable, an alternate explanation may be that the type of molecular ions formed in these solutions is different from those in solutions of the aliphatics. Another difference between phenylalanine and tryptophane on the one hand, and tyrosine on the other hand, is that both the regions of selective absorption and of the onset of the ultraviolet continua of the latter are shifted towards the red in alkaline solutions while those of the former are not affected. Such shifts occur in the spectra of alkaline solutions of the aliphatic amino acids.[18]

Since the aromatic amino acids are common constituents of proteins and are separated from each other by at least two atomic distances, their characteristic bands may be expected to occur independently in protein spectra. If the protein contains both tryptophane and tyrosine, whose bands overlap, the resulting effect in the protein spectrum produced with a spectrograph with limited resolving power will be a wide band with unresolved structure. But, if the resolving power is adequate, structure appears according to the proportionate compositions, which are given in Table I for the proteins investigated.

In Fig. 2 the absorption curves for egg albumin and gelatin in aqueous solutions and for lactalbumin and gelatin in alkaline solutions are reproduced. Both aqueous solutions show strong selective absorption with a maximum in the 280-mμ region. The curves are by no means smooth but have definite structures.

The egg albumin was at its isoelectric point, pH = 4.8, and studied at 0°C. The band structure, curve I, was observed for a concentration of 0.3 g/cc, using total exposures not exceeding five minutes, in which time no large percentage of the protein is denatured by irradiation. The predominant band appears at 279 mμ; the structure is not difficult to identify. The maxima a_1 and a_2 at 289 and 279 mμ are obviously tryptophane bands; the b_1 and b_2 tyrosine bands at 280.4 and 275.5 mμ must be partly responsible for the width of the 279-mμ band. The b_3 tyrosine band is slightly evident as an irregularity at 268 mμ in the down slope of the main band. The bands of phenylalanine, indicated by the c's, are superimposed on the region of minimum absorption between the main band and the ultraviolet continuum.

These constituents do not account for all the structure in the selective absorption region nor its magnitude. Two additional maxima d_1 and d_2 appear at 284 and 274 mμ. Since the other constituents of proteins exhibit no absorption in this region, the only remaining seat of absorption is the peptide linkage, thought to be responsible for the two component band at 286 and 276 mμ in the spectrum of glutathione.[13] Since the frequency of occurrence of this linkage in a protein depends on the number of the constituents, there are many chances for the absorption of energy in the breaking of the numerous linkages between

TABLE I.*

PROTEIN	FREQUENCY OF OCCURRENCE OF PHENYLALANINE	TRYPTOPHANE	TYROSINE
Egg albumin	5.1	1.3	4.2
Lactalbumin	1.3	2.7	2.0
Gelatin	1.4	0.0	0.0

* The quoted values are taken from C. L. A. Schmidt, *The Chemistry of the Amino Acids and Proteins* (Chas. L. Thomas, Chicago, Illinois, 1938), p. 217.

[18] M. L. Foster, G. A. Anslow and D. Barnes, J. Biol. Chem. **89**, 665 (1930); G. A. Anslow, M. L. Foster, and C. Kingler, *ibid.* **103**, 81 (1933).

the groups. Hence a considerable proportion of the absorbed energy must be ascribed to this process.

To test this hypothesis gelatin, which is very poor in tryptophane and tyrosine, was studied in an aqueous solution of pH=4.5. The usual chemical tests for the presence of tryptophane and tyrosine indicated no trace of the former and only a slight reaction typical of the latter. In the spectrum the bands at d_1 and d_2 fall in the same region as those in the spectrum of egg albumin. There is no indication of tryptophane or tyrosine bands, the remaining structure being that of phenylalanine.

For further information the simple peptide, acetanilide, was studied in various solutions and a comparison made with the bands previously recorded for the peptides, glutathione[13] and stearic anilide.[19] Their spectra and those of gelatin and lactalbumin are graphed in Fig. 3, which shows both the location of the peptide bands in aqueous solutions and the effect of solvents on their positions and intensities. All aqueous solutions yield the two-component band at about 280 mμ, the longer wave-length component being the narrower. The wave number separation of these components is about 1200 for all the proteins and the amino acid peptide studied, and about 850 for the anilides. In the aqueous solution of acetanilide, pH=4.5, the narrow band appears at 279.5 mμ and the wide band has its center at 272 mμ. The latter is difficult to indicate on the graph since it is superimposed on the onset of an extremely strong ultraviolet continuum on which appears a strong band with center at about 235 mμ, the band found for stearic anilide by Rideal and Mitchell and which may be identified as that of the phenyl group of the anilides. In alcohol and particularly in cyclohexane solutions of these anilides both this band and the two peptide components show little damping by the solvent and are well resolved.

The solvents employed, because of their polarity, shift the peptide band of the amphoteric protein and amino acid solutions toward the visible, but have only a slight effect on the anilides. The shift produced in 0.5 normal NaOH solutions of all the amphoterics is very nearly the same, about 2200 wave numbers. The shift occurring in absolute EtOH solutions of glutathione is about half that produced in alkaline solutions. The ultraviolet continua of these solutions are also shifted toward the visible.

The relative intensities of the two components are affected by the solvent. For alcohol solutions of acetanilide and of glutathione the narrow band is the more intense; for cyclohexane solutions of

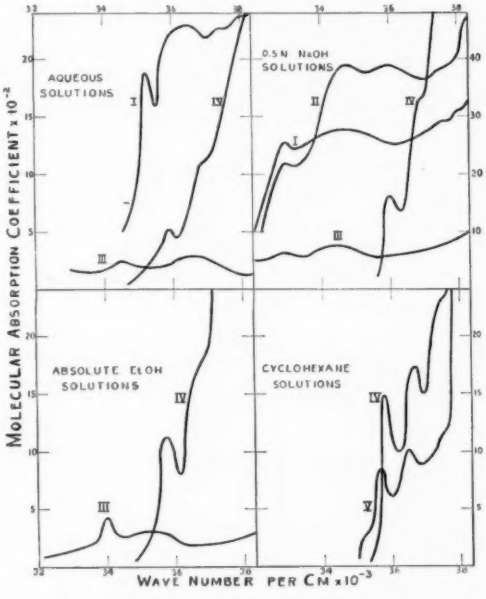

FIG. 3. Absorption curves of I—gelatin; II—lactalbumin; III—glutathione (reference 13); IV—acetanilide; V—stearic anilide (reference 19). The NaOH curves are plotted at half the scale of the others and the lactalbumin values are reduced $\frac{1}{3}$.

acetanilide and stearic anilide the two components are of nearly equal intensity and width; whereas for alkaline solutions of gelatin, glutathione, and acetanilide the wide band is the more intense, the general absorption in the region of the bands being much greater than in other solutions. The effect is not immediately clear in the alkaline solution of lactalbumin because of the superposition of the tryptophane and tyrosine bands on those of the peptide linkage. Both the tyrosine and the peptide bands have been shifted toward the visible, the tryptophane bands being undisplaced, with the result that the tyrosine

[19] I. E. K. Rideal and J. S. Mitchell, Proc. Roy. Soc. **A159**, 206 (1937).

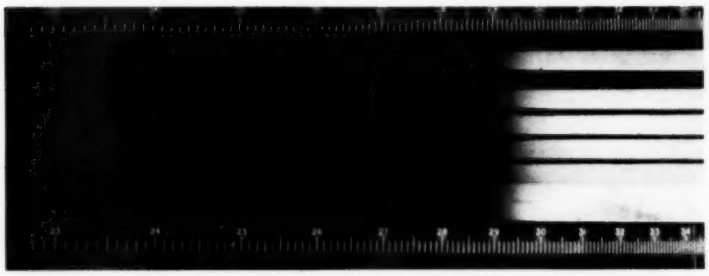

FIG. 4. Effect of irradiation on the absorptivity of egg albumin.

longer wave-length components fall in the region of the 289-mμ band of tryptophane and its short wave-length component near the 279 tryptophane band, and that the two peptide components are shifted to the same locations as those of gelatin, the shorter wave-length component falling near the long wave-length component of the tryptophane band. Since the 289-mμ region contains bands caused by tryptophane, tyrosine and the peptide and the 279-mμ region only those of tryptophane and tyrosine, the former is of the greater intensity. Similarly, the peptide band for egg albumin in 0.5 normal NaOH solution, not plotted, becomes stronger and is shifted into the same region as those of the other proteins, the resultant spectrum resembling that of lactalbumin but showing less separation between the 289- and 279-mμ bands because of the larger percentage of tyrosine in the protein, the b_1 and b_2 components broadening the 289-mμ absorption region.

Confirmation of the present conclusions is available in the results of other investigations dealing with the spectra of both simple peptides and proteins. In an extensive study of simple peptides Allen and co-workers[20] found that "when the hydrozyl of a carboxyl group of an acetylbipeptide is replaced by an NHC_6H_5 residue, marked increase in absorption occurs and bands appear at 280 and 245 mμ." The latter corresponds to the region of the bands produced by the benzene derivatives, the former is that just identified as characteristic of the peptide linkage. The results obtained by Fruton and Lavin[21] for tyrosine containing peptides can be interpreted in the light of the present information as the resultant of the tyrosine bands and those of the peptide linkage. The protein spectra which show the greatest structure and permit comparison with the present results are those produced by the protein component of viruses reported by Lavin, Loring and Stanley.[12]

Thus it appears that the band structure in the 280-mμ region in peptides lacking tryptophane and tyrosine is caused solely by the peptide linkage, while in proteins containing these two constituents it is the resultant of the independent absorption by tryptophane, tyrosine, and the peptide linkage.

The physical effect of irradiation on protein

A solution of egg albumin of *p*H 4.8 was irradiated at 0°C. During the first hour flocculation appeared accompanied by a bad smell. The precipitate settled in less than 24 hours. The solution was decanted and its concentration compared with that of a fresh one by the interferometer method. A slight decrease in concentration was consistently observed on different trials, an unexpectedly small decrease considering the amount of the precipitate. Two possibilities explain this result. Either because of the size of the protein molecule a fairly large quantity must precipitate to affect the concentration, or more probably, the solute is denatured before flocculation by breaking into smaller particles, a process which causes greater refraction and counterbalances the decrease due to flocculation.

It was observed that on frequent shaking of the solution under irradiation more flocculation was formed. If the solution was irradiated without agitation the change in concentration was negligible and the flocculation was confined to a thin layer against the wall adjacent to the source.

[20] A. G. Allen, R. E. Steiger, M. A. Maguill and R. A. Franklin, Biochem. J. **31**, 195 (1937).
[21] J. S. Fruton and G. I. Lavin, J. Biol. Chem. **130**, 375 (1939).

This indicates, as a result of irradiation, the formation of a protective layer, such as found in tissue by Spiegel-Adolf,[5] which absorbs the energy required to affect the peptide linkage. Additional information concerning this effect is furnished by the spectra reproduced in Fig. 4, which are results of one-second exposures of egg albumin solutions, the successive exposures being taken after irradiating for 0, 5, 30 min., and additional 1-, 2-, 3- and 4-hour intervals, respectively. The solution rapidly becomes more absorptive, but after several hours of irradiation becomes more transparent.

These physical effects must be caused by the breaking of the peptide linkage, followed by combinations forming hydrophobic molecules. Consequently, about 4.4 electron volts of energy (calculated from the mean wave-length of the peptide bands in aqueous solutions), are absorbed in breaking this linkage. The effect of solvents like alcohol and NaOH is a decrease in the required energy and an increase in the fraction of the energy absorbed, which suggests that if tissue proteins are treated with such solvents before irradiation increased efficiency may result. Moreover, in these solvents sunlight even after transmission through ordinary glass can affect dissociation.

The Shape of Stereoscopic Images

JOHN T. RULE
Massachusetts Institute of Technology, Cambridge, Massachusetts
(Received November 7, 1940)

THIS article deals with the determination of the shapes of stereoscopic images. It develops formulae for locating image points and a graphical method of projecting any object plan directly into the resultant image plan when the conditions of photographing and projecting are given. The purpose is to supply an exact tool for the analysis of stereoscopic effects so that it may become possible to determine the reasons for observable distortions and to predict the results of any proposed optical system. A further purpose is to furnish a base for the comparison of the psychological interpretation of images with their shapes on geometrical principles in order to open the way for the study of the degree of variation from orthostereoscopic images which is permissible in practical projection without annoyance. The entire considerations here, however, are geometrical.

The errors in image shape introduced by considering camera and projector lenses as thin lenses are of a very minor order compared to those introduced by slight changes in position of the observer and by the normally varying human interocular. We shall therefore treat all lenses as points, or, from the geometric standpoint, as centers of projection.

Geometrically we are dealing with a double projective system. The object is projected through two centers of projection, the camera lenses, onto a projection plane—the plate of the camera. The two resultant projections may then be enlarged or reduced and changed in separation. This may be accomplished with prints or by projecting onto a screen, such projection being only a magnifying device. They are then reprojected, in the geometric sense, using two new centers of projection, the eyes, to form an image determined by the intersections of corresponding rays of projection.

It is our purpose to develop a method of determining the plan view of the resultant image, having given the plan view of the object and the conditions of photographing, projecting and viewing. We will show that it is possible to substitute for the complicated system above a single projection plane and center of projection and obtain on the projection plane the stereo image plan directly from the object plan—that is, that the image plan is always in projective relationship to the object plan and may be obtained graphically by a single perspective projection.

We have the following variables:

(1) The distance between the camera lenses $=e_c$.

(2) The distance from the camera lens to the plate $=f$. This depends, of course, on the distance for which the camera is focused. Except for close work it is substantially equal to the focal length of the lenses. It will be called the focal length throughout this article. The correction should be made where necessary.

(3) The enlargement or reduction of the two resultant images either as a print or projected on a screen $=M$.

(4) The change in separation between the two images. The separation on the plate of the two images of a single space point is a function of the distance of this point from the plane of the lenses. The images of every point in any plane parallel to this plane have the same separation. Thus it is possible and helpful to express the separation in the resultant images in terms of the distance to the plane of points for which the separation is to be zero after any change in separation has been made, that is, the distance from the lenses to the plane, the two images of which are to be superimposed in the final stereograph. Such a plane always exists theoretically, though it may be at a negative distance —in back of the camera—when the images are to be moved apart. This distance $=d_0$. ($d_0=f$ when no shift occurs.)

(5) The human interocular $=e$.

(6) The viewing distance from the eyes to the stereograph (whether a print or a projection on a screen) $=V$.

We shall assume that the observer shall be so placed that his center line of vision with respect to the stereograph shall be coincident with the previous position of the axis of the camera, as this is the proper and normal viewing position. Distortions caused by a variation from this line of sight will not be considered here.

We shall consider an object plan and the resultant image plan cut by the plane containing the lens centers and the axis of the camera—in effect a top view of the entire system.

Figure 1 shows the conditions of photographing any point, X, in the object plan. d_x=distance from X to plane of lenses. O=point in plane of superposition in final stereograph. d_0=distance from O to plane of lenses. W_0=distance on plate between two images of O=change in separation between taking and viewing of two halves of stereograph. W_x=distance on plate between two images of X. S_x=distance between two images of X after change in separation but before magnification.

For convenience the plate of the camera may be considered at a distance of f in front of the camera lenses, rather than behind it, as the print in viewing is effectively placed in this position, the images in the two positions being congruent.

We have immediately:

$$S_x = W_x - W_0$$

from similar triangles

$$W_x = \frac{e_c(d_x - f)}{d_x} \quad \text{and} \quad W_0 = \frac{e_c(d_0 - f)}{d_0},$$

whence

$$S_x = e_c f\left(\frac{1}{d_0} - \frac{1}{d_x}\right). \tag{1}$$

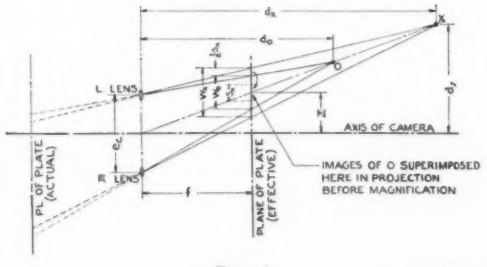
L. LENS
R. LENS
AXIS OF CAMERA
PL. OF PLATE (ACTUAL)
PLANE OF PLATE (EFFECTIVE)
IMAGES OF O SUPERIMPOSED HERE IN PROJECTION BEFORE MAGNIFICATION

FIG. 1.

Figure 2 shows the viewing conditions after magnification. (The order of change in separation and magnification is immaterial.) The plane of the stereograph and the central line of sight are taken as the Y and X axes of coordinates, respectively. M=magnification of stereograph over plate. V=viewing distance, i.e.,distance of eyes from plane of stereograph. I=stereo image of X. I_x=distance of I from plane of stereograph.

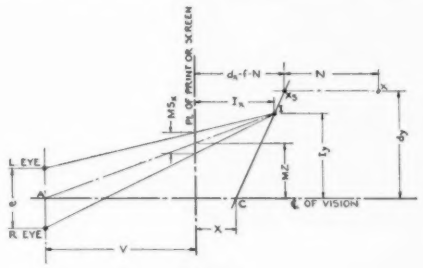

FIG. 2.

From similar triangles:

$$\frac{I_x}{I_x + V} = \frac{MS_x}{e},$$

whence

$$I_x = \frac{VMS_x}{e - MS_x}. \tag{2}$$

Substituting from (1) and (2) and simplifying

$$I_x = \frac{e_c MfV(d_x - d_0)}{ed_x d_0 - e_c Mf(d_x - d_0)}. \tag{3}$$

This is the basic formula for determining the depth of any point in a stereoscopic image.

We can now proceed to consider the graphic relationship between the object plan and its resultant image plan. It will be shown later that a difference between the distance between camera lenses, e_c, and the human interocular, e, may be treated entirely as a matter of scale. We need at the moment, therefore, consider only cases in which $e_c = e$.

In these cases formula (3) becomes:

$$I_x = \frac{MfV(d_x - d_0)}{d_x d_0 - Mf(d_x - d_0)}. \tag{3a}$$

If the object plan and the image plan are in projective relationship, the center of projection

must lie on the X axis because of considerations of symmetry. As will be seen, they are not immediately in projective relationship but may be so placed by shifting the object plan parallel to the X axis, a distance equal to N. It is necessary to determine this distance. From the coordinates of $I(I_x, I_y)$ and of $X_s(d_x-f-N, dy)$ we derive the equation of the line through these

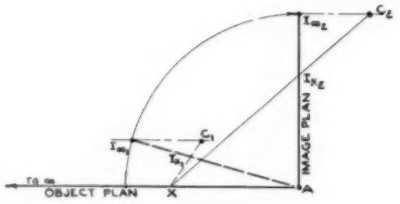

FIG. 3.

two points. This equation is:

$$\frac{y-I_y}{X-I_x}=\frac{I_y-d_y}{I_x-(d_x-f-N)}. \qquad (a)$$

If there is a value for N which places the object and image in projective relationship the center of projection, since it lies on the X axis, must be the intersection of the above line from X_s through I and the X axis, that is the point in this line where $y=0$.

Placing $y=0$ in (a) and solving for X we obtain

$$X=\frac{I_y(f+N)+I_xd_y-I_yd_x}{d_y-I_y} \qquad (4)$$

from similar triangles in Fig. 1 =

$$Z=\frac{fd_y}{d_x}$$

and from similar triangles in Fig. 2 =

$$Z=\frac{I_yV}{M(I_x+V)},$$

eliminating Z and solving for d_y

$$d_y=\frac{I_yVd_x}{Mf(I_x+V)}. \qquad (b)$$

If we now substitute into Eq. (4) the value of I_x from Eq. (3a) and of d_y from Eq. (b) we may reduce the resultant equation to the following form—

$$X=\frac{Mfd_0[N-(V-f)]}{(d_0-Mf)d_x}+\frac{Mf(V-d_0)}{d_0-Mf}. \qquad (5)$$

Now the value of N which will place the object and image in projective relationship must be such that X in Eq. (5) will remain a constant for all positions of the line—that is, that the lines from all points in the object through their images will meet at a common point, the desired center of projection.

Since the second term in Eq. (5) is a constant any value of N which would make the first term vanish would fulfill the above condition. Obviously such a value is $N=V-f$ whence

$$X=\frac{Mf(V-d_0)}{d_0-Mf}.$$

Consequently if the ground plan is shifted a distance, $V-f$, it comes into projective relationship with the image plan, the single center of projection being at a distance from the plate of

$$\frac{Mf(V-d_0)}{d_0-Mf}.$$

We now have a projective system for obtaining the image plan from the object plan, However, the object plan, the image plan and the center of projection all lie in the same plane which makes the image plan graphically indeterminate from the object plan as the points of intersection of the rays from the object plan with the plane of the image plan cannot be obtained. It is consequently necessary, and also convenient, to rotate the projection plane containing the image plan through 90° and relocate the center of projection accordingly. This reduces the system to a standard perspective projection and makes the image plan directly obtainable from the object plan by any of the common perspective methods.

If the object plan is considered to extend to the camera lenses it can be shown geometrically that the images of all points on the line connecting the optical centers of the lenses will lie on the line in the image plan connecting the eyes. As the geometrical proof would require

considerable space the same result can be obtained by substituting zero for d_x in Eq. (3a) whence $I_0 = -V$.

Since this line in the object and its image are a distance apart equal to $V-f$ they will be coincident after the shift of N of the object. Hence the image plan may be rotated about this line.

Though this is a common perspective procedure it will be well to include the explanation here.

Figure 3 shows a side elevation of the object plan, image plan and center of projection just after the start of rotation ($I_{\infty 1}$, C_1, I_{x1}) and after 90° of rotation ($I_{\infty 2}$, C_2, I_{x2}). It can be seen from similar triangles that so long as the line $I_\infty C$ is maintained constant in length and parallel to the object plan, that with C as a center of projection, the projection of any point in the object plan onto the image plan will be at a fixed point, that is, the distance $I_{x1}A$ will always equal the distance $I_{x2}A$.

Now setting $d_x = \infty$ formula (3) may be reduced to

$$I_\infty = \frac{VMf}{d_0 - Mf},$$

whence

$$I_\infty C = \frac{VMf}{d_0 - Mf} - \frac{Mf(V-d_0)}{d_0 - Mf}$$

or

$$C_y = \frac{Mfd_0}{d_0 - Mf}. \qquad (c)$$

This is the distance of the center of projection from the rotated projection plane. The distance of this center above the plane of the object plan will be I_∞ or

$$C_x = \frac{VMf}{d_0 - Mf}. \qquad (d)$$

It now only remains to develop a treatment for the case $e_c \neq e$.

The stereoscopic projections of any object on a plate are exactly the same shape and size as those of a similar larger object farther away with a proportionally increased interocular. This is shown in Fig. 4. Consequently by a change in scale we can adjust e_c to be equal to e without changing the two projections but only the distance between them.

This is obviously accomplished by using the scale e/e_c and constructing the object plan with this scale starting from the plane of the lenses as a zero line, having the plane of the plate however, at its true distance. This affects our formulas only in changing the value of d_0 to d_1 such that $d_1 = ed_0/e_c$. We then use this value of d_1 for d_0 in formula (c) and (d) to locate the center of projection. These formulas then become

$$C_y = \frac{Mfd_1}{d_1 - Mf} \quad (b) \qquad C_x = \frac{VMf}{d_1 - Mf}. \quad (7)$$

We now have an extremely simple method of obtaining the image plan directly from the object plan by a single perspective projection as shown pictorially in Fig. 5.

It is to be remembered that this projection is not a perspective of the image plan but the image plan itself.

It can also be seen that the image plan can be obtained at any desired scale simply by shifting the projection plane parallel to itself without shifting the center of projection.

Results

Conditions for orthostereoscopy and true shape

For our purposes an orthostereoscopic image is one in which the image plan is congruent to

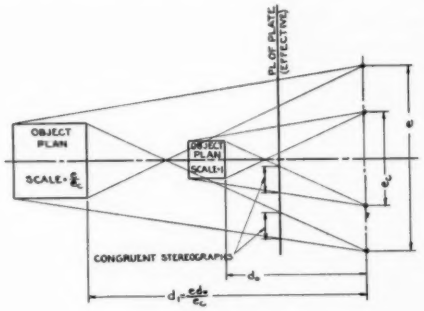

FIG. 4.

the object plan. It is also possible to have images similar to their objects but of different sizes.

It will be noticed from Fig. 5 that if the center of projection is at infinity in a direction such that the projection rays make an angle of 45° with both planes, the image plan will then be

congruent to the object plan at the scale to which the object plan has been drawn. Thus when $C_x = C_y = \infty$ an orthostereoscopic view is obtained when the scale of the object plan is unity, and a true shaped view when this scale is other than unity,—that is for cases in which $e_c \neq e$.

Now from (c) and (d) $C_x = C_y = \infty$ only when $d_0 = Mf = V$. This is the standard parallel projection system in which the two views are projected parallel, the proper viewing distance being the focal length times the magnification and in which the plane fused on the screen was at a distance from the camera equal to the viewing distance.

If $e_c \neq e$ we get from (6) and (7)

$$d_1 = Mf = V \quad \text{or} \quad \frac{ed_0}{e_1} = Mf = V.$$

This is the standard variable interocular system in which distance between camera lenses is so chosen that the near object in the scene will fall in the plane of the screen when projected parallel, the resultant shape of the image being similar to the shape of the object but changed in size by the ratio e/e_c, the proper viewing distance being correspondingly increased.

A few studies of image shapes will show the usefulness of this tool. One such study[1] was made to show the image shape of superimposed stereographs of small size. Under the conditions of taking and viewing used the distance from the camera lenses to infinity was compressed into $1\frac{1}{2}$ inches of depth. Since these Vectographs are

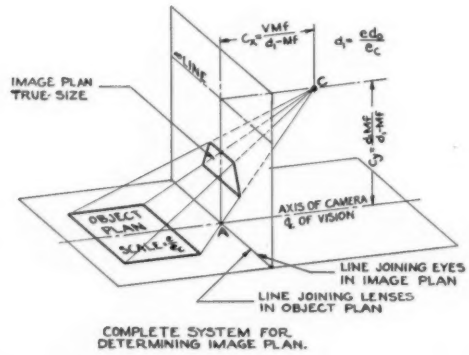
IMAGE PLAN TRUE SIZE
LINE
OBJECT PLAN
AXIS OF CAMERA & OF VISION
LINE JOINING EYES IN IMAGE PLAN
LINE JOINING LENSES IN OBJECT PLAN
COMPLETE SYSTEM FOR DETERMINING IMAGE PLAN.

FIG. 5.

[1] Edwin H. Land, J. Opt. Soc. Am. **30**, 230 (1940).

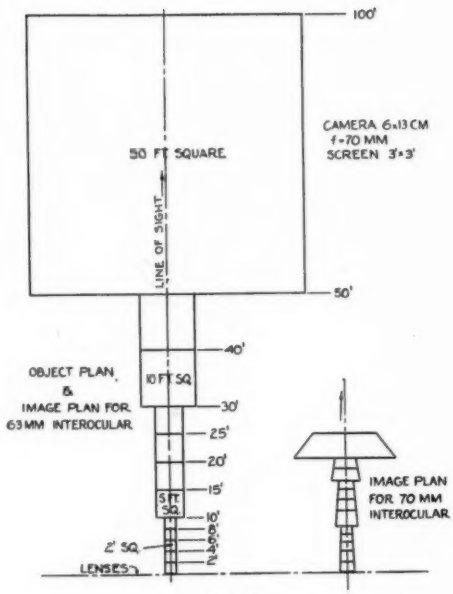

FIG. 6.

extremely pleasing in effect and do not appear overdistorted, the necessary conclusion is that a great deal of distortion is permissible in small stereographs in the direction of reduction of depth.

Cardboarding

Many observers of stereographs complain of a "cardboard" effect, that is, that though the objects appear to lie in planes at different depths, they themselves appear flat. This has been ascribed to a number of different causes such as lack of color, psychological appreciation of the fact that a stereograph is in reality flat, etc.

Figure 6, shows an object plan composed of squares increasing in size with distance and its image plan to 100 ft. of depth of the object plan for a scene taken by a standard stereo 6×13-cm camera, 70-mm focal length, and projected on a 3-ft.×3-ft. screen, the conditions so set as to yield an orthostereoscopic view for an individual of average interocular, 63 mm, but actually viewed by an individual of large interocular, 70 mm.

It is apparent that the squares in the object plan have become trapezoids in the image plan with decreased depth and that this loss of depth

becomes more pronounced as the distance from the camera increases. If the two halves of the stereograph are shifted closer together than the ideal, as is almost always the case in small scale projection in order to make fusion easier, this effect is much more highly exaggerated. It is thus apparent that the "cardboard" effect is a real one and not a subjective one. The problem of eliminating it can consequently be approached from an optical standpoint. Obviously it would be eliminated if projection conditions were set for the widest human interocular. This would cause a slight divergence for distant points and an increase in depth for near points for individuals of small interocular. The question of introduction of eye-strain by such a procedure needs investigation.

It is obvious that problems of eye-strain and psychological interpretation may be studied in the laboratory with the object of determining the limits of change in image shapes in various directions which are permissible in practical viewing without causing uncomfortable eye-strain or displeasing distortions. Ideal conditions are not to be expected in practical work and it is therefore valuable to have a single method for obtaining image shapes so that permissible variation from the ideal may be experimentally determined.

I want to acknowledge the great help received from Professor Earle F. Watts of the Section of Graphics of the Massachusetts Institute of Technology in developing the theory described in this paper.

Construction and Test of a Goniophotometer

PARRY MOON AND JACQUES LAURENCE
Electrical Engineering Department, Massachusetts Institute of Technology, Cambridge, Massachusetts
(Received October 18, 1940)

1. INTRODUCTION

THERE is a growing need for more information on the angular distribution of reflected light from surfaces. An investigation of the subject was begun several years ago in the Illuminating Engineering Laboratories of the Massachusetts Institute of Technology, and a photoelectric goniophotometer was built for this research. The present paper describes the goniophotometer and presents some of the experimental results obtained in testing the adequacy of the instrument. Future papers will give data on the reflection characteristics of various materials.

2. THE GONIOPHOTOMETER

Essentially, a goniophotometer is a very simple piece of apparatus consisting of a lamp, a device for holding and rotating the sample, and a light-sensitive detector arranged so that it can be placed in known angular relation to the sample. If a large number of routine measurements are to be made on similar materials, there is an advantage in designing the goniophotometer particularly for these materials and in building all necessary light shields and apertures permanently into the instrument. On the other hand, there are advantages in leaving the instrument in a very flexible form, as was done in the present case. In this way, light sources, lens systems, detectors, filters, and apertures can be changed, and the best conditions can be found for testing each kind of surface. Also check runs can be made under completely different conditions to insure that the results are actual characteristics of the surface being tested and not characteristics of the goniophotometer.

Figures 1 and 2 show the construction of the chassis, while Fig. 3 gives the appearance of the table to which the sample is attached. A heavy iron casting (Fig. 1) is bolted to a bed plate. A similar casting (on the right) is pivoted about a vertical axis, with ball-bearing supports. Screwed to these castings are two Zeiss "optical benches," each one meter long. On these bars can be placed any number of Zeiss riders equipped with lenses, shields, and other apparatus. A steel scale is attached to the bottom of each bar and suitable pointers are fastened to the riders so that their exact positions are easily determined.

A steel table 203 mm in diameter is mounted on ball bearings on the same shaft that supports the moving arm. The sample to be tested is placed vertically on this table, with its front surface accurately set at a line scribed across the

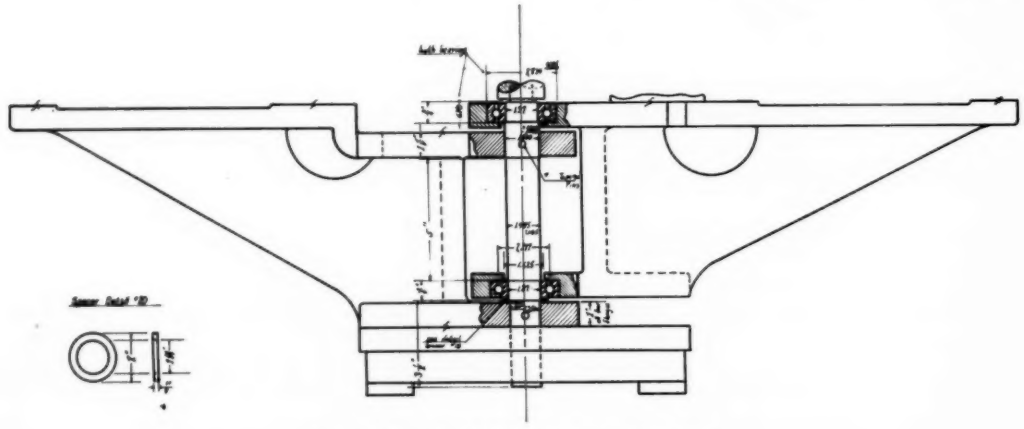

FIG. 1. Elevation of the goniophotometer chassis.

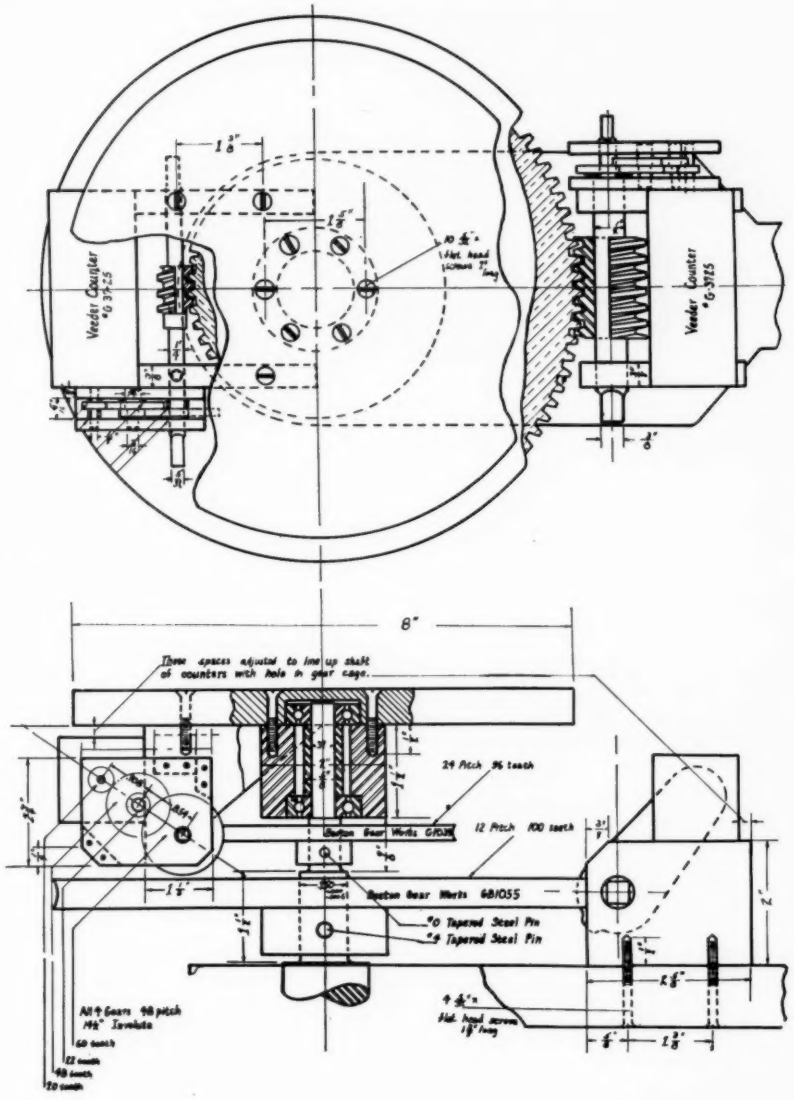

FIG. 2. The table.

top of the table. The sample is clamped against a vertical support (Fig. 3). The large opening in the support allows transmission measurements to be made. To date, all measurements have been made with a vertical sample; and the data apply, therefore, only to the plane which includes the source, the detector, and the normal to the surface. If desired, however, the vertical sample support may be replaced by a tilting support to give data in other planes.

Pinned to the fixed vertical shaft are two bronze worm wheels, and movements of the arm and of the table are effected by means of hardened steel worms engaging with these worm wheels. The worms are geared to Veeder counters which read angles directly in radians. The smallest reading is 0.001 radian, and the total backlash in the gear train amounts to less than this minimum reading. The table is turned by means of a knurled knob, but the moving arm is driven by

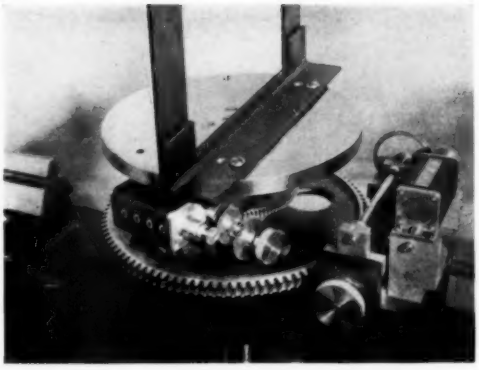

FIG. 3. The goniophotometer, showing gears and counters.

a small synchronous motor mounted on the side of the right-hand casting. This arrangement will allow the goniophotometer to be provided with automatic recording if this change seems advisable. Visual measurements can also be made, if desired, by attaching a brightness meter of the visual comparison type to one of the arms.

A 500-watt, 120-volt projection lamp is mounted on one of the Zeiss riders and is provided with a housing to eliminate stray light. The lamp is ordinarily used on the stationary arm at approximately one meter from the sample. A spherical mirror is provided, as well as a number of lenses. The lamp is operated from a storage battery and the voltage at the socket is kept constant to within ± 0.1 volt. The voltage is read by means of a laboratory-standard voltmeter.

The detector is mounted on the moving arm. Several kinds of barrier-layer cells have been tried, but most of the tests have been made with a No. 782 Electrocell. The cell is usually placed at the end of a light-tight housing which reaches almost to the sample and which is provided with a removable entrance aperture and fixed internal baffles. This arrangement is found very effective in eliminating stray light.

For linear response and for a minimum of fatigue, the barrier-layer cell must be operated under short circuit conditions. This is accomplished by using a compensating circuit, the schematic diagram for which is shown in Fig. 4. A battery and a drop wire introduce an additional current in the same direction as that produced by the barrier-layer cell. The value of R_1 is varied until the galvanometer G reads zero, when the cell is operating under short circuit conditions with a short circuit current i_2. Evidently,

$$i_2 = i_1 \frac{R_1}{R_1 + R_2} \cong i_1 \frac{R_1}{R_2}. \qquad (1)$$

The readings R_1 of a calibrated drop wire will be directly proportional to the short circuit photoelectric current i_2, provided $i_1 = \text{const.}$ and $R_2 \gg R_1$.

The actual arrangement of the compensating circuit is shown in Fig. 5. A 3-volt battery provides a current of 3×10^{-3} ampere through a set of General Radio decade resistors adjusted to 0.1 percent (except in the lowest decades). Two decades with one-ohm steps are mounted back-to-back and attached to one shaft. The same arrangement is used with the ten-ohm decades, so the battery current in the resistors remains constant, irrespective of the position of the dials. A galvanometer shunt is included in the case that houses the compensating circuit.

A Leeds and Northrup Type R galvanometer is used as a null detector. It is mounted on a Julius suspension, and with a scale distance of 3 meters gives 1 mm deflection with 10^{-9} ampere and has a critical damping resistance of 2200 ohms. The

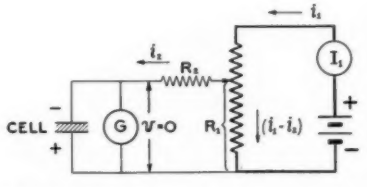

FIG. 4. Schematic diagram of the compensating circuit for a barrier-layer cell.

actual cell current corresponding to a reading of 1 on the lowest dial is, according to Eq. (1),

$$i_2 = 3 \times 10^{-9} \text{ amp.},$$

which gives a galvanometer deflection of approximately 3 mm. Vibration is entirely negligible, so the position of the light spot of the galvanometer can be read to 1 mm, corresponding to a luminous flux on the cell of approximately 2×10^{-6} lumen.

3. Accuracy

A factor that limits the accuracy of results obtained with the goniophotometer is fatigue in the barrier-layer cell. Figure 6 shows how the current decreases with time when an Electrocell is used with the compensating circuit of Fig. 5. The cell was completely dark adapted and was then exposed to steady light at $t=0$. Ordinarily the error caused by cell fatigue will be less than ± 1 percent because the illumination of the cell is usually lower than that in Fig. 6 and no readings are taken until the cell has been exposed to light for several minutes. Nevertheless, fatigue is found to limit the accuracy of the measurements. Higher illuminations than those used in Fig. 6 can be measured by employing a higher battery voltage in the compensating circuit, but this change is never made because of the great increase in fatigue at higher illuminations. It is also found that colored light usually increases fatigue in a marked manner.

Experience has shown that the maximum errors to be expected in using the instrument are approximately as follows:

Fatigue, barrier-layer cell	±1.0 percent
Departure from linearity, barrier-layer cell	±0.5
Variation in lamp voltage	±0.4
Random fluctuations in cp of lamp	±0.1
Variation in compensating current	±0.1
Error in distance measurement	±0.2
Stray light	0.0

The effect of variations in lamp voltage can be reduced to a negligible value by using a potentiometer for reading the lamp voltage; but there is little incentive for making this change, in view of the large effect of fatigue. Higher accuracy could be obtained by replacing the barrier-layer cell by a photoelectric flicker photometer,[1] but the present arrangement is sufficiently accurate for most engineering requirements.

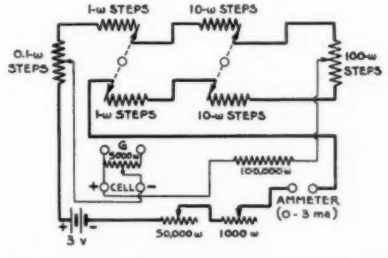

Fig. 5. Actual wiring diagram of the compensating circuit.

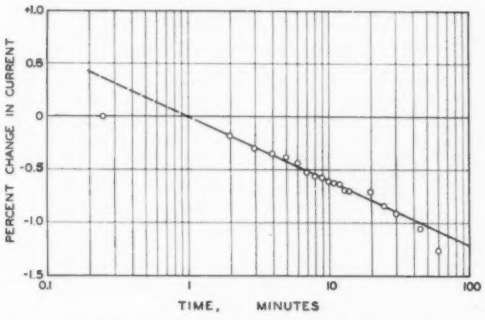

Fig. 6. Fatigue of barrier-layer cell. Dark-adapted cell exposed to constant illumination at $t=0$.

Beyond the items listed above, there are a number of sources of serious error that may enter unless suitable precautions are taken.[2] It is never possible to get perfectly unidirectional illumination of the sample or to obtain an absolutely uniform brightness over the field of view of the photometer. The best check on errors caused by these factors is an experimental one, the aperture size being decreased until further reduction causes no appreciable change in the apparent reflection factor.

The testing of selective materials requires a receptor which responds in accordance with the C.I.E. standard lamprosity (visibility) function. Proper green filters have been developed for the selenium barrier-layer cell, and their use insures that color will not produce an objectionable error. If nonselective materials are tested (as in the present research), the green filter can be omitted with consequent increase in response.

4. Specular Reflection

Specular reflection and diffuse reflection are subject to entirely different laws and must be measured with different arrangements. The *spec-*

[1] P. Moon and D. P. Severance, "The design of photoelectric flicker photometers," I. E. S. Trans. **34**, 801 (1939); M.I.T., Elect. Eng. Dept. Contribution No. 168 (1939).

[2] H. J. McNicholas, "Absolute methods in reflectometry," Bur. Stand. J. Research **1**, 29 (1928); R. S. Hunter, "Methods of determining gloss," J. Research Nat. Bur. Stand. **18**, 19 (1937); D. B. Judd, "Note on the choice of apertures in the definitions of specular gloss and contrast gloss," J. Opt. Soc. Am. **27**, 225 (1937).

ular reflection factor of a specular surface may be defined as

$$\rho_s(\theta)=\frac{B_i(\theta)}{B_s}, \tag{2}$$

where $B_i(\theta)$ = brightness (candle m^{-2}) of image and B_s = brightness of source.

Equation (2) can be written also as

$$\rho_s(\theta)=\frac{I_i(\theta)}{I_s}, \tag{2a}$$

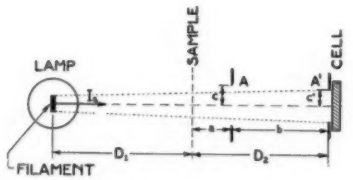

FIG. 7. Arrangement for the measurement of specular reflection.

where $I_i(\theta)$ = apparent intensity (candles) of the image of a source whose dimensions are small compared with the distances under consideration, and I_s = intensity of actual source.

The *diffuse reflection factor* of a diffusing surface is defined as

$$\rho_d(\theta_1, \theta_2)=\frac{\pi B_r(\theta_1, \theta_2)}{E(\theta_1)}, \tag{3}$$

where $E(\theta_1)$ = illumination (lumen m^{-2}) of sample; $B_r(\theta_1, \theta_2)$ = brightness (candle m^{-2}) of sample, illuminated at angle θ_1 and viewed at θ_2; θ_1 = angle of incidence; θ_2 = angle of view.

Other diffuse reflection factors correspond to the illumination through a large solid angle, but they will not be considered here.[2]

For the measurement of the reflection factor ρ_s of a *purely specular surface*, a satisfactory arrangement is shown in Fig. 7. The movable arm is first set at π radians, with no sample, so that the light from the lamp falls directly on the cell. Apertures are inserted of such size that every point of the lamp filament illuminates every point of the aperture A'. A neutral filter is introduced at the cell to bring the readings within the range of the compensating circuit; and a reading is taken which calibrates the instrument for specular reflection. A sample is now inserted at the distance D_1 from the lamp, and the movable arm is brought into a position where reflected light from the sample reaches the cell. If the specular reflection factor of the sample be 100 percent, with no diffuse reflection, the reading will be identical with that obtained in the calibrating position; but with actual samples the readings will always be less than the calibration reading. For calibration, the luminous flux to the cell is

$$F_c=\frac{I_s A'}{(D_1+D_2)^2} \text{ (lumen)}, \tag{4}$$

where A' = area of aperture at cell (m^2), I_s = intensity of source (candles), along axis of goniophotometer, D_1, D_2 = distances (m).

With the sample in position, the luminous flux at the cell is, by Eq. (2a),

$$F_r=\frac{\rho_s I_s A'}{(D_1+D_2)^2} \tag{5}$$

and

$$\rho_s=F_r/F_c. \tag{6}$$

If linear cell response is assumed,

$$\frac{F_r}{F_c}=\frac{k_r i_r}{k_c i_c}, \tag{7}$$

where i_r and i_c are photoelectric currents and k_r and k_c are constants. If the sample is a nonselective reflector and if the same portion of the cell surface is uniformly illuminated in both cases, $k_r=k_c$, and the specular reflection factor is

$$\rho_s(\theta)=i_r(\theta)/i_c. \tag{6a}$$

Thus for specular reflection, the goniophotometer is an absolute instrument and the specular reflection factor is equal to the ratio of two photoelectric currents.

5. Diffuse Reflection

For measuring the reflection factor of a *diffuse sample*, one may use the same arrangement (Fig. 7), provided measurements are taken only with small values of θ_2 and provided there is sufficient reflected light from the sample to give a satisfactory reading. If readings are to be taken at large angles from the normal to the test surface, however, smaller apertures must be used. Figure

8 shows the arrangement. The lamp filament provides essentially uniform illumination over a distance w measured perpendicular to the axis of the instrument.

Evidently the apertures c and c' must be sufficiently small so that rays reaching the cell do not originate from parts of the sample beyond Q. Let β be the maximum deviation of rays from normal incidence on the cell. Consider the triangle with angle β, opposite side ($w \sec \theta_1$), and adjacent side ($a+c \cot \beta$). Using the fact that

$$\tan \beta = \frac{c+c'}{b}$$

one obtains

$$c^2(D_2^2-M^2)+2c[c'(aD_2-M^2)-bKD_2] + [c'^2(a^2-M^2)-2abc'K+K^2b^2]=0$$

or

$$c = \frac{c'(M^2-aD_2)+bKD_2 \pm bM(c'+K)}{D_2^2-M^2}, \quad (8)$$

where $D_2=a+b$; $M=w \sec \theta_1 \sin \theta_2$; $K=w \sec \theta_1 \times \cos \theta_2$.

The $\pm$ sign refers to the two extreme rays. Only the one that gives the smaller value of c is of interest, so the width c for a given width c' should be

$$c \leqq \frac{c'(M^2-bM-aD_2)+bK(D_2-M)}{D_2^2-M}. \quad (8a)$$

For the special case of equal width of openings, Eq. (8a) becomes

$$c \leqq \frac{bK(D_2-M)}{D_2^2+aD_2-2M^2+bM}. \quad (8b)$$

The obvious disadvantage in using small apertures is the reduction in photoelectric current. If the sample has a uniform brightness B_r over the angle $\pm\beta$ (Fig. 8), and if the apertures are small compared with the distance b, the illumination at the exit aperture A′ is

$$E = B_r \frac{A}{b^2}$$

and the flux to the cell is

$$F = B_r \frac{AA'}{b^2} \text{ (lumen)}, \quad (9)$$

where B_r = brightness of sample (candle m^{-2}), A, A' = areas of apertures (m^2).

For circular apertures,

$$F = B_r \left(\frac{\pi cc'}{b}\right)^2. \quad (9a)$$

For slits of semiheight h, h' and semiwidth, c, c',

$$F = B_r \frac{16hh'cc'}{b^2}. \quad (9b)$$

It can be shown that for a given angle β, the largest flux is obtained with slits of equal width, $c=c'$. It is also easy to prove that with the dimensions used in the M.I.T. goniophotometer, the error introduced by the use of the inverse square relation in Eq. (9) is less than 0.1 percent.

Having decided on the slit-width by consideration of Eq. (8a), one can next find if the resulting photoelectric current will be sufficient. By the

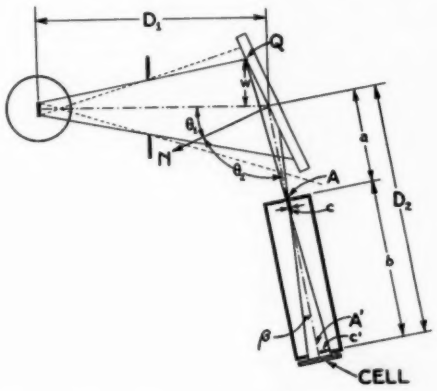

FIG. 8. Arrangement for the measurement of diffuse reflection.

definition of diffuse reflection factor, Eq. (3),

$$B_r = \rho_d \frac{I_s \cos \theta_1}{\pi D_1^2}.$$

Substitution of this expression in Eq. (9b) gives, for equal slits of semiwidth c,

$$F = \rho_d \frac{16h^2c^2I_s \cos \theta_1}{\pi b^2 D_1^2}. \quad (10)$$

For a given cell and a given spectral distribution of the irradiation,

$$\frac{i}{F}=s=\text{const.}$$

Let $i_{\min}$ be the minimum current that will allow good readings—say the current equivalent to a dial reading of 100. Then the semiwidth of the slit must be at least

$$c\geqq\frac{1}{4}\left(\frac{\pi i_{\min}}{s\rho_d I_s\cos\theta_1}\right)^{\frac{1}{2}}\frac{bD_1}{h}. \tag{11}$$

If the numerical values obtained from Eqs. (8a) and (11) are consistent, everything is satisfactory. If not, shorter spacings may be used or a lens system may be placed between the lamp and the sample.

The goniophotometer can be calibrated for diffuse reflection factor ρ_d by replacing the sample by a matt plate having a known reflection factor,

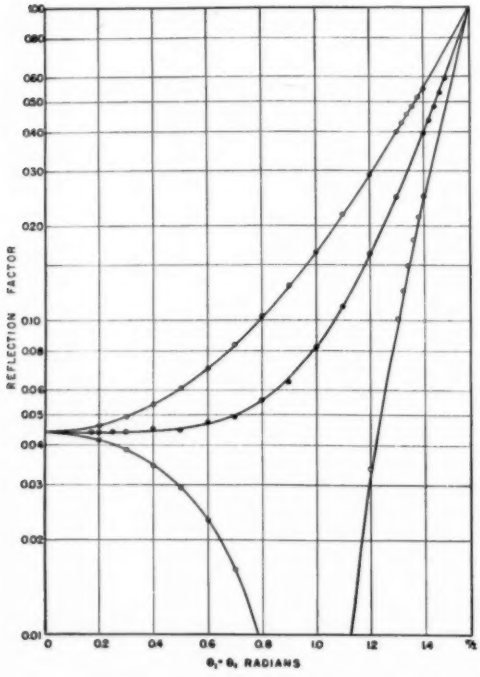

FIG. 9. Specular reflection factor of polished black glass ($n_D=1.53$). ○ Polarized light, one run. ● Natural light, average of 2 runs. — Theoretical curve, according to Fresnel formula.

or absolute measurements can be made. The method for absolute measurements will now be described. The arrangement of Fig. 7 is used, with large apertures so that every part of the filament illuminates every part of the area A'. The flux to the cell is

$$F_c=\frac{I_s A'}{(D_1+D_2)^2}\quad\text{(lumen)}. \tag{4}$$

The sample is now introduced and the moving arm swung so that θ_2 is small. The illumination of the sample is

$$E=\frac{I_s}{{D_1}^2}\cos\theta_1\quad\text{(lumen } m^{-2}) \tag{12}$$

and from Eqs. (3) and (9a)

$$B(\theta_1,\theta_2)=\frac{\rho_d}{\pi}\frac{I_s}{{D_1}^2}\cos\theta_1,$$

$$F_r=\frac{\pi\rho_d I_s c^2 c'^2}{b^2{D_1}^2}\cos\theta_1. \tag{13}$$

Therefore,

$$\frac{F_r}{F_c}=\frac{\rho_d c^2}{b^2}\left(\frac{D_1+D_2}{D_1}\right)^2\cos\theta_1$$

or

$$\rho_d(\theta_1,\theta_2)=\left(\frac{b}{c}\right)^2\left(\frac{D_1}{D_1+D_2}\right)^2\left(\frac{F_r}{F_c}\right)\sec\theta_1. \tag{14}$$

If the sample is nonselective, or if a suitable color correcting filter is used in the cell, Eq. (7) applies with $k_1=k_2$, and the ratio of fluxes in Eq. (14) can be replaced by the ratio of currents. Thus the goniophotometer is an absolute instrument for the measurement of diffuse reflection factor. If measurements are to be made at large values of θ_2, a secondary calibration is easily effected by taking two readings at small θ_2, one reading with the large circular apertures of Fig. 7, and the other with the narrow slits to be used in the subsequent measurements.

For polished samples having *both specular and diffuse reflection*, a separation of the two components is most easily obtained by measurements at the angle of regular reflection ($\theta_1=\theta_2$) and at some distance from this angle. The curve of ρ_d *vs.* θ_2 for constant θ_1 is then extrapolated to

$\theta_2=\theta_1$, and this extrapolated value is subtracted from the reading at $\theta_1=\theta_2$ to give ρ_s. With proper arrangements, the diffuse component may be made negligible in comparison with the specular component so that the subtraction can be omitted.

The flux to the cell, caused by the specular component, is

$$F_s=\frac{\rho_s I_s A'}{(D_1+D_2)^2}.$$

For the diffuse component (and circular apertures),

$$F_d=\frac{\rho_d \pi c^2 c'^2 I_s \cos\theta_1}{b^2 D_1^2}.$$

Thus,

$$\frac{F_d}{F_s}=\frac{\rho_d}{\rho_s}\left(\frac{c}{b}\right)^2\left(\frac{D_1+D_2}{D_1}\right)^2\cos\theta_1. \qquad (15)$$

For values of $D_1=D_2$, $\cos\theta_1=1$, Eq. (15) becomes

$$\frac{c}{b}\leqq\frac{1}{2}\left(\zeta\frac{\rho_s}{\rho_d}\right)^{\frac{1}{2}}, \qquad (15a)$$

where ζ = allowable error caused by presence of diffuse component (expressed as fraction of specular component). For example, if $\zeta=0.01$, $\rho_s=\rho_d$,

$$\frac{c}{b}\leqq 0.05.$$

For $\zeta=0.01$, $\rho_d=0.90$, $\rho_s=0.04$,

$$\frac{c}{b}\leqq 0.01.$$

Therefore, by making the aperture small in comparison with the distance b, the effect of the diffuse component can be greatly reduced.

6. Results

An example of the results obtained in measuring *specular reflection factor* is shown in Fig. 9. A polished black-glass sample (Pittsburgh Black Carrara) was used. The index of refraction for sodium light was measured and found to be $n_D=1.53$. Measurements were then made of the specular reflection factor for various values of angle ($\theta_1=\theta_2$), using unmodified light from the incandescent lamp. For the measurement with plane-polarized light, a Polaroid disk was used in the incident beam. Since Polaroid does not polarize at either end of the visible spectrum, however, a filter was introduced to eliminate radiant energy at wave-lengths less than 0.49μ and greater than 0.65μ. This filter consisted of a Schott GG-11 yellow filter (2 mm) and 50 mm of an 0.8-percent solution of cupric chloride in distilled water.

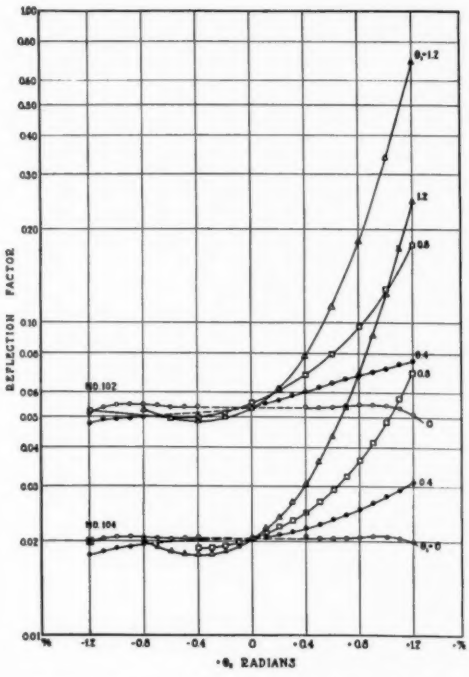

FIG. 10. Diffuse reflection factor of gray cloths.

The curves of Fig. 9 were calculated[3] by use of the Fresnel formula, while the points were obtained with the goniophotometer. The agreement between the two is as good as can be expected with the present set-up.

For the measurement of *matt samples* at large angles, a narrow slit must be used and a lens system is introduced into the incident beam to give a high illumination of the sample. Figure 10 gives some results obtained on samples of gray worsteds used for men's suits (Cornwall Mills, Incorporated, Holyoke, Massachusetts). With normal incidence ($\theta_1=0$), the diffuse reflection factor is seen to be almost independent of the

[3] Parry Moon, "A table of Fresnel reflection," J. Math. Phys. **19**, 1 (1940).

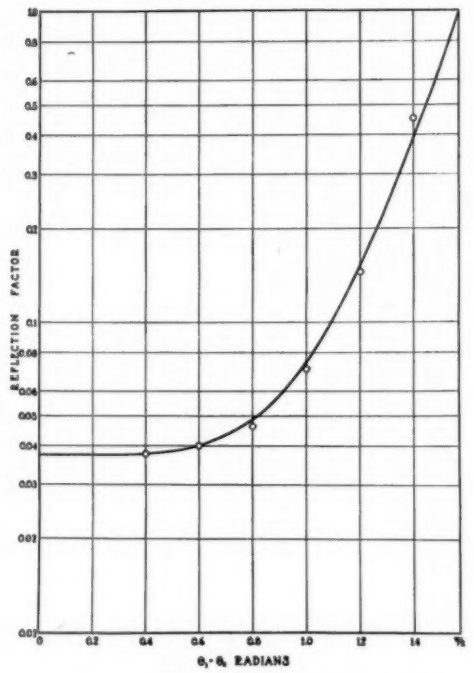

FIG. 11. Specular reflection factor of polished white opal glass ($n_D = 1.48$). ○ Experimental results, average of 2 runs. — Theoretical curve, according to Fresnel formula.

angle of view between -1.2 and $+1.2$ radians. As the angle of incidence is increased, however, the curves dip slightly at negative angles and rise in a very marked manner for $\theta_2 > 0$. Thus the samples are by no means as thoroughly diffusing as would be thought from casual inspection or from consideration of the curve for $\theta_1 = 0$. It is interesting to note that there is no peak in the curves such as would be obtained if any specular reflection were present.

The only indication of the accuracy of the curves was obtained by measurement of the samples with the Hardy color analyzer. The spectral curves were nearly flat, with a slight dip in the violet and a rise in the red end of the spectrum; so variations in the spectral distribution of the incident radiation are unimportant. The ordinates were multiplied by 0.980 to compensate for the reflection factor of the magnesium oxide comparison surface of the color analyzer. The results are given in Table I. The values obtained with the goniophotometer are for $\theta_1 = 0$, $-1.2 < \theta_2 < +1.2$. The color analyzer measures the total reflected flux with $\theta_1 = 0$. The two sets of readings are not strictly comparable, though they do serve as a rough check on the goniophotometer.

The *two components of reflection* are easily separated for polished samples. Figure 11 shows the results obtained on a sample of polished white opal glass 9 mm thick (Pittsburgh White Carrara) which was tested with no backing. With $\theta_1 = 0.200$ radian, for instance, the following readings were taken:

θ_2	READING
0.60 radian	105
0.70	106
0.80	106
0.90	105
1.00	105

The variation is within the probable error of the instrument, so the brightness of the sample, at angles where the specular component is absent, can be considered as independent of θ_2. The value of diffuse reflection factor, calculated from the foregoing readings is

$$\rho_d = 0.787.$$

The set-up was then completely changed, a lens system was introduced, and a different lamp was used. Readings were taken with various values of θ_1 and θ_2, and again no appreciable change could be found in the diffuse reflection factor:

θ_1	ρ_d AV. AT NONSPECULAR VALUES OF θ_2
0.40 radian	0.785
0.60	0.767
0.80	0.782
1.00	0.800
	AV. = 0.784

Thus one can conclude that, within the limits of experimental error, *the diffuse reflection factor of this sample of polished opal glass is a constant:* $\rho_d = 0.78$.

The specular component was obtained by subtracting from the reading at $\theta_1 = \theta_2$ the average reading for the diffuse component obtained at the same θ_1. This gave the values shown by the circles of Fig. 11. The index of refraction of the sample of glass was measured and found to be 1.48. The curve of Fig. 11 is the calculated curve[3] for this index. A scattering somewhat greater than in the previous graphs will be noticed in the experi-

mental points. This decrease in accuracy is caused by the fact that each value of ρ_s is obtained by subtracting two experimental values, each of which is subject to error.

7. Conclusions

A photoelectric goniophotometer is described and methods of operation are discussed. The instrument will give absolute measurements of reflection factor for either specular samples or matt samples; and with polished materials exhibiting both specular and diffuse reflection, the two components are easily separated. The unavoidable errors in the present set-up, after factors such as non-uniform illumination and improper slit width are taken care of, are believed to be within ± 2 percent of the correct reading, which is good enough for most engineering work. A large part of this error is caused by fatigue in the barrier-layer cell, and this error can be eliminated by using a photoelectric flicker arrangement.

Table I.

	Reflection Factor	
Sample	Goniophotometer	Color Analyzer (Integrated Values for C.I.E. Illuminant *A*)
No. 104, "Oxford gray"	0.0205	0.0208
No. 102, "Dover gray"	0.054	0.0547

Test results are given to indicate the possibilities of the goniophotometer. A check is obtained with the Fresnel formula for a polished black-glass sample illuminated with natural and with polarized light. Results are also given for the measured reflection factor of samples of wool cloth at various angles of incidence and various angles of view. The values at normal incidence are checked against results obtained with the Hardy color analyzer. Data are also given for the separation of the two components of reflection for a sample of polished white opal glass.

In conclusion, we wish to thank Mr. T. Wroblewski for a few of the data used in the graphs; Dr. S. Q. Duntley, who made the measurements with the color analyzer; and the manufacturers who supplied samples of glass and cloth for the tests.

An Arc Employing High Streaming Velocity for Spectrochemistry*

M. F. HASLER
Applied Research Laboratories, Los Angeles, California

IT is a well-known fact that one of the most important factors determining the rapidity, accuracy, and percentage range covered in spectrochemical analysis, is the spectral source. To illustrate this point one has only to survey the most successful applications. One of the most widely known and used is the A.S.T.M. method for zinc and zinc die casting analysis.[1] This employs an acid solution of the metal, standards, and a d.c. arc. Another example that has received widespread recognition largely through the excellent results reported at these conferences[2] is the analysis of cast iron and steel. Cast pegs of the sample furnish electrodes directly, and a high voltage spark produces the discharge. Standards are used only to obtain the working curves and for occasional checks. The third example is the analysis of caustic liquors also reported at this conference.[3] The liquor is dried directly on electrodes. The discharge is produced with a high voltage alternating-current arc between two such electrodes. Working curves are employed in the usual manner.

The three examples mentioned above represent outstanding examples of the use of three kinds of discharges in quantitative spectrochemistry namely, the d.c. arc, the high voltage a.c. spark, and the high voltage a.c. arc. The recognition of the fact that at present there is no universally best source has led to the installation of these three sources in most modern laboratories so that the source best suited for a particular job may be used. Figure 1 shows the three Applied Research Laboratories source units. The first is the d.c. arc; the second, the high voltage spark; and the third, the a.c. arc.

The chief characteristics of these sources as they are now employed are: the d.c. arc—adaptability to metallic or nonmetallic analysis, high concentrational sensitivity, large concentrational working range, relatively poor reproducibility; the high voltage spark—adaptability to metal bar or solution analysis, nonadaptability to nonmetallic solid analysis, low concentrational sensitivity, large concentrational working range and high reproducibility; the high voltage a.c. arc—adaptability to metallic or nonmetallic analysis, high concentrational sensitivity, small concentrational working range, fair reproducibility.

In reviewing these characteristics it appears that the greatest need at present is for a source that is more reproducible than the d.c. arc, more sensitive than the spark, and with a greater working range than the a.c. arc. It must, of course, be usable for the analysis of both metals and nonmetallics.

The source about to be described possesses these properties to a considerable extent and so should find many applications. However, it is not presented as a perfect source or even a new source as it employs no electrical innovations. It is merely a departure from the conventional arc that seems to possess certain inherent

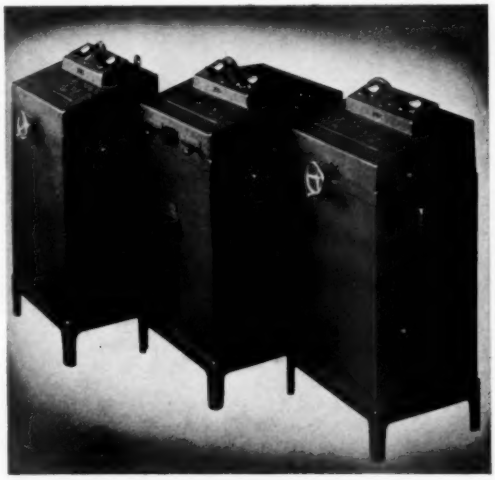

FIG. 1. Three source units.

* Presented at the Eighth Summer Conference on Spectroscopy and Its Applications at Massachusetts Institute of Technology, July, 1940.

[1] C. C. Nitchie, Ind. Eng. Chem. Anal. Ed. **1**, 1 (1929).

[2] H. B. Vincent and R. A. Sawyer, *Proceedings of the Seventh Summer Conference on Spectroscopy and Its Applications (1939)*, (John Wiley and Son, 1940), p. 16.

[3] O. S. Duffendack and R. A. Wolfe, *Proceedings of the Fifth Summer Conference on Spectroscopy and Its Applications (1937)*, (John Wiley and Son, 1938), p. 24.

advantages. As it is an arc, most laboratories have the electrical equipment necessary to produce this discharge, which should facilitate its general use.

Figure 2 shows the arrangement of electrodes and samples. The first arc is used for the analysis of powders either nonmetallic or metallic, the second arc is for the direct analysis of metal rods. In the first, the powdered sample is mixed with a carrier medium such as ammonium chloride or specially reactive carbon produced by heating sucrose. The mixture is placed in the space between the carbon center post and the carbon sleeve, the latter being electrically insulated from the electrode with a Transite bushing. This bushing is protected from heat by a layer of carbon produced by filing a carbon electrode. When the arc is struck the heat generated causes the carrier to produce a large volume of gas which, in blowing out of the orifice, carries the powdered sample up into the arc. In four seconds of arcing at ten amperes from 50 to 100 mg of sample can be blown through the arc, the exact amount depending upon the carrier used. The intensity of such an arc is several times greater than that of an ordinary arc so that a single four-second exposure suffices to produce a spectrogram of sufficient density to detect minimum amounts of all elements detectable. Since each sample particle is blown into the arc in a manner completely independent of the vapor pressure of its constituents, the fractional distillation effects of the more usual discharges are avoided.

In the second arc the same sort of action takes place except that the metal melted by the discharge is blown into the arc. By using the right carrier medium the metal is vaporized just as rapidly as it melts so that no bead is formed and no fractional distillation occurs. Just as in the case of powders, large amounts of material can be made to pass through the discharge in a very short time; 50–100 mg in four seconds with a 10-amp. arc.

In general, this type of arc produces a spectrum that is similar to that obtained with the high current density arc described by King.[4] Despite the fact that normal arcing currents are employed, atomic concentrations equal to those obtained in a 100-ampere arc are apparently produced. These conditions of high atomic density favor the neutral atom spectrum by limiting electron velocities in the arc. This minimizes spark spectrum and conditions of high excitation and thus reduces background so that the net result is a large increase in the concentrational limit of detection and measurement of many elements. This reduction of background

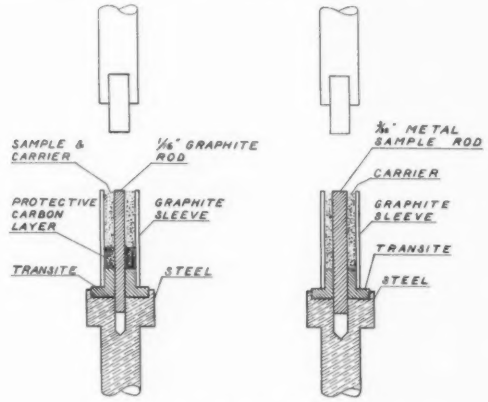

FIG. 2. Arc electrodes.

is particularly marked in the case where a metallic rod is arced with an ammonium chloride carrier, as the various carbon compound bands hardly register.

The absolute intensity of this type of arc is from 2 to 5 times as intense as the normal sample-graphite arc employing the same current. This implies that, corresponding to the increase of atom density, there is also an increase in the number of atoms excited. However, because of the high atomic densities, some of the spectrum lines of the major constituent are reversed while many are widened, often in an asymmetrical manner. However, in general, all the minor constituent lines appear normal. At first hand these manifestations of high atomic concentrations might lead one to expect much self-absorption of spectral lines of minor constituents as well as major ones. This is not the case. In fact, perfectly linear relationships between intensity and concentration have been obtained for lines of elements present up to five percent

[4] A. S. King, Astrophys. J. **62**, 238 (1925).

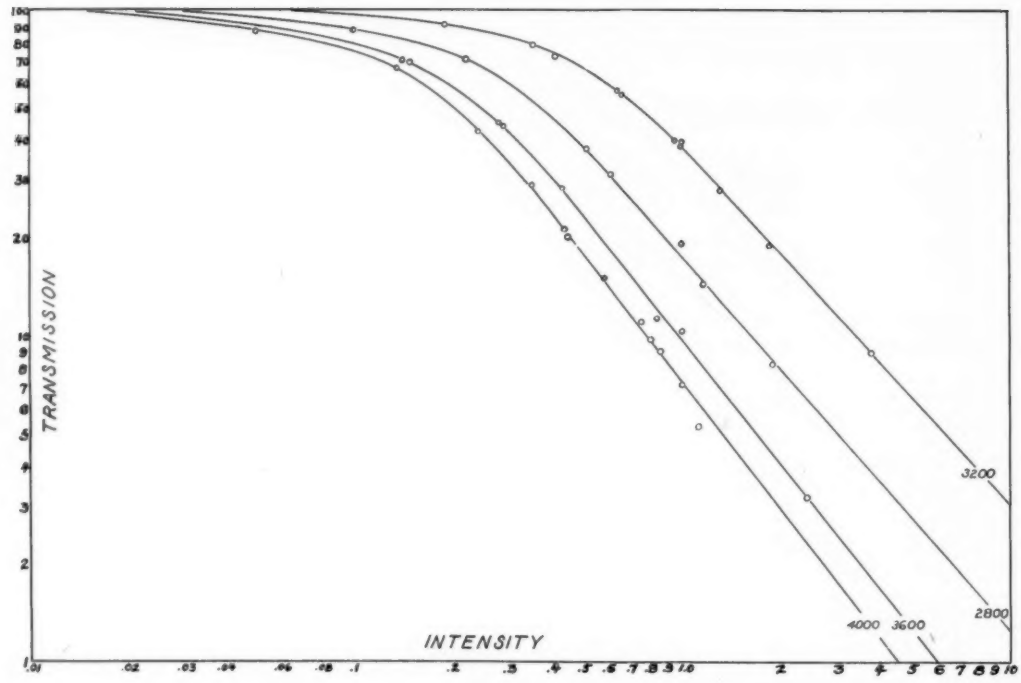

FIG. 3. Film blackening curve.

provided, of course, suitable lines were chosen. Since this condition is rarely found in the more usual types of discharge it would seem that the high streaming gas velocities of this arc prevent the formation of large absorbing clouds of cold vapor in front of the discharge and thus minimize self-absorption. Besides this, the high streaming velocities together with the geometrical arrangement stabilize the arc very markedly so that good reproducibility of both absolute and relative line intensity is obtained.

However, to insure that reproducibility and to minimize background, light from a certain portion of the discharge must be used. This was determined by studying the change of spectral intensity along the discharge which is related to the motion of particles of sample through the arc. This was done by focusing an image of the arc onto the secondary slit of the spectrograph. This arrangement produces a spectrum, each line of which is an arc image in the vertical direction. In the case of a metal oxide, low relative atomic line intensity is obtained directly above the orifice due to the evaporation of most of the sample in the molecular form. However, as the vapors pass up through the arc, these molecules are decomposed so that the line intensities increase rapidly toward the top of the arc as more atoms are available for excitation. In the case of a metal rod, on the other hand, evaporation produces large quantities of atoms immediately which give a very intense line spectrum above the orifice. This is reduced in intensity as the atoms move up through the arc and combine with negative radical atoms to form fairly stable molecules. In general, the most suitable radiation to use for spectrochemical work is that from the portion of the arc $\frac{3}{16}''$ to $\frac{1}{4}''$ above the lower electrode as first set up, when a $\frac{3}{8}''$ spacing is used between electrodes. In actual practice this region was centered on the optical axis of the spectrograph but the arc was defocused by working without a condensing lens, and positioned 24 cm from the secondary slit of the astigmatic grating spectrograph.

With such a source available, having good

stability, high concentrational sensitivity and linear change of intensity with concentration, a number of problems involving both metal and nonmetallic analyses were investigated with considerable success. Before discussing these, however, a more fundamental problem solved by the use of this arc will be considered. This problem is that of film density calibration.

This problem is much more diverse than most operators realize. The tendency often is to construct a single H and D film blackening curve and expect that it be applicable in all regions of the spectrum irrespective of the particular plates, films or developers used. Another error is to compare line intensities between lines widely separated in the spectrum. The only way to obtain consistent results day after day and month after month when it is necessary to compare lines further apart than, say, 400 angstroms in the spectrum, is to have a source rich in lines and very reproducible in the relative intensities of its lines. With such a source the relative intensities of a group of lines close together can be determined once and for all and these lines can then be used to determine a blackening curve in that region of the spectrum. This can be repeated in several regions of the spectrum to give as many blackening curves as are necessary. These can be set up to always bear a definite ratio to each other by calling a certain iron line in each group, unit intensity. Then by reading each line's intensity from the blackening curve relating to its region of the spectrum, ratios of intensities can be obtained that are independent of variations of speed of the spectrograph or of speed and contrast of film emulsion. This is the case because, instead of reading an intensity ratio directly, one reads the ratio $I_1(2800)/I_{Fe}(2800)$ to $I_2(4000)/I_{Fe}(4000)$ which is independent of the changes mentioned above as long as the iron source maintains a constant intensity ratio between its lines irrespective of the region of the spectrum in which they occur. Consistent use of such a system should allow direct comparison of intensity ratios between different laboratories.

Such a group of calibration curves is shown in Fig. 3 covering the spectral range 2400–4600A. Instead of using $\log 100/T$ as the ordinate, where T is the transmission in percent of the spectrum lines, $\log T$ is plotted, as then no reciprocals need be taken. This is just an inversion of the usual H and D curve. The iron arc used employs portions of nails, $\frac{3}{32}''$ in diameter and $\frac{7}{8}''$ long. These are placed in a holder similar to that depicted in Fig. 1. The carbon sleeves are produced from $\frac{1}{4}''$ rod and are $\frac{5}{8}''$ long with a wall thickness of 0.020". Ammonium chloride is used as a carrier. This is the C.P. grade obtained commercially with a particle size of about 0.5 mm. It is kept in a desiccator over sulphuric acid. The current in the arc is adjusted to give 10 amperes with a $\frac{3}{8}''$ spacing at the moment the arc is opened. A four-second arcing, terminated by means of an electrical timer on the arc rectifier, is used. Accurate spacing and positioning of electrodes is achieved with the projection system on the standard arc-spark stand employed. The iron lines used are in most cases successive lines in the iron spectrum produced by this source, chosen to calibrate a certain region of the spectrum. The mere fact that no special choice of lines had to be made, indicates the great reproducibility of relative line intensities for this arc. The wave-lengths of the lines and their relative intensities are given

TABLE I.

WAVE-LENGTH	INTENSITY	WAVE-LENGTH	INTENSITY	WAVE-LENGTH	INTENSITY	WAVE-LENGTH	INTENSITY
2788.1	1.92	3175.5	4.20	3661.4	0.141	3953.8	0.136
2786.8	.219	3173.7	.97	3659.5	1.00	3948.8	1.20
2786.2	.126	3172.1	.64	3659.1	.148	3948.1	.86
2781.8	.619	3171.4	1.00	3657.9	.286	3947.5	.57
2778.8	.519	3168.9	.65	3657.1	.277	3947.0	.44
2778.2	1.18	3167.9	.96	3656.2	.432	3945.1	.46
2767.5	1.00	3166.4	1.95	3655.5	.84	3943.4	.24
		3165.9	1.32	3651.5	2.40	3942.4	.77
		3164.3	.35			3940.9	.80
		3163.9	.42			3940.0	.066
		3163.1	.22			3852.6	1.00

TABLE II. *Repeat metal peg analyses of zinc die casting pig.*

	1	2	3	4	5	6	7	8	AVERAGE	STANDARD DEVIATION
Aluminum	3.75	3.92	3.84	3.84	3.84	3.92	4.09	3.92	3.89	2.5%
Copper	1.13	1.10	1.13	1.12	1.12	1.17	1.10	1.09	1.12	2.3%
Magnesium	.035	.037	.035	.037	.038	.037	.041	.036	.037	5.2%
Iron	.022	.022	.021	.021	.022	.023	.020	.019	.021	6.3%
Lead	.0031	.0027	.0029	.0032	.0033	.0028	.0029	.0028	.0030	7%
Cadmium	.0027	.0027	.0030	.0026	.0025	.0025	.0023	.0023	.0026	9%
Tin	.0010	.0009	.0009	.0010	.0010	.0008	.0008	.0008	.0009	10%

$$\text{Standard deviation} = \frac{1}{\text{mean}}\left(\frac{\Sigma(\text{deviation from mean})^2}{n-1}\right)^{\frac{1}{2}}$$

in Table I. Differences in optical arrangement and direct-current facilities may vary these ratios somewhat. However, such variation should not be great so that these figures should be of value.

In using this arc in analytical work, a number of possibilities present themselves since the sample and/or internal standard can be made the rod at the center of the arc or mixed with the carrier powder surrounding the rod. In metal rod analysis, the usual procedure has been to employ the major constituent as the internal standard, though doubtlessly an internal standard could be mixed with the carrier. Iron, aluminum, zinc and zinc die casting alloys have been analyzed directly from metal pegs. Oxides prepared from these same metals have been analyzed as powders which has made possible a comparison with prepared oxides of known composition. Thus, this method of arcing allows the calibration of a direct, metal peg, spectrochemical analytical method by a spectrochemical powder method.

The fact that a calibrating method was available decided the first problem studied, namely zinc die casting analysis. This is a problem that severely taxes any source as the constituents range in percentage from a few parts per million for some elements up to four percent for others. A single arcing on a metal rod had to produce the analysis of tin, cadmium and lead from 0.001–0.01 percent, of magnesium and iron from 0.01–0.1 percent, of copper from 0.1–3 percent, and of aluminum from 3.5 to 4.5 percent. The results given in Table II indicate that this has been done with considerable success. A more detailed presentation of the method will be published elsewhere.

The most interesting point connected with these results is that most of the working curves relating intensity ratios to concentration turned out to be straight lines. This means that for a suitable range of line intensities, lines of every element could be found that varied in intensity proportionately to the number of atoms of that element in the sample. This held despite the several thousandfold variation of atomic concentration between the several kinds of atoms for which tests were made. This extremely simple relationship can, of course, only be obtained if low intensity lines are corrected for background. This is done by the usual procedure of calculating both the intensity of the line plus background and the background from the H & D blackening curve and subtracting the latter from the former to obtain the intensity of the line alone.

In connection with the final commercial method developed, an arcing procedure similar to that used for the iron calibration arc was employed with ammonium chloride again as the carrier. Either cast or turned pegs are used as sample electrodes. One calibrating iron spectrum and eight sample spectra could be placed on a single film. This takes about two minutes per sample or eighteen minutes for photography. The film is processed in about seven minutes making a total of 25 minutes to prepare a film. Reading the film on the densitometer takes about thirty minutes as does plotting the film calibration curves and calculating the final percentages. Thus, a total time of about an hour and a half allows the completion of fifty-six element determinations. This is less than two man minutes per analysis.

The accuracy shown in Table II can be obtained day after day, thanks to the iron arc film

calibrating method. These accuracies illustrate that this arc approaches the accuracy of a spark for all lines that are of reasonable intensity. For lines that approach background intensity, the errors are greater. However, it is gratifying to see that even at the limit of detection of lead, cadmium, and tin, at 0.0006 percent, 0.0009 percent and 0.0007 percent, respectively, answers accurate to one part in a million can still be achieved.

The analysis of zinc oxide is a good example of what can be achieved in nonmetallic analysis. The oxides investigated were prepared to simulate oxides obtained from zinc die casting alloys which allowed the standardization of the metal peg system. Certain advantages of this type of sample preparation such as that drillings may be used to obtain average sampling, makes this suitable for commercial analysis in place of the A.S.T.M. method.[5] Also, concerning cadmium, lead and tin, lower percentages can be detected and measured than with the metal peg method. The limits by the oxide method are cadmium 0.0007 percent, lead 0.0003 percent and tin 0.0002 percent. The cadmium limit could be considerably extended by using the 2288A line in place of the 3261A line employed in these tests. However, the latter line is more suitable for testing the usual commercial alloys possessing a few thousandths of a percent of cadmium.

It was found that great care had to be exercised in preparing oxides of die casting metal because of the four percent aluminum. Converting a large mass of acid solution to oxides by simple heating proved very unsatisfactory as the formation of complex oxides seemed to vary from preparation to preparation. The most satisfactory method was to heat a silica dish very hot and then drop the solution into it drop by drop so that a number of small portions of the solution were converted to solids. (Since several hundred drops per gram of metal are dried, an average of all the possible complex oxides is obtained.) This material was scraped from the dish and ground in an agate mortar. A one-to-one mixture of sample and carbon was prepared. The carbon is formed by heating sucrose until it is thoroughly carbonized and then grinding it in an agate mortar. Fillings of this mixture in electrodes having a $\frac{1}{16}$" carbon center post and the usual insulated sleeve, produced the arc. The accuracies obtainable for the higher percentages are slightly less than with the metal pegs though still quite acceptable with the exception of aluminum, the analysis of which possesses an 8 percent standard deviation. However, due to the increased intensity of lines over background for the trace elements, better accuracies could be obtained for these than with the sample in the peg form. Again, very linear relationships between line intensity and concentration could be established, indicating that just as with the metal arc, the oxide arc does not tend to self-absorb lines to any great extent.

Thus, in conclusion, an arc source has been developed that is more stable than the usual d.c. arc, more sensitive than the spark, and possesses a greater percentage working range than the a.c. arc. It should, therefore, find use in many applications of spectrochemistry that up to now have required several sources, or have been limited in scope.

[5] A.S.T.M. "Tentative method of test for quantitative spectrochemical analysis of zinc alloy die castings for minor constituents and impurities." Designation: E 27-37 T.

Temperatures in Spectroscopic Sources Used in Analytical Work*

O. S. DUFFENDACK AND J. M. LARUE
University of Michigan, Ann Arbor, Michigan

THIS report deals with some measurements on the temperature parameters in d.c. and high voltage a.c. arcs between spectroscopic carbon electrodes and between these electrodes with a thin layer of caustic soda on their ends. The arcs were operated in the manner commonly employed in spectrochemical analysis. The temperature parameters were determined from measurements on the distribution of intensity among the rotational lines of the λ4216 band of CN in accordance with well-established theories and procedures. The investigation is not yet complete, but the results thus far obtained are of interest in themselves and hence are reported at this time.

The intensity of a spectral line emitted from an assemblage of radiating systems depends upon the number of emitters present in the assembly that are in the initial energy state E_j concerned in the transition giving rise to the line and to the probability of the transition. By intensity of a spectral line emitted by a source we shall mean the amount of energy per second radiated by the source at the frequency of the line in question and caused by transitions between energy states of the molecules of the source. A certain portion of this energy will pass through the slit of the spectrograph and fall at a particular position on the photographic plate and produce there the latent slit image which permits the recording of the line by the photographic plate. The well-developed techniques of spectral photometry enable one to determine the relative intensities of the spectral lines in the source from measurements on the slit images recorded on the photographic plate. It must always be borne in mind that spectrochemical analysis rests fundamentally on the relative intensities of the spectral lines as emitted by the source, and so any investigation of the factors controlling the intensities of emitted lines is pertinent to the general problem of spectrochemical analysis.

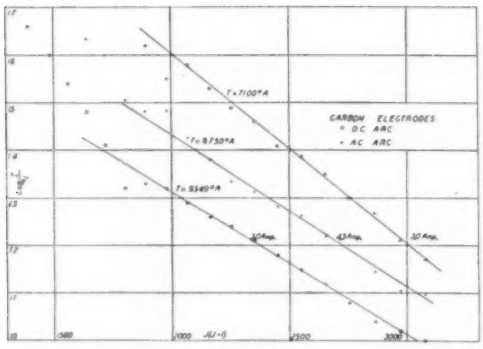

FIG. 1. Arcs between electrodes of spectrographic graphite.

The intensity of a spectral line radiated by an assemblage of molecules is given by

$$I = N_j A_{jj'} h\nu_{jj'},$$

where N_j = number of molecules in the energy state E_j, the initial state of the transition producing the line; $A_{jj'}$ = transition probability of the transition from energy state E_j to energy state $E_{j'}$ in the molecule; $\nu_{jj'}$ = frequency of the spectral line emitted; h = Planck's constant.

$A_{jj'}$ is the Einstein transition probability and may be shown to be given by

$$A_{jj'} h\nu_{jj'} = \frac{64\pi^4 \nu_{jj'}^4}{3c^3} P_{(jj')}^2,$$

where $P_{(jj')}$ is the electric moment of the molecules for the transition $j \rightarrow j'$; c = velocity of light.

The number of molecules in the energy state E_j depends upon the conditions prevailing in the gas (as e.g. the temperature) and will vary with the excitation conditions. For a condition of thermal equilibrium, this number is given by

$$N_j = \frac{N}{\sigma} g_j e^{-E_j/kT},$$

where N = total number of molecules in the assembly (all states); σ is a normalizing factor

* Presented at the Eighth Summer Conference on Spectroscopy and Its Applications at Massachusetts Institute of Technology, July, 1940.

($\sigma=\Sigma g_j e^{-E_j/kT}$); g_j is the statistical weight or *a priori* probability of the state j.

$$\therefore \qquad I=\frac{N}{\sigma}\frac{64\pi^4\nu^4}{3c^3}g_j P^2_{(jj')}e^{-E_j/kT}.$$

The product $g_j P^2_{(jj')}$ is proportional to an intensity factor, i, which can be evaluated for a given molecular transition in diatomic molecules by the quantum mechanics.

For a diatomic molecule the total energy of a given state is made up of three component parts which may be ascribed, in the main, to the energy associated with the electronic, vibrational, and rotational states, respectively, so that $E_j=E_e+E_v+E_J$, where e, v, and J characterize these states. For a given electronic and vibrational transition, and therefore for the lines of a given band in a band system of a molecule, E_e and E_v are invariant, and so the only variable in the Boltzmann factor which enters into the expression for the intensity of a given line is the rotational part, and, if one is interested only in the relative intensities of the lines of a single band, one needs to take account only of E_J in this factor.

$$E_J=\frac{J(J+1)h^2}{8\pi^2 I},$$

where J is the rotational quantum number of the initial state and I=moment of inertia of the molecule in this state. Furthermore, since the frequencies of the lines of a band are not very different (the lines extend over a narrow region of the spectrum) the factor ν^4 may be taken as constant over the lines of a single band and likewise σ is very slowly varying and may be taken as constant so that

$$I_{JJ'}=Ci\exp\left[-\frac{J(J+1)h^2}{8\pi^2 IkT}\right].$$

For a band of the class of the CN band used in the measurements, the intensity factor, i, may be shown to be given by: $i_p=2(J+1)$ for the P branch of the band and $i_r=2J$ for the R branch of the band, and so can be evaluated for the several lines of the band. Now it will be observed that

$$\log\frac{I_{JJ'}}{i}=\text{const}-\frac{J(J+1)h^2}{8\pi^2 IkT}$$

so that a graph of $\log I_{JJ'}/i$ *vs.* $J(J+1)$ will be a straight line of slope $-h^2/8\pi^2 IkT$, and, from this measured slope, the temperature, T, can be determined.

This method has been employed for the determination of the temperature of the sun and particularly by Ornstein[1] and his pupils in determining the temperatures in electric arcs. While the relations developed apply strictly only to sources where the conditions of thermal

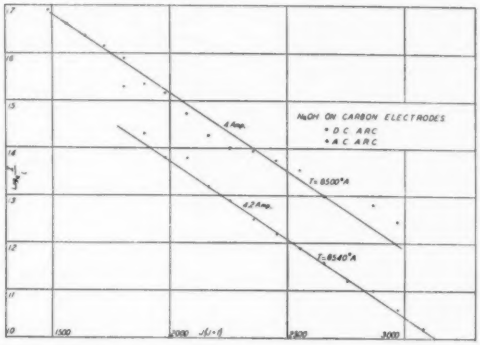

FIG. 2. Arcs between graphite electrodes coated with NaOH.

equilibrium prevail, we[2] at Ann Arbor and others[3] as well, have demonstrated that the distributions of intensities one encounters in excitations by electron impact and by impacts of the second kind simulate that of thermal equilibrium so that a value of the factor T in the intensity equation can be obtained. The value of T does not give the temperature of the assembly of molecules in the source in such cases and should not be spoken of as the temperature of the source. We have formed the habit of referring to it as the "temperature parameter" of the source. It is related to the distribution in energy of the *excited* molecules revealed by the spectrum in the same way as is the true temperature of the gas in cases where thermal equilibrium prevails, and by means of it one can calculate the portion of

[1] L. S. Ornstein and H. Brinkman, Proc. Roy. Acad. Amst. **34**, 33 and 498 (1931); Physica **1**, 797 (1934); W. Lochte-Holtgreven and H. Maecker, Zeits. f. Physik **105**, 1 (1937).

[2] O. S. Duffendack, R. W. Revans and A. S. Roy, Phys. Rev. **45**, 807 (1934); O. S. Duffendack and K. T. Chao, Phys. Rev. **56**, 176 (1939).

[3] F. L. Mohler, J. Research Nat. Bur. Stand. **16**, 227 (1936); G. O. Langstroth and D. R. McRae, Can. J. Research **16**, 17 (1938).

the excited molecules that will be found in any given excited state and can make other important deductions about the excitation of spectral lines in the source.

Figures 1 and 2 show typical graphs from which the temperatures of the arcs were determined. Because we did not have the necessary transformers available for our source with our 21-foot concave grating, all of the spectrograms of the high voltage a.c. arcs were taken with a large

TABLE I. *Arcs between pure spectroscopic graphite electrodes.*

SPECTROGRAPH	SOURCE	CURRENT AMP.	TEMPERATURE °K
Grating	d.c.	1.7	6600
"	"	3.6	5600
"	"	3.6	6230
"	"	3.6	7100
"	"	7.0	6100
Littrow	"	3.0	9340
"	"	3.0	7100
"	"	3.0	6840
"	"	3.0	8390
"	"	3.7	7200
"	"	4.0	8000
"	a.c.	4.3	8750
"	"	4.3	8800
"	"	4.3	8750
"	"	2.6	9430
"	"	2.6	9040
"	"	2.6	7740
"	"	2.6	7800

Littrow glass spectrograph. Some of the spectrograms of d.c. arcs were taken with the same instrument and some were taken with the 21-foot grating. The resolution of the spectrograph was not sufficient to permit measurements on the lines near the null position in the band and it will be noted that the graphs depart from straight lines for the lower values of $J(J+1)$.

The spectra were photographed without any lens between the source and the slit and so light from all parts of the arc fell upon the photographic plate. However, since the cyanogen bands are excited much more strongly in the positive column than in the cathode layer, the temperatures are those prevailing in the positive column and the values determined from these measurements are of the same order of magnitude as those reported by other observers[4] for the positive column of carbon arcs.

[4] See reference 1; also G. G. Suits, Physics **6**, 190, 315 (1935).

The results of the measurements are given in Table I for arcs, both high voltage a.c. and d.c., between spectrographic graphite electrodes and in Table II for high voltage a.c. arcs between such electrodes coated on their ends with a thin layer of NaOH. Some measurements were made on d.c. arcs between NaOH-coated electrodes but the intensity measurements fluctuated so widely it was impossible to deduce any temperatures from them. The most consistent set of measurements for these arcs is reproduced in Fig. 2.

It will be noted that the temperature parameters are not dependent upon the arc currents. The gap lengths likewise were varied by a factor of two without producing any change in the temperature. Similar observations have been reported before.[4] The d.c. arcs made the electrodes white hot, but the high voltage a.c. arcs between pure graphite electrodes produced only a cherry red and a very slow wasting away of the material. The high voltage a.c. arcs between the electrodes coated with NaOH did not heat them hot enough to show any color at all. Nevertheless the temperature parameters for the high voltage a.c. arcs were within the range of those of the d.c. arcs and the presence of NaOH on the electrodes caused no reduction in the temperature parameter. The average value of the temperature parameters of the high voltage a.c. arcs was higher (8616°K for pure graphite) than that of the d.c. arcs (7136°K) and the measurements were more consistent.

It seems probable, as contended by Ornstein,[1] that conditions in the arc column of a d.c. arc are approximately those of thermal equilibrium. This is, however, quite likely not the situation in the high voltage a.c. arc. This being the case, differences in the distribution in intensity of the spectral lines in the two types of sources may be expected and were observed. In spite of the fact that the temperature parameters were in the same range of values, spectral lines from higher terms are more commonly observed in the high voltage a.c. arcs than in the d.c. arcs. The relative intensities of higher series members with respect to lower series members is greater in the high voltage a.c. arcs and the presence of NaOH on the electrodes does not alter this observation. Thus, the high voltage a.c. arc is advantageous

when it is desirable to use spectral lines from the higher terms or the higher series members. The d.c. arc seems to be more sensitive, i.e., one can detect a lesser amount of an element, if the lines from the lower terms fall in a region of high plate sensitivity and if, as in the case with the metallic elements, their excitation potentials are relatively low. The high voltage a.c. arc is, according to our experience, a much more consistent source than the d.c. arc when materials are put upon the spectrographic graphite electrodes for analytical purposes.

Since thermal equilibrium does not prevail in the high voltage a.c. arc, the exciting electrons may have higher average energies than those corresponding to the temperature parameters whereas the average energies of the electrons in d.c. arcs are those corresponding to the prevailing temperatures. Hence the exciting electrons in the high voltage a.c. arcs are of relatively higher energy with respect to the energy of those at the maximum of the excitation function of a spectral line than in the d.c. arc. The more remote the electron energies are from the value at the maximum of the excitation function, the less sensitive is the probability of excitation to variations in the energies of the exciting electrons. Therefore, one may understand why the high voltage a.c. arc gives more consistent results than does the d.c. arc in exciting the spectra of materials being analyzed. Further studies on the conditions prevailing in spectroscopic sources used in quantitative spectrochemical analysis are desirable in order that more reliable sources for analytical purposes may be developed.

TABLE II. *Arcs between spectrographic graphite electrodes coated with* NaOH.

SPECTROGRAPH	SOURCE	CURRENT AMP.	TEMPERATURE °K
Littrow	a.c.	4.2	8570
"	"	4.2	8540
"	"	2.5	8700
"	"	2.5	7870
"	"	2.5	7950

Electrode Concentrations and Total Intensity of Spectral Lines*

HENRY HEMMENDINGER†
George Eastman Research Laboratories of Physics, Massachusetts Institute of Technology, Cambridge, Massachusetts

THE work to be reported on at this time was prompted by astrophysical studies of emission line intensities. In the light of these studies, an attempt has been made to extend the interpretation of line intensities in a laboratory source, in the hope of removing some of the present limitations on spectrographic analysis.

INTRODUCTION

Let us first review some of the facts concerning atomic transition probabilities and their significance in the interpretation of line intensities.[1] Consider an assembly of atoms in thermal equilibrium. They will be divided among the various atomic levels according to Boltzmann's equation,

$$\frac{N_m}{g_m}=\frac{N_n}{g_n}e^{-(E_m-E_n)/kT}, \tag{1}$$

in which N_i is the number of atoms in level i, whose statistical weight (or degeneracy) is g_i, and excitation potential E_i; T is the temperature. We may define a quantity f_{nm}, called the oscillator strength, or Ladenburg f, such that the intensity of the line of frequency ν emitted by atoms in the upper state m in spontaneously jumping to the lower state n is given by

$$I=\frac{N_m}{g_m}g_n f_{nm}\nu^3\frac{8\pi^2\epsilon^2 h}{mc^3}, \tag{2}$$

where ϵ and m are the charge and mass, respectively, of the electron.

This equation is valid where the emitting layer of gas is optically thin. Consider now what happens as the layer of gas becomes thicker—though still all in thermal equilibrium at a given temperature—such that it exhibits an appreciable opacity for the frequency of the line being considered. At first the line contour remains the same, merely growing in intensity, at a rate proportional to the number of emitting atoms. Over this range of intensity the line contour is determined predominantly by the Doppler shifts of the quanta emitted by atoms in thermal motion. As the line continues to increase in total intensity, its shape gradually begins to change; the center of the line attains a maximum intensity (equal to the intensity of radiation at the same frequency from a blackbody at the temperature of the gas), and the continued growth in the line intensity is due to an increase in its width. Over this range of growth the line shape is no longer controlled by Doppler effect, but by the natural width of the atomic energy levels; and the intensity of the line increases in proportion to the square root of the number of atoms producing the line. The curve representing the rate of change of intensity with a change of the number of atoms in the emitting layer is called the "curve of growth." In the case of the transparent (thin) emitting layer we are concerned only with the first portion of the curve of growth; in the case of the thicker layer, for which the intensity increases less rapidly than the number of atoms, we say that the line is undergoing "self-absorption."

The foregoing is to be distinguished from the case ordinarily occurring in the laboratory, in which, even if we may still, at least as a first approximation, speak of thermal equilibrium, we do not have a homogeneous layer of gas, but rather a central core surrounded by external portions at a lower temperature. Under these circumstances, in addition to the self-absorption just discussed, there is a diminution in the intensity of the lines due to self-reversal; that is, light emitted by the central hot portion is partially absorbed on its way out through the outer cooler layers.

The atomic transition probabilities, or the f values, are known for certain types of lines.

* Presented at the Eighth Summer Conference on Spectroscopy and Its Applications at Massachusetts Institute of Technology, July, 1940.

† Bausch and Lomb Fellow.

[1] For complete discussion of the theory, see, for instance, E. U. Condon and G. H. Shortley, *The Theory of Atomic Spectra* (Cambridge University Press, 1935), Chapter IV; A. C. G. Mitchell and M. W. Zemansky, *Resonance Radiation and Excited Atoms* (MacMillan, New York, 1934), Chapter III; A. Unsöld, *Physik der Sternatmosphären* (Springer, Berlin, 1938), Chapters VIII, IX.

For the lines of hydrogen and helium they may be computed sufficiently rigorously. They are available also, from empirical methods, for a number of other transitions, such as the doublet series of the alkalies. Of greatest importance for the present study is the series of relative f values for neutral iron and titanium determined in a painstaking study by R. B. and A. S. King.[2] They have measured the integrated intensity of absorption lines formed by metallic vapor in an electric furnace at a known temperature. By confining their measures to the first linear portion of the curve of growth, they have been able to use the relative populations of the various atomic levels to deduce f values from the observed intensities. The availability of these f values has determined the choice of electrodes for the experimental work to be discussed, in which we shall consider the intensities of iron and titanium lines in emission in a direct-current arc.

Observations

The observational procedure may be summarized briefly. The arc was imaged, full size, on the 0.1-mm slit of a thirty-five foot grating in a Wadsworth mounting. The wave-length range covered on a ten-inch plate was 3500–4300A. On the same plate standards were photographed: a line source, weakened at the slit by a logarithmic step-sector, to make possible a calibration of the optical density of the emulsion as a function of impressed intensity, and the ribbon filament of a tungsten lamp, operated at a known temperature, to make possible the determination of the absolute values of the observed intensities for all wave-lengths. Eastman 33 plates were generally used, with a few Eastman Process. All plates were brushed during development in rodinal, to minimize Eberhard effect. Measurement of the line densities was made with a nonrecording microphotometer. Calibration curves were drawn for hundred-angstrom intervals, to eliminate errors arising from the dependence of photographic contrast on wave-length.

A study of the errors of the experimental procedure was undertaken by repeated measurement of the line intensities in a Pfund arc operated at a low arc current, with the geometry and electrical characteristics of the arc maintained as nearly constant as possible. Exposures were made on four different plates, each separately standardized and developed, and about one hundred line intensities were measured on two exposures on each plate. From comparison of the observed intensities the probable error of the observations was found to be 0.013 unit in the logarithm of the intensity. This probable error includes both the errors of measurement and the inevitable slight variations in the physical conditions of the source.

Arc Temperature

Interpretation of the observed intensities requires some knowledge of the temperature of the source. An arc burning in air is not truly in thermal equilibrium, and cannot be completely characterized by a single temperature. It has been found[3] however, that populations of atomic levels of different excitation potentials may be closely represented by Boltzmann's formula; we shall, therefore, define the "excitation temperature" T_e as the parameter in terms of which the observed populations may be most closely represented by that equation. The temperature thus defined may be expected to correspond fairly closely to the kinetic temperature.

We may rewrite Eq. (2) with the quantity N_m/g_m replaced by its value according to Eq. (1), and find that

$$\log_{10}\frac{I}{g_n f_{nm}\nu^3}=\text{constant}-\frac{5040E_m}{T_e}. \qquad (3)$$

Since I is observed for each line, and $g_n f_{nm}\nu^3$ is known, Eq. (3) enables us to determine the excitation temperature. The value observed by the author for the center of the positive column of a freely burning arc of iron or titanium, or of mixtures of the two elements, has been found to be insensitive to changes in arc length or arc current. Figures 1(a) and 1(b) show graphically typical series of measurements from which the temperature has been derived. Here the ordinate is

[2] R. B. and A. S. King, Astrophys. J. **87**, 24 (1938) or Mt. Wilson Contribution No. 581.

[3] For review of this point, see L. B. Loeb, *Fundamental Processes of Electrical Discharges in Gases* (Wiley, New York, 1939), pp. 616–622.

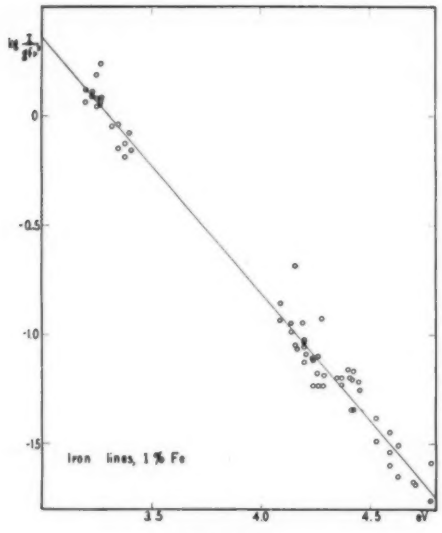

FIG. 1(a).

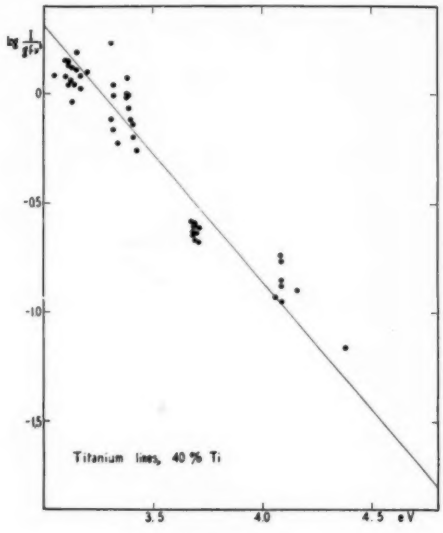

FIG. 1(b).

$\log I/g_n f_{nm} \nu^3$ and the abscissa is the excitation potential in electron volts. The data are for an arc 18 mm long operated at a low arc current (1.0 ampere), with 110-volt direct current across the electrodes; the arc with ballast was operated from the 220-volt mains. Figure 1(a) shows the data for iron lines in electrodes containing 1 percent iron, 99 percent titanium, and Fig. 1(b) shows the data for titanium lines in a mixture of 40 percent titanium and 60 percent iron. The values of the excitation temperatures deduced from these two series are 4200°K and 4060°K respectively. Observations at other concentrations and arc currents gave accordant results for the temperature, with the exception of circumstances in which the equations used in its derivation (implying an optically thin layer) might no longer be expected to apply, for reasons to be discussed subsequently. On the basis of all available measurements, the temperature 4200°K was adopted for the arc temperature.

LINE INTENSITIES

Let us consider first the intensities in an ordinary Pfund arc, with pure iron. The arc was operated from the 220-volt direct-current line, with an electrode separation of 18 mm. The microphotometer observations were made at a point of the image corresponding closely to the center of the positive column (the region of minimum arc intensity per unit area of the source), which was several millimeters distant from the edge of the perceptible cathode flare.

To facilitate the interpretation of the observed intensities, we shall define a quantity F, proportional to the theoretical intensity for a thin emitting layer:

$$\log F = \log g_n f_{nm} \nu^3 - 5040 E_m / T_e. \qquad (4)$$

Figure 2(a) shows a comparison of $\log F$ with the observed intensities of about one hundred lines of Fe I, for an arc operated at 1.2 ampere and 110–115 volts drop across the electrodes. The large circles represent lines to the ground state of the atom; the intermediate circles represent transitions whose upper level has an excitation potential of about three-quarters of an electron volt, and the small circles represent transitions to levels of about one-and-one-half volts excitation potential. It will be observed (a) that the points fall fairly closely along a line inclined at 45° to the axes, as is to be anticipated from Eq. (2) for the case of a thin emitting layer, and (b) that there is no marked segregation of the plotted points according to excitation potential, such as would be caused by an

incorrect value of the temperature used in the computation of log F. When, however, the arc current is increased to 4.0 amp., as is shown in Fig. 2(b), a marked change occurs. The more intense lines no longer fall on a line inclined at 45° to the axes; and the ones of lowest excitation potential deviate more than those of higher excitation. This is the typical behavior to be expected when self-reversal takes place.

For the study of titanium intensities, use has been made of the technique of pressing electrodes of mixtures of powdered metals, and then sintering them in an electric furnace at a temperature slightly below the eutectic point to obtain a near-alloy by metallic diffusion. Iron and titanium have been mixed in this way in proportions ranging from 1 to 99 percent. The method has the disadvantage that it is impossible to obtain completely uniformly crystallized alloys, and there is, therefore, greater scatter in some of the results to be shown later than would be expected if the use of true alloys were possible. In addition, titanium reacts sufficiently readily with atmospheric gases so that observation with the higher percentages of titanium becomes difficult.

The next several figures present comparisons of the observed intensities with the theoretical intensities for three mixtures of different proportions of iron and titanium. (It should be remarked at this point that the experimental f values are relative only, with arbitrary zero points for each element.) In the case of electrodes of 70 percent Fe+30 percent Ti (Fig. 3(a)), the titanium lines are considerably weaker than the iron lines characterized by the same value of log F; the titanium lines are substantially unreversed, the stronger iron lines slightly reversed. As the relative proportion of titanium in the electrodes is increased (Figs. 3(b), (c)), the intensities of the titanium lines increase relative to those of iron, and at the same time the stronger titanium lines show a tendency to grow in strength less rapidly than the weaker ones, while the iron lines become less subject to self-reversal.

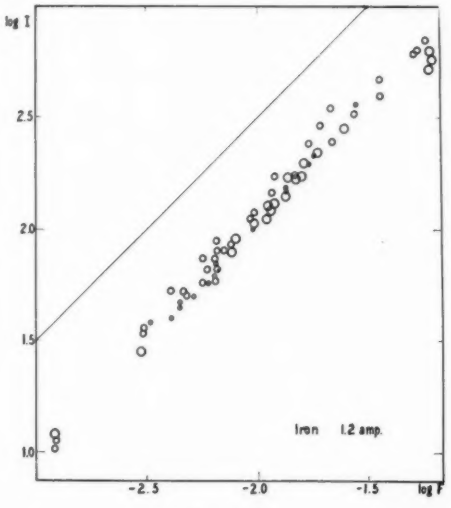

FIG. 2(a).

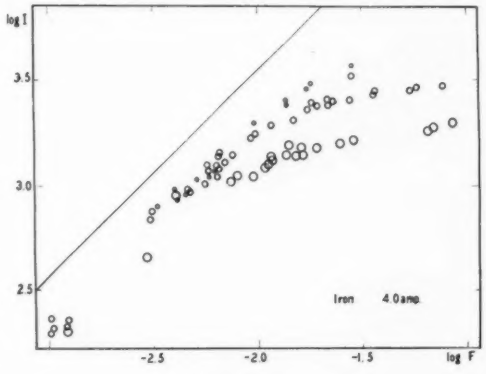

FIG. 2(b).

Figure 4 shows data similar to that for the previous figure, and using the same electrodes, but at a higher arc current. Here again the differences in self-reversal as a function of arc current are apparent. At the same time another feature is marked in Fig. 4 that had been indicated in the intensity measures at lower currents. Both elements, iron and titanium, exhibit a tendency to attain a maximum intensity, but that intensity is about four times as great for titanium as for iron. Furthermore, the intensities of the iron lines exhibit the dependence on excitation potential which is typical of, and may probably be ascribed to, the self-reversal of the lines; but for titanium such a dependence on excitation potential is not evident.

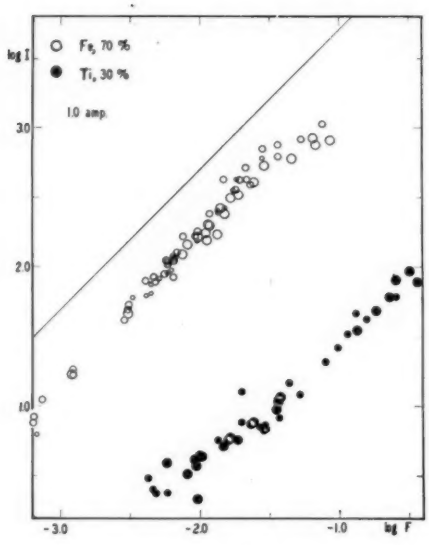

FIG. 3(a).

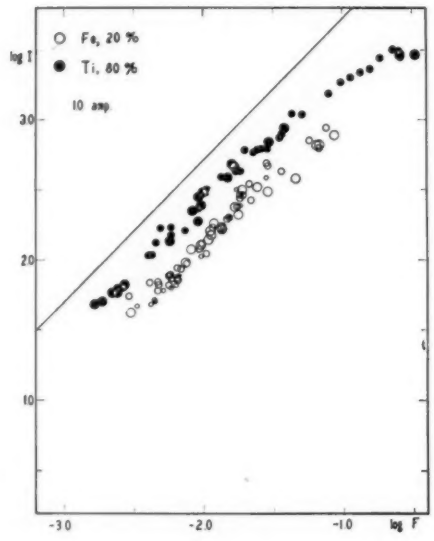

FIG. 3(b).

The difference in these two respects in the behavior of the two elements leads one to suggest the hypothesis that the diminution in intensity of the stronger titanium lines may be due not to self-reversal but to self-absorption. Further study of this question can best be accomplished by considering the true line profiles.

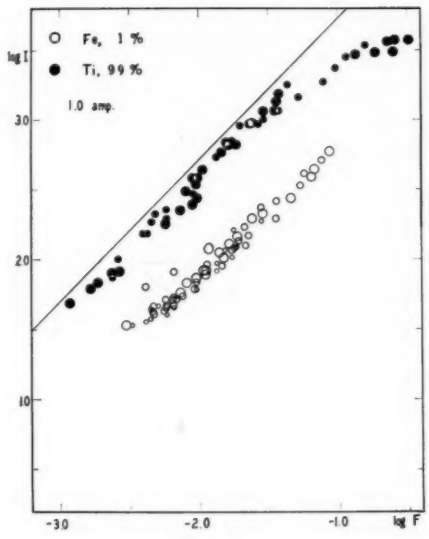

FIG. 3(c).

POSSIBLE APPLICATIONS TO ANALYSIS

The question now arises, to what extent we can avoid the limitations on analysis imposed by the foregoing observations, of self-reversal or of self-absorption, as the case may be. Let us return to Figs. 3(a)–(c). We see that a rational criterion of concentration ratio may be taken as

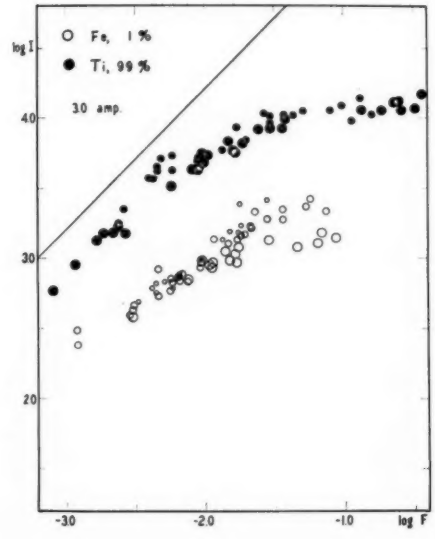

FIG. 4.

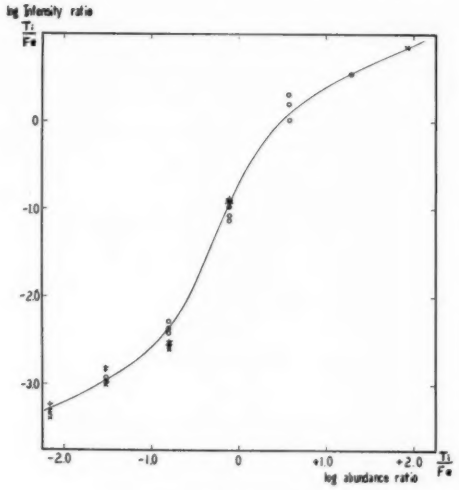

FIG. 5.

the intensity ratio of any two points on the straight-line portions of these graphs. Or, since it is difficult to choose two lines which will always be available, at different levels of intensity, let us choose the actual distance (which is a ratio, since the scale is logarithmic) between the two straight-line portions. This is best accomplished by denoting by $\log I_0$ the intercept of the straight-line portion with the abscissa $\log F=0$, and then using as the criterion of intensity ratio the quantity

$$\log I_0(\mathrm{Ti}) - \log I_0(\mathrm{Fe}).$$

Determinations of this parameter have been carried out, using the range of concentrations 1 percent to 99 percent, and a low arc current. Observations were made on three separate occasions, approximately one week apart. The resulting data are shown in Fig. 5, in which three different symbols are used to denote the different series of measurements. While the scatter is appreciable (probably due, as indicated above, to the grain size of the electrode components), there is a continuous curve between the observed points. Moreover, the curve does not flatten off at intermediate values of the concentrations, as do the usual working curves, so that the parameter here considered may be interpreted as a valid criterion of the proportions of the two components of the electrodes throughout the entire possible range of concentration ratios.

The point of inflection in Fig. 5 is at first quite startling, but it may at least partially be explained by reference to the absolute value of

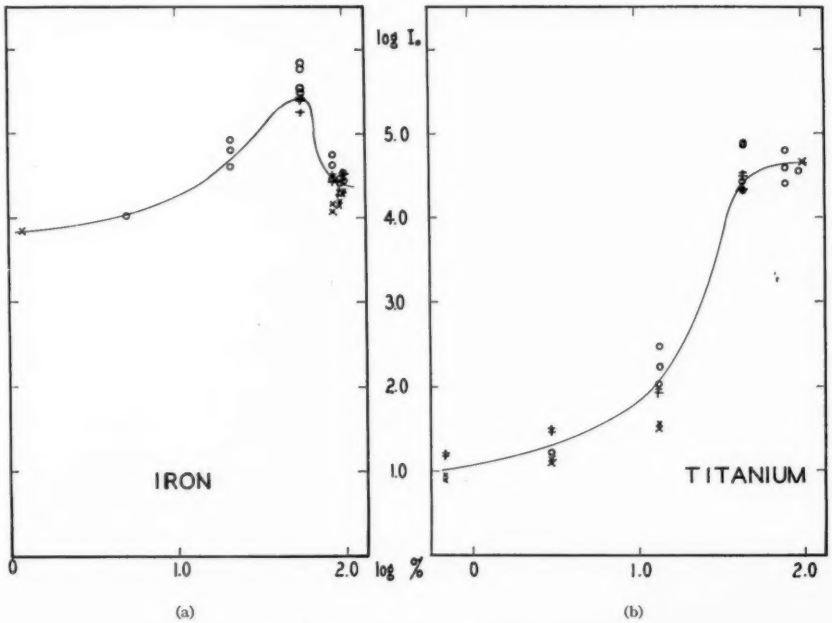

FIG. 6.

the intensities of the lines of the two elements, using, as above, the intercept I_0 as a measure of the absolute intensity of the element in question. The relevant data are shown in Fig. 6(a), (b). The absolute intensity of the iron lines increases throughout the range of low concentrations, reaches a maximum at about 50 percent, then diminishes. The titanium intensity, on the other hand, varies over a wider range, and reaches a flat-top maximum at about 50 percent. Very probably these effects can be ascribed to interactions between the ions of the two elements in the formation of the arc; their further investigation, and extension of the investigation to cases involving other elements, might be expected to throw considerable light on the problems of analysis caused by the anomalous influences of extraneous elements. An extension of this investigation, and of some problems raised by it, is in progress.

Emission Spectra of the Rare Earth Elements*

WILLIAM F. MEGGERS
National Bureau of Standards, Washington, D. C.

SCARCELY anyone will now deny that modern spectrographic methods are competing successfully with conventional chemical methods of making routine analyses of metals and alloys. For various reasons standardized chemical methods, at this moment, possess certain advantages over atomic emission spectra in the analysis of gases and nonmetals. There are, however, two groups of chemical elements, the noble gases and the rare earths, that cannot be determined quantitatively by ordinary chemical methods for the simple reason that the first group forms no chemical compounds, and the second group forms essentially identical compounds. For routine analyses of mixtures of noble gases or of rare earths, spectrographic methods are the same in principle as for metals and alloys, and they require only calibration to make them available. Analysis of noble gas mixtures will require some specialized technique and will be handicapped in sensitivity by the fact that their strongest lines are shorter than 1800A and by the relatively large range of ionization potentials (Rn = 10.69v, He = 24.46v).

The rare earths, on the other hand, have low ionization potentials (5 to 7v) so that the strongest lines of their first two spectra occur in the visible or adjacent ultraviolet. Although the ionization potentials are nearly identical, large differences in absolute sensitivity of individual rare earths may be expected because of wide variations in spectral structure. Whereas neutral noble gases with closed shells emit spectra constructed on the same general plan (singlets and triplets) the rare earths exhibit the entire range of spectral term multiplicities from one to eleven. Furthermore, it is easy to excite the first spectra of noble gases without a trace of the second spectra, but the conventional arc shows a confusing mixture of successive spectra when rare earths are present. Finally, the first two spectra of each of the noble gases are among the best described and analyzed, whereas the rare earths are characterized in general by poorly described spectra of great complexity, and until recently nothing was known about the structures of their spectra. In every case the practical applications of spectra in chemical analysis are greatly facilitated by reliable descriptions of the spectra (to insure against misidentifications) and by classification of the stronger lines (so that proper lines may be chosen for quantitative analysis). In 1927, when Hund[1] developed the general correlation of spectral terms and valence electron configurations, he remarked that typical spectra had been analyzed in nearly all the periods, "Nur an einer Stelle des periodisches Systems klafft eine grosse Lücke. Von den seltenen Erden ist noch kein Spektrum in Terme geordnet."

In recent years considerable progress has been made in the interpretation of rare earth spectra, but this group of elements still remains the outstanding problem in spectroscopy. The purpose of this paper is to summarize what is now known concerning the term structures of rare earth spectra.

A dozen years ago, I attacked the first two spectra of cerium, searching for constant wave number differences among lines for which King[2] had supplied temperature classification. Of course, many repeating differences were found, but every attempt to set up a significant quadratic array was frustrated and it was concluded that the observed regularities were fortuitous.

A few years later two papers purporting to give regularities in cerium spectra were published in Germany. The first is by Karlson[3] who claims to classify 540 lines of the arc spectrum, and the second by Haspas[4] who reports a classification for 430 Ce II lines. The results of both papers appear to be entirely artificial; they are excellent examples of the "snare and delusion" possibilities of complex spectra, especially those of rare earth elements. To this date no true interpretable

* Presented at the Eighth Summer Conference on Spectroscopy and Its Applications at Massachusetts Institute of Technology, July, 1940.

[1] F. Hund, *Linienspektren und Periodisches System der Elemente* (Julius Springer, Berlin, 1927), p. 175.
[2] A. S. King, Astrophys. J. **68**, 194 (1928).
[3] P. Karlson, Zeits. f. Physik **85**, 482 (1933).
[4] K. Haspas, Zeits. f. Physik **96**, 410 (1935).

regularities in the first spectrum of Ce have been published.

In 1935, Professor Harrison and I attacked the Ce II spectrum with the automatic interval sorter.[5] A plausible quadratic array was set up but it was abandoned when attempts to extend it met with no success. This spectrum finally succumbed to systematic analysis by Albertson and Harrison on the basis of new wave-length data,[6] and, since more than 3400 lines are now accounted for, it probably leads all complex spectra in the completeness of its line placement. The new wave-length data give an average difference of observed and computed wave number values of less than 0.02 cm^{-1}. The probability of finding by accident a solid array of even four columns and ten rows with this tolerance is less than one in a million, starting with any random interval and the actual density of Ce II lines. If the tolerance were doubled the probability would increase to 1 in 10. With the data formerly available and tolerances of more than 0.2 cm^{-1}, such chance arrays become very numerous. The lowest term in the Ce II spectrum is $(4f\ 5d\ 6s)\ {}^4H_{3\frac{1}{2}}{}^\circ$.

Russell and King[7] have accounted for 294 Ce III lines as combinations of 33 triplet and singlet terms, but no terms associated with the electron configuration $4f^2$ (which probably includes the normal state) have been found.

Several lines of the Ce IV spectrum have been classified[8] but the lowest state has not been found.

Having failed to find real regularities in Ce spectra, I looked in 1930 at the other end of the period and was impressed by the relative simplicity of Lu spectra. Systematic subtractions of the wave numbers of the stronger arc lines from one another immediately disclosed a recurring difference of 1994 cm^{-1} which was assumed to belong to $(4f^{14}\ 5d\ 6s^2)\ {}^2D$. Improved data on wave-lengths and intensities enabled Meggers and Scribner[9] to classify and interpret the principal lines of the first three spectra of Lu. The (normal state) lowest term of Lu II was found to be represented by $(4f^{14}\ 6s^2)\ {}^1S$, and of Lu III by $(4f^{14}\ 6s)\ {}^2S$.

We next turned our attention to Yb spectrum and in connection with new wave-length and intensity data announced the term combinations for the principal lines of the first two spectra.[10] The normal state of Yb atoms was found to be represented by $(4f^{14}\ 6s^2)\ {}^1S$, and of Yb^+ ions by $(4f^{14}\ 6s)\ {}^2S$.

Because most of the earlier available samples of Lu and Yb were contaminated by Tm, it was necessary to study Tm spectra with some care in order to identify its lines as "impurities" in other spectra. During the past year I have completed a list[11] of more than 5000 Tm lines (2200 to 9000A), and only a month ago I found the first real regularities among Tm lines. By selecting a group of 70 easily excited spark lines and subtracting their wave numbers from each other, two significant differences (236.95 and 187.78 cm^{-1}) were found to connect 50 of the lines. Zeeman patterns indicate that these four levels are identifiable as $(4f^{13}\ 6s)\ {}^3F^1F$, and ${}^3F_4{}^\circ$ is the lowest level. The normal state of neutral Tm atoms is probably represented by $(4f^{13}\ 6s^2)\ {}^2F_{3\frac{1}{2}}{}^\circ$, but this is not yet established definitely.

TABLE I. *Electron configurations and lowest terms.*

Atomic Number	Element	Theoretical Electrons	Term	Experimental			
				Neutral Atoms		Ionized Atoms	
				Electrons	Term	Electrons	Term
58	Ce	$f\,d\,s^2$	${}^3H$	$(f\,d\,s^2)$	$({}^3H)$	$f^2\,s$	${}^4H$
59	Pr	$f^2\,d\,s^2$	${}^4K$	$(f^2\,d\,s^2)$	$({}^4K)$	$f^3\,s$	${}^5I$
60	Nd	$f^3\,d\,s^2$	${}^5L$	$(f^4\,s^2)$	$({}^5I)$	$f^4\,s$	${}^6I$
61	Il	$f^4\,d\,s^2$	${}^6L$	$(f^5\,s^2)$	$({}^6H)$		
62	Sm	$f^5\,d\,s^2$	${}^7K$	$f^6\,s^2$	${}^7F$	$f^6\,s$	${}^8F$
63	Eu	$f^6\,d\,s^2$	${}^8H$	$f^7\,s^2$	${}^8S$	$f^7\,s$	${}^9S$
64	Gd	$f^7\,d\,s^2$	${}^9D$	$f^7\,d\,s^2$	${}^9D$	$f^7\,d\,s$	${}^{10}D$
65	Tb	$f^8\,d\,s^2$	${}^8H$	$(f^8\,d\,s^2)$	$({}^8H)$		
66	Ds	$f^9\,d\,s^2$	${}^7K$	$(f^{10}\,s^2)$	$({}^6I)$		
67	Ho	$f^{10}\,d\,s^2$	${}^6L$	$(f^{11}\,s^2)$	$({}^4I)$		
68	Er	$f^{11}\,d\,s^2$	${}^5L$	$(f^{12}\,s^2)$	$({}^3H)$		
69	Tm	$f^{12}\,d\,s^2$	${}^4K$	$f^{13}\,s^2$	${}^2F$	$f^{13}\,s$	${}^3F$
70	Yb	$f^{13}\,d\,s^2$	${}^3H$	$f^{14}\,s^2$	${}^1S$	$f^{14}\,s$	${}^2S$
71	Lu	$f^{14}\,d\,s^2$	${}^2D$	$f^{14}\,d\,s^2$	${}^2D$	$f^{14}\,s^2$	${}^1S$

[5] G. R. Harrison, Rev. Sci. Inst. **3**, 753 (1932); *ibid.* **4**, 581 (1933).

[6] W. E. Albertson and G. R. Harrison, Phys. Rev. **52**, 1209 (1937); *ibid.* **57**, 1073 (1940).

[7] H. N. Russell and R. B. King, Phys. Rev. **52**, 456 (1937).

[8] R. C. Gibbs and H. E. White, Phys. Rev. **33**, 159 (1929); J. S. Badami, Proc. Roy. Soc. (London) **43**, 53 (1931).

[9] W. F. Meggers and B. F. Scribner, Bur. Stand. J. Research **5**, 73 (1930).

[10] W. F. Meggers and B. F. Scribner, J. Research Nat. Bur. Stand. **19**, 651 (1937).

[11] W. F. Meggers, unpublished.

The tendency for d type electrons to fill or half-fill their shells prematurely was discovered years ago when the spectra of neutral atoms in the first long period were analyzed. It now appears from the analysis of rare earth spectra that f type electrons exhibit a similar tendency. The shell of f electrons is expected to be complete with 14 in Lu, but the spectra show that it is already complete in Yb, and that Tm probably has 13 f electrons instead of the 12 expected. In like manner, with regular addition of f electrons, the shell would not be half-filled until Gd, but analyses of spectral structure disclose that Eu already has seven, and Sm has six instead of the theoretical five.

The analysis of the Gd I spectrum is due to Albertson[12] who finds that the normal configuration and lowest state is $(4f^7\ 5d\ 6s^2)\ {}^9D_2{}^\circ$, in agreement with theory.[1] Unpublished results of Gd I analysis by Albertson and Russell include multiplets belonging to the undecet system. All possible multiplicities of spectral terms from 1 to 11 are thus established.

According to Albertson *et al.*,[13] the normal electron configuration of singly ionized gadolinium is $4f^7\ 5d\ 6s$, which gives ${}^{10}D_{2\frac{1}{2}}{}^\circ$ as the ground state of Gd II.

The Eu I spectrum has been almost completely classified by Russell and King[14] who identified terms belonging to sextet, octet and decet systems and fixed the lowest level as $(4f^7\ 6s^2)\ {}^8S_{4\frac{1}{2}}{}^\circ$.

The principal features of the Eu II spectrum have been interpreted by Albertson[15] who has shown that the lowest level is $(4f^7\ 6s)\ {}^9S_4{}^\circ$.

[12] W. Albertson, Phys. Rev. **47**, 370 (1935).
[13] W. Albertson, H. Bruynes and R. Hanau, Phys. Rev. **57**, 292 (1940).
[14] H. N. Russell and A. S. King, Astrophys. J. **90**, 155 (1939).
[15] W. Albertson, Phys. Rev. **45**, 499 (1934); *ibid.* **46**, 1023 (1934).

Albertson has also analyzed the first[16] and second[17] spectra of Sm. For the Sm I spectrum the lowest level is demonstrated to be $(4f^6\ 6s^2)\ {}^7F_0$, while for Sm II it is $(4f^6\ 6s)\ {}^8F_{\frac{1}{2}}$.

The only other rare earth spectra that have thus far yielded to analysis are the second spectrum of praseodymium and of neodymium. The lowest term in the Pr II spectrum is $(4f^3\ 6s)\ {}^5I_4{}^\circ$, according to Harrison and Rosen,[18] while in the Nd II spectrum it is $(4f^4\ 6s)\ {}^6I_{3\frac{1}{2}}$ according to Albertson.[19]

Theoretical configurations[1] and experimental findings in neutral rare earth atoms are summarized in Table I. Values in parentheses are predicted by Albertson.[17] Experimental results for singly ionized atoms of rare earths are collected in the last column of Table I.

The results may be summarized as follows: With considerable certainty the lowest spectral terms have been established spectroscopically for six rare earths in the neutral state and for nine in the singly ionized state. In most cases there is present a premature addition of f type electrons to fill or half-fill the $4f$ shell. Divergences between theoretical and experimental results are mainly due to the fact that the first theory neglected to take account of this tendency of larger shells to hasten their completion. This also accounts for the divalent properties of Sm, Eu and Yb. It appears that ionization usually occurs through the removal of one of two outermost s type electrons, and the spectra of ionized rare earths will consequently contain intense lines resulting from a simple $s \rightarrow p$ excitation.

[16] W. Albertson, Phys. Rev. **47**, 370 (1935); *ibid.* **52**, 644 (1937).
[17] W. Albertson, Astrophys. J. **84**, 26 (1936).
[18] G. R. Harrison and N. Rosen, unpublished.
[19] W. Albertson, unpublished.

Commercial Applications of Visual Spectroscopic Analysis*

F. H. EMERY
The Harshaw Chemical Company, Cleveland, Ohio

THE largest commercial application of the visual spectroscope is for qualitative analysis. It serves as a rapid means of proof of the identity of an alloy. Three or four dozen such instruments are in use in various parts of the world for sorting steels. The United States has not as yet adopted this method as extensively as it has been adopted in England and other parts of Europe. The presence of the alloying constituents specified for the alloy, and the absence of more than residual amounts of other alloying elements serves to prove the identity of a sample. The examination can be made by one man in a minute or less. The following elements occurring in steels can be identified spectroscopically, by examination of the arc spectrum: aluminum, columbium, cobalt, copper, chromium, lead, manganese, molybdenum, nickel, sulfur, silicon, titanium, tungsten, and vanadium. There are several limitations to this list. Many of these elements will not be detected by the spectroscope if less than 0.1 percent is present. Aluminum can be found in nitriding stock, but the aluminum in a rimmed or killed steel cannot be detected. Nickel must be present to the amount of 1 percent before it can be detected. Sulfur is detectable in free machining screw stock only. Because of the fact that the only visible silicon line available in the arc is at 3905A at which point the eye has less than 1 percent of its green sensitivity, about 2 percent silicon must be present before most eyes can see it.

Mixed stock is a real problem to manufacturers who make or use steel. It occasionally happens that a few bars of the wrong analysis will be mixed into a bundle. After the bundle has been put through a riveting machine, for example, each of a number of kegs will contain a number of rivets of the wrong analysis. After heat treatment these are certain to be either too soft, too weak, or too hard, so the customer cannot use them. In this case the entire shipment of rivets will be returned, and the manufacturer is faced with the problem of sorting or scrapping a considerable investment. Some companies offer a standing reward of $2 to any workman who discovers a misplaced bar. The metal perhaps will not swage or draw properly and the workman reports it. Most companies have a man who is an expert spark tester. The sample is held against an emery wheel and the amount and character of the sparks noted. This method is complementary to spectroscopic analysis since it is most accurate for the determination of carbon, for which the spectroscope is not suited. Many men can determine the amount of carbon up to forty points with an accuracy of better than 10 percent of the amount present. They can do this on plain carbon steels only, and the presence of alloying constituents seriously interfers with the accuracy. If these spark testers were to be provided with spectroscopes in addition to their usual equipment, they would acquire the ability to do surprisingly accurate semiquantitative analysis.

The basic instrument used in such work is a visual spectroscope, such as those manufactured by Bausch and Lomb, Hilger, or Gaertner. Hilger is the pioneer in the development, having sold the Spekker Steeloscope for over ten years. Spectroscopes built for steel analysis have a scale marked with the symbols of the common steel alloying elements. The operator sets the index to the element it is desired to determine. He then observes the spectrum produced by the instrument and compares it with standard prints furnished with the instrument. These photographic reproductions of spectra from standard alloys make it easy for an operator to locate the exact position of a line due to the alloying element. If the line has a standard intensity relative to a neighboring iron line, the element is present in the proper amount. The standard charts and indexed element symbols make it easy to train an unskilled operator to identify steel alloys.

Since nonferrous spectra are less complex than

* Presented at the Eighth Summer Conference on Spectroscopy and Its Applications at Massachusetts Institute of Technology, July, 1940.

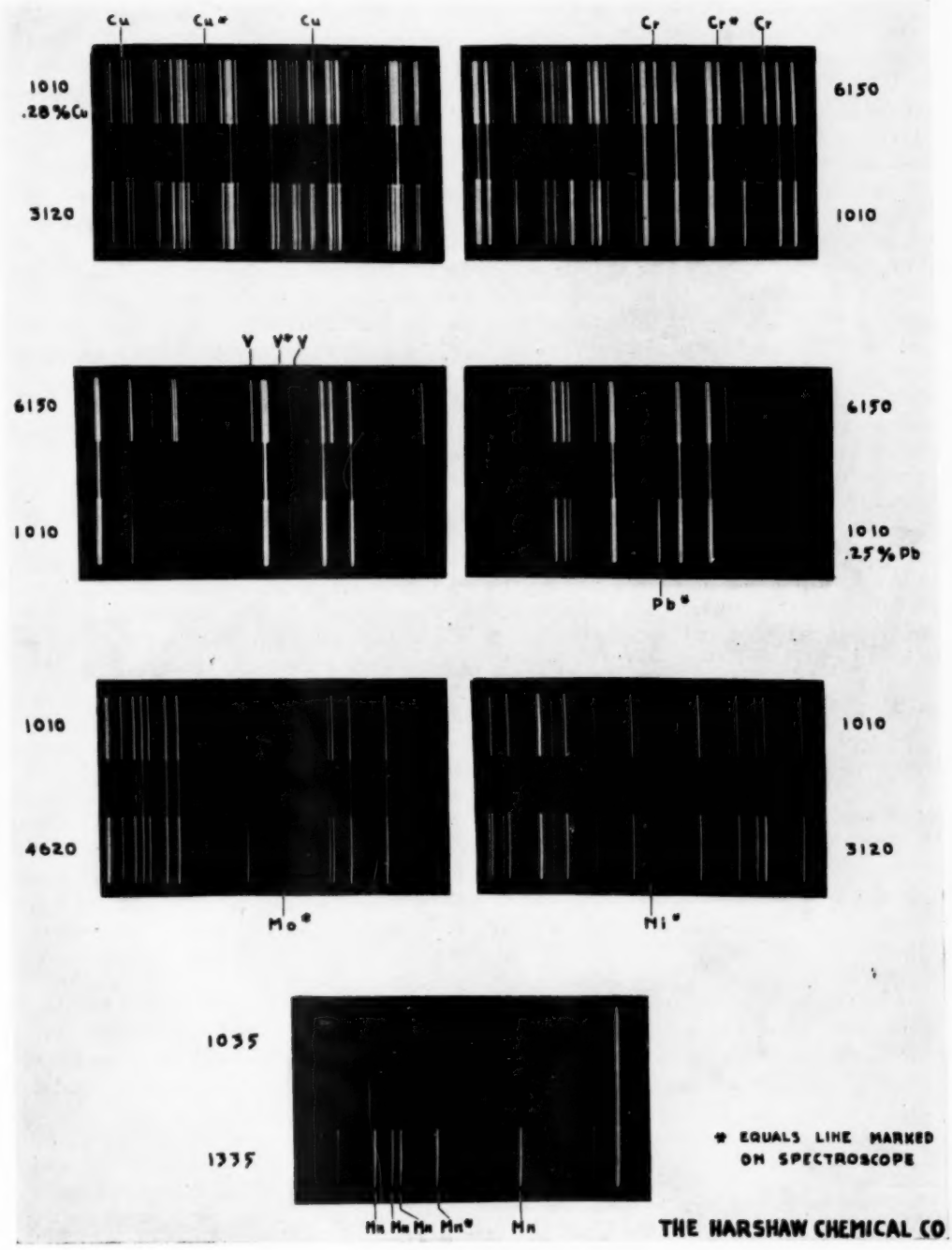

FIG. 1. Spectroscopic steel chart.

other spectra, the various alloys of aluminum, copper, lead, cadmium, etc. can be identified with ease and certainty. The spectroscope may also be used for quantitative analysis of both ferrous and nonferrous alloys.

The equality of two light sources may be judged by the eye with great accuracy. Whenever it is possible spectroscopically to correlate the equality of two neighboring lines with a percentage composition, quantitative analysis can be carried out. Match points can be set up according to Gerlach and Schweitzer's[1] internal standards method. The line from the element to be analyzed may be correlated with a faint line of the major constituent, or it may be matched with a line caused by a secondary constituent present in known amounts. The auxiliary standard method may also be used where the line from the element to be analyzed is matched against a line from a standard lamp or iron arc. The two sources may be viewed at once by the use of a prism before half the slit. If a standard lamp is used, its intensity may be varied until a match is obtained. The percentage composition can then be obtained from a previously made calibration curve.

Another way of producing a continuously variable line to be used as a standard for matching is to use the method of Wendt and Heun.[2] They match a spark line of the major constituent against an arc line of the element to be determined, using a spark from an oscillating circuit, in which the inductance may be varied. This method takes advantage of the difficulties which the Feussner[3] circuit aims to eliminate. The Feussner circuit introduces great damping or quenching so that only the initial high voltage spark-like spectrum is obtained. Wendt and Heun use variable damping but always less than Feussner. The less damping the circuit has, the longer the duration of the spark and the greater the number of arc-like oscillations. With little damping, the spark line will be fainter and the arc line stronger. The damping is varied by varying the inductance. A standard curve is made by plotting the amount of inductance in the circuit against the composition of the sample when a selected pair of arc and spark lines are of equal intensity. A variation of this method is to match the selected line of the substituent element against an air line, the intensity of which can be easily varied by changing the inductance.

The Barratt[4] method is based on the statement that two equivalent sparks in series will show equal line intensity only if the elements to be analyzed are present in equal amounts. The method can be used for elements present to the amount of 5 percent or more. It does not, however, have any better accuracy than other methods, and one must be prepared to accept errors which are large compared to those obtainable by chemical methods, when large amounts are analyzed.

Another English development is the Insta[5] eyepiece developed and sold by Adam Hilger. This device uses the spectrum from one source. The lines are divided in the center and means are provided for moving the top half relative to the bottom. In this way, lines a considerable distance apart can be brought into coincidence. The eyepiece also contains wedges by which the intensity of one-half of the spectrum can be varied until a match is obtained. Wedge settings are plotted against compositions.

As in all spectral analysis, the greatest source of error in all these methods is the variation of the light source. Difficulties from this cause will be greater than in spectrographic methods since the eye does not integrate while a plate does. It is possible to avoid some of this error, by viewing the lines at some definite time after striking the arc, and by disregarding any spectrum produced by a hissing arc. An accuracy of 10 percent of the amount present, or perhaps a little better, can be obtained. The method is not suitable for production use by one man since it is too fatiguing to the eye.

Future developments should include instruments having greater dispersion and longer range than those now available. An ultraviolet spectroscope fitted with a fluorescent eyepiece would enable one to detect small amounts of Ni in steel.

[1] W. Gerlach and E. Schweitzer, *Foundations and Methods of Chemical Analysis by the Emission Spectrum* (Adam Hilger, Ltd., London).
[2] A. Wendt and H. Heun, Zeits. f. Physik **93**, 92–9 (1934).
[3] U. S. Patent No. 1,971,215.
[4] L. J. Spencer, J. Sci. Inst. **8**, 229–32 (1931).
[5] U. S. Patent No. 1,902,109.

Some Horticultural Applications of Spectrochemical Analysis*

B. C. BRUNSTETTER AND A. T. MYERS
Division of Fruit and Vegetable Crops and Diseases, Bureau of Plant Industry, United States Department of Agriculture, U. S. Horticultural Station, Beltsville, Md.

THE purpose of this paper is to describe briefly some of the horticultural problems that the spectrographic laboratory of the United States Horticultural Station at Beltsville, Maryland, has been attacking cooperatively with various staff specialists during the past two years.

In cooperation with Dr. C. A. Magoon, a series of studies has been made on the mineral composition of grape leaves, with the hope that light might be thrown on various problems of vineyard management and differences in varietal performances. The spectrochemical technique used has already been described.[1] Leaves were sampled before the application of Bordeaux spray about 3 weeks before flowering. From each vine, leaves were taken from corresponding positions on the canes and were therefore comparable with respect to stage of development.

In Table I analytical data are summarized for 8 elements in leaves of 25 varieties of American bunch grapes. It will be noted[2] that there is quite a wide range in concentration of the different elements among the varieties. In the cases of iron and aluminum, however, because of possible dust contamination of samples from 2 varieties, the range is probably abnormally great. This varietal survey is the first comprehensive analysis of grape leaves ever made in this country, and it was made possible by the peculiar advantages of the spectrochemical technique.

One result of this survey is that varieties showing extremes of concentration have been spotted for future study. For example, the variety Peabody showed a concentration of 12 parts per million of copper in the dried leaves whereas there were 52 parts per million in those of the Lucile variety. Detailed study of single varieties by Dr. Magoon has revealed a number of suggestive relationships between mineral concentration and biological properties of the varieties.

In the two studies represented by the data in Table II, samples were collected from 20 vines of the Concord variety, 18 of the Ontario variety, and 17 of the Delaware variety. The figures seen are based on 609 analyses in triplicate. An example of the comparisons made possible by this study is found in the cases of phosphorus and magnesium. The leaves of the Ontario variety showed a significantly greater concentration of phosphorus than those of the Concord and Delaware varieties, but had a lower concentration of magnesium. Each of these three varieties were given two cultural treatments, clean cultivation *vs.* mulch, and two fertilizer treatments, complete fertilizer *vs.* nitrate of soda. Detailed analysis concerning the effect of these different treatments, have been published elsewhere.[3,4]

The coefficients of variability seen in Table II are interesting because they show that for some elements, such as potassium, phosphorus, magnesium, and copper the over-all variation is quite low. The sampling variations appear to be only slightly in excess of the analytical errors. An interesting point in this connection is that the rapidity of the spectrochemical method makes it possible to replicate sufficiently so that vari-

TABLE I. *A survey of 8 mineral elements in leaves of 25 varieties of grapes.*

ELEMENT	[PERCENTAGES OF DRY WEIGHT] MEAN	RANGE
K	2.05	1.46 –3.00
P	0.50	0.36 –0.73
Ca	1.35	0.87 –1.98
Mg	0.31	0.17 –0.49
Al	0.042	0.025 –0.14
Fe	0.017	0.0093–0.048
Mn	0.022	0.016 –0.034
Cu	0.0025	0.0012–0.0052

* Presented at the Eighth Summer Conference on Spectroscopy and Its Applications at Massachusetts Institute of Technology, July, 1940.

[1] B. C. Brunstetter, A. T. Myers, H. L. Wilkins and M. A. Hein, *Sixth Summer Conference on Spectroscopy and Its Application* (John Wiley, 1939), p. 14.

[2] B. C. Brunstetter, A. T. Myers, I. W. Dix and C. A. Magoon, Proc. Am. Soc. Horticultural Sci. **37**, 635 (1939).

[3] C. A. Magoon, A. T. Myers, I. W. Dix and B. C. Brunstetter, Proc. Am. Soc. Horticultural Sci. **36**, 485 (1938).

[4] A. T. Myers, B. C. Brunstetter, I. W. Dix and C. A. Magoon, Proc. Am. Soc. Horticultural Sci. **37**, 645 (1939).

ability can be measured and the significance of differences can be calculated. Thus differences in inorganic composition, which though small are significant, may be readily detected.

Other spectrochemical studies of the inorganic composition of grape leaves are in progress. The goal of these analyses is to learn whether a knowledge of the inorganic nutrition of grape vines will answer questions such as these: What varieties persistently exhibit peculiarities of absorption of one or more elements? What is the minimum concentration of an essential element in the leaf required to sustain growth and give an acceptable yield? What is the range of concentration in the leaf that will indicate that a fertilizer application will give little or no response because the vine is able to absorb enough of the element from the soil for its needs? To what extent is there an inorganic nutritional basis for such undesirable grape varietal characteristics as fruit cracking, "shattering," or dropping of the fruit from the vines prematurely, poor yield, vine weakness, premature loss of foliage, or for poor or uneven coloring of the fruits?

A number of investigations with other horticultural crops are in progress. Pecan leaves have been analyzed to learn the increase of copper content in the interior of the leaves after spraying with Bordeaux mixture; other samples have been studied to learn whether trace element deficiency is the cause of pecan leaf scorch. Often apple trees show a physiological disease of the bark known as "measles"; samples of bark have been analyzed to learn whether the concentrations of inorganic elements were in any way responsible. Samples of skin and flesh of apples from different regions in Maryland are being studied to learn whether differences in keeping quality in cold storage are associated with differences in mineral composition. Spindling-sprout disease of potatoes is being studied by analysis of normal sprouts in comparison with spindle sprouts. This list of problems and activities is by no means complete but serves to illustrate the range of applicability of spectrochemical analysis to horticultural problems.

TABLE II. *Comparison of mineral content of leaves of 3 varieties of grapes.*

	[PERCENTAGE OF DRY WEIGHT]					
	CONCORD		ONTARIO		DELAWARE	
ELEMENT	MEAN	C.V.	MEAN	C.V.	MEAN	C.V.
K	1.97	11.8	2.20	18.6	2.44	10.2
P	0.61	13.6	0.76	11.6	0.59	12.7
Ca	0.57	21.4	0.47	17.9	0.72	22.2
Mg	0.28	15.0	0.22	10.9	0.27	13.3
Al	0.045	18.7	0.041	13.7	0.048	14.6
Fe	0.019	30.0	0.022	41.4	0.020	11.9
Mn	0.018	24.4	0.022	18.2	0.016	17.3
Cu	0.0041	9.8	0.0047	11.1	0.0048	16.7
B	0.0017	28.5	0.0016	18.8	—	—

TABLE III. *Chemical vs. spectrochemical determination of sodium.*

	[PERCENTAGE OF DRY WEIGHT]			
	ASH	SODIUM		
PLANT PART	PERCENT	CHEMICAL PERCENT	SPECTROCHEM. PERCENT	DEV. FROM MEAN PERCENT
Kale				
Old petioles	20.3	3.11	3.57	6.9
Medium petioles	13.3	1.29	1.50	7.5
Young petioles	12.2	0.42	0.59	16.8
Young petioles	11.4	0.82	1.07	13.2
Red beet				
Old petioles	25.8	2.98	3.09	1.8
Old petioles	19.0	0.98	0.99	0.5
Old petioles	24.5	5.26	5.31	0.5
Young petioles	18.6	3.46	3.95	6.6
Young petioles	17.8	2.07	2.02	1.2
Young petioles	17.0	1.05	1.15	4.5
Young leaves	16.2	0.47	0.69	19.0
Sugar beet				
Young petiole	13.3	0.69	0.79	6.8
Young petiole	13.3	1.46	1.99	15.4
Young petiole	14.9	0.83	1.33	23.2
Old leaves	17.2	1.37	1.66	9.6
Old leaves	20.7	4.28	4.46	2.1
Old leaves	20.7	4.47	5.29	8.4
Young leaves	13.2	2.53	2.30	4.8
Swiss chard				
Leaves	11.8	1.45	1.86	12.4
				Av. 8.5

In Table III analytical data are presented for sodium, an element not often investigated in horticultural work, because it is not considered an essential element and does not usually occur in plant tissue in amounts above a few tenths of a percent. In cooperation with Dr. J. S. Caldwell, a number of samples were analyzed for sodium. The samples listed in Table III represent only a small fraction of those taken in an extensive fertilizer investigation where one of the objectives was to study the effect of excessive

applications of nitrogen in the form of sodium nitrate.

It appeared to be a good opportunity to compare spectrochemical with chemical determinations of sodium, obtained by the use of Kolthoff's zinc uranyl acetate method.[5] The total salt content of the spectrochemical standards and samples was made approximately constant by the addition of suitable amounts of potassium chloride. No internal standard was used and the plates were not calibrated. For the most part analyses were made in duplicate only by both methods.

As shown in Table III, in 17 out of 19 cases the spectrochemical method gave higher results. The average deviation from the mean of the two methods was 8.5 percent, a degree of concordance sufficient for the purpose in hand.

Another example of a comparison between chemical and spectrochemical data has been made possible by the cooperation and courtesy of Dr. L. P. Batjer, who has been analyzing leaves and fruits of apples for boron in order to get an idea of the concentrations indicating deficiency and to learn the degree of response by measuring the increased boron concentrations when that element is injected into the trees, sprayed on the trees, or applied to the ground about the trees. The method of boron analysis employed by Dr. Batjer was an electrometric titration technique devised by Wilcox.[6]

The salient features of Table IV from the analytical standpoint can be summarized by the following statements:

(1) The average deviation from the mean of triplicate spectrochemical analyses was 10.4 percent. The precision of the chemical data was much better, averaging 1.7 percent.

(2) The average deviation from the mean of chemical and spectrochemical analyses was 13.1 percent.

These boron analyses were made on samples ranging from 10 to 20 mg in weight, with the exception of the orange leaves where it was necessary to use a 1-mg sample size. Two sources of error decreased precision: First, with the high amperage used (22 amperes) and the short, high purity, high cost, upper electrodes, the arc occasionally flashed from the tip of the upper electrode to its base. In two cases noted this happened as soon as the arc was struck and lasted for several seconds. Two values for sample No. 104, to which potassium carbonate had been added, were correspondingly low; the triplicate values read 29.1, 31.9, and 43.5 parts per million of boron. A second source of error, it is believed, was caused by occasional irregularities in drying solutions of the samples in the lower electrodes. After ashing, addition of hydrochloric acid solution, and drying down in the electrodes, occasionally salts were deposited near the top of the cavities. In these cases more or less loss of material may occur when the arc is struck.

This spectrochemical method for boron appears to be sufficiently accurate for survey purposes. Samples 107 and 108 were pear leaves taken from check trees to which no boron had been applied; samples 109 and 110 were leaves from trees each of which had received a pound of borax applied to the soil. The spectrochemical as well as the chemical method detected the higher concentrations of boron in the leaves caused by the addition of boron to the soil. Similarly, in the apple leaves, sample 103 was taken from an untreated or control tree, whereas

TABLE IV. *Chemical vs. spectrochemical determination of boron.*

		[Dry Weight Basis]		
		Av. Boron Content in Parts per Million		
No.	Plant Part	Chemical[1]	Spectrochem.	Dev. from Mean Percent
101	Orange leaves (Valencia)	873.0	549.0	22.8
103	Apple leaves (Ben Davis)	34.5	29.9	7.1
104	do	37.8	45.0	8.7
104[2]	do	37.8	34.8	4.1
105	do	38.3	40.2	3.3
106	York fruit	29.5	20.9	17.1
106[2]	do	29.5	17.8	24.7
107	Pear leaves (Bosc)	21.5	14.5	19.4
108	do	19.8	16.6	8.8
109	do	32.9	24.4	11.5
110	do	29.6	21.3	16.5
				Av. 13.1

[1] Samples and chemical data supplied by Dr. L. P. Batjer.
[2] Ashed in presence of K_2CO_3.

[5] I. M. Kolthoff and E. B. Sandell, *Quantitative Inorganic Analysis* (Macmillan, New York, 1937), p. 395.
[6] L. V. Wilcox, J. Ind. Eng. Chem. Anal. Ed. **12**, 341 (1940).

samples 104 and 105 were leaves from trees that had been treated with boron. Here also the spectrochemical as well as the chemical method indicated an increased boron content.

Mercury disinfection is extensively used to control basal plate storage rot of narcissus bulbs. The floricultural project of the Beltsville station wanted to know whether mercury could be found in the interior of narcissus bulbs that had previously been treated with solutions of mercury compounds. Using a simple spectrochemical technique for the determination of mercury, analyses of dozens of bulbs showed that mercury was present in all parts of the interior of treated bulbs. The main features of the technique developed may be noted briefly. After removal of several outer scales and the exterior of the basal plate to avoid surface contamination, each bulb was dissected into basal plate, embryonic flower, and an inner and an outer sample of scale tissue. These various parts were cut into small pieces, dried at 60°C, and ground to 40 mesh.

The samples were not ashed before they were burned in the arc. Usually the sample size was 10 or 25 mg of dried plant tissue. In narcissus tissue containing mercury, the larger the sample size burned in the arc, the less the blackening of the mercury line at 2537A. To compensate for this effect of organic matter on mercury radiation, the same weight of narcissus tissue previously found to be free of mercury was added to various dilutions of a bichloride of mercury standard whose concentration ranged from 0.05 to 1.0 microgram of mercury per 0.1 ml.

Another important factor affecting sensitivity is the depth of the cylinder bored in the lower electrodes. For a given amount of mercury, blackening of the mercury line at 2537A increased as the depth of the cylinder increased, reaching a maximum at 15.0 mm.[7]

At the present time no data are available to measure the accuracy of this technique. Precision is only moderate, though adequate for the purpose of this preliminary survey. The average deviation from the mean of duplicate determinations ranged from 7 to 15 percent from plate to plate.

The concentration of mercury found in different parts within narcissus bulbs usually was less than 10 parts per million, dry weight.

In conclusion, there are two main types of situations in horticulture where spectrochemistry is invaluable. Ample material for analyses may be available, but the number of samples may be so great, as in surveys, that only by spectrochemical analysis can the data desired be secured in a reasonably short length of time. The reverse generally occurs in regional analysis where the distribution of one or more elements among the parts of a plant structure such as a bulb or a flower is desired. Here the small amount of sample available makes the spectrochemical technique indispensable.

[7] A. T. Myers and B. C. Brunstetter, J. Ind. Eng. Chem. Anal. Ed. **11**, 218 (1939).

Geochemical Study of Saratoga Mineral Waters by a Spectrochemical Analysis of Their Trace Elements*

LESTER W. STROCK AND S. DREXLER
New York State Research Institute of the Saratoga Spa, Saratoga Springs, New York

THE natural mineral waters of Saratoga Springs contain approximately equal amounts of the bicarbonates and chlorides of Na, K, Ca and Mg. The relative proportion and absolute amounts of these substances vary from spring to spring, but 15,000 mg/l of total solids are present in some of the waters, in addition to three to four volumes of free carbon dioxide.

This paper is the first report of a detailed investigation of the lesser abundant constituents of these waters, whose composition and origin are being studied from a geochemical standpoint. The experimental data is provided largely by quantitative spectrochemical analysis of groups of elements isolated chemically from the waters, as well as the geological formations of the region.

CHEMICAL ISOLATION OF Fe, Ti, V AND Zr BY CUPFERRON

The most conspicuous minor element in Saratoga mineral waters is approximately 5 mg/l iron. A spectrochemical analysis of the iron precipitated from the waters by various reagents offered a promising means of enriching, by a factor of 3000, those particular trace elements which are precipitated with iron. For this purpose a 7.5-liter sample of water was neutralized with HCl, concentrated to 500 cc and the iron precipitated with Cupferron in acid solution. This Cupferron precipitate of the iron was ignited to Fe_2O_3, mixed with two parts carbon powder, and arced. Its spectrum revealed the presence of surprisingly large amounts of zirconium, in fact, so much that a solid cap of unvaporized zirconium nitride remained on the cathode after arcing.† The presence of zirconium was previously unknown in these waters, and no record has yet been found of any reported concentration of this element in any other natural mineral water. Since both Ti and V are considerably more abundant than Zr in the earth's lithosphere,[1,2] this enrichment of Zr is of great geochemical interest.

In contrast with the large amount of zirconium present, no titanium or vanadium was detected in the spectra of the same sample of Fe_2O_3, in spite of the fact that all three elements are known to be precipitated by Cupferron[3–5] in acid solution. It was, therefore, necessary to study the effect of acidity and salt concentration on the Cupferron precipitation process, in order to prove that the absence of Ti and V was not due to an incompleteness in their precipitation. This was especially advisable in view of the high salt content of the acidified and concentrated mineral water samples, which contained approximately 110 grams of Na, K, Ca and Mg chlorides per 500 cc. Accordingly, a series of experiments were made with test solutions containing 25 mg Fe, and 0.125 mg each Ti, V and Zr in a total volume of 250 cc. Two series of these test solutions were precipitated with Cupferron at various acidities ranging from 15 percent HCl to $p\mathrm{H}=7$; one series from water solution and the other from salt solution equivalent to a concentrated mineral water sample. Neither the gravimetric nor spectrographic results showed any convincing effect of the acidity over the range from 15 percent HCl to $p\mathrm{H}=3$, while the only positive effect of high salt was to partially precipitate Ti from the test solution. The reproducibility of the spectrographic results, especially of Zr, were rather poor, and in order to evaluate their spread in terms of concentration, the amount of Ti, V and Zr in the test

* Presented by title at the Eighth Summer Conference on Spectroscopy and Its Applications at Massachusetts Institute of Technology, July, 1940.

† The sample was packed into the 1.5×4-mm crater of a 3.5-mm pure carbon cathode and arced for 3 min. 10 sec. at 6 amp. The zirconium nitride cap could not be completely vaporized by prolonged arcing even at 10 or 12 amp.; and even then it disappeared from the cathode by tiny explosions which contributed little or nothing to the spectral line intensity.

[1] G. v. Hevesy and K. Würstlin, Zeits. f. anorg. Chemie **216**, 305–11, 1934.

[2] V. M. Goldschmidt, Skr. Norske Vid.-Akad. Oslo, Mat.-Naturv. Kl., No. 4, 100 (1937).

[3] O. Baudisch, Arkiv. f. Kemi, Min. Geol. **12B**, No. 8, 1935.

[4] G. Frederick Smith, "Cupferron and Neo-Cupferron," Columbus, 1938.

[5] G. E. F. Lundell and J. I. Hoffman, *Outlines of Methods of Chemical Analysis* (New York, 1938), p. 117.

solutions was varied over the range 0.015 to 3.1 mg; keeping the Fe constant at 25 mg. The precipitations were made at 5 percent HCl. All the above experiments proved conclusively that Ti and V are actually very low or absent in the water.

Spectrographic Analysis of Fe–Cupferron Precipitate

Attempts to devise a quantitative spectrochemical method for analyzing the three elements concerned in Fe_2O_3 on the basis of the data obtained have led to great difficulties which have been partially solved after restricting the problem to a determination of Zr alone in Fe_2O_3.

The results of this attempt to determine zirconium in iron oxide illustrates, on a very exaggerated scale, the manner in which slight variations in operating technique—such as preheating in the arc—or in chemical combination of the elements in the sample can influence the intensity of the spectral lines. Such influences are frequently mentioned, but seldom accompanied by sufficient experimental data.

Determination of Zr in Fe_2O_3 in Presence of Ti and V

Figure 1 contains the Δ log T values* (exposure time ratio)[6,7] for the lines Zr 3273.04A and Fe 3280.26A from individual spectra of various amounts of Ti, V and Zr precipitated along with 25 mg Fe from the test solutions by Cupferron at 5 percent HCl. Similar plots were made for Ti and V, but the individual values for both of these elements showed a considerably smaller deviation from an average curve. In general, the values for V were the most constant, and those for Zr the least constant. These points were obtained from duplicate and even triplicate precipitates; but even for the same precipitate variations of as much as 0.5 in Δ log T were found. Two features of these data, as yet unexplained, are the high exposure-ratio values at 0.125 mg, and the results obtained by a mechanical dilution of some precipitates with iron oxide. These high values at 0.125 mg mark a sharp inflection of an average curve for all three elements, which was checked by additional precipitations and spectra. In the case of Ti and V, the curve flattened out suddenly at this point, rising again at approximately 0.35 mg concentration to continue as a straight line of about half the slope of the curve immediately below the 0.125-mg point. But with Zr, the average curve passed through a distinct maximum before continuing on with a constant lower slope. The dashed curve also shown in Fig. 1 was obtained from mechanical mixtures of the dry oxides. This curve, it will be noted, coincides closely with a possible average curve for the precipitated mixtures at higher concentrations. Additional work is still in progress, which, it is hoped, will provide some explanation for these results, but the data which follow for the simplified mixtures, will suggest a partial source of the apparent irregularities.

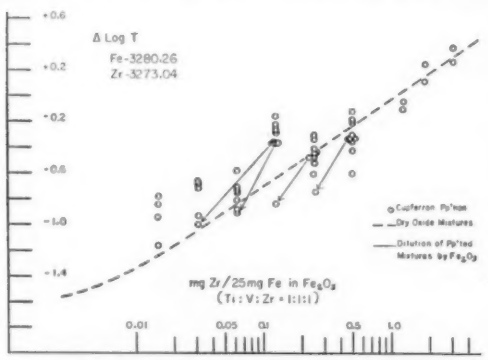

Fig. 1. Individual intensity ratios (expressed as log relative intermittent exposure times = Δ log T) of Fe/Zr for Cupferron precipitated mixtures of Fe plus Ti, V and Zr as minor constituents in proportions 1 : 1 : 1. Dashed line is average curve for dry oxide mechanical mixtures.

Determination of Zr in Fe_2O_3 in Absence of Ti and V

Figure 2 contains the individual values of exposure time ratio for the same Zr and Fe lines as before, but for precipitated mixtures containing Zr alone with Fe. These values show the same, or even wider, spread than did those

* The relative time scale from which these Δ log T values were obtained involves intermittent time exposures prepared with a rotating step-sector. Δ log T is a practical numerical expression of log intensity ratio, but is not always identical with it. See especially reference 7.

[6] L. W. Strock, *Proceedings of the Seventh Annual Summer Conference on Spectroscopy* (Wiley and Sons, 1939), pp. 134–41.

[7] L. W. Strock, Spectrochim. Acta **1**, 117–22, 1939.

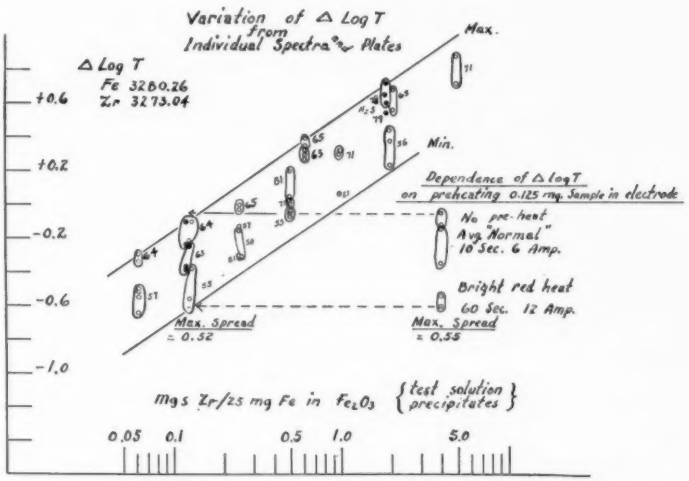

FIG. 2. Individual log relative intermittent exposure times for Fe/Zr in precipitated Fe—Zr mixtures in absence of Ti and V. Numbered fields enclose data obtained from same plate. Solid and open circles distinguish different precipitates at same concentration. See text concerning preheating data projected to right of figure.

referred to in Fig. 1. The numbered enclosures designate the plate from which the enclosed values were obtained. For the most part, all values for the same concentration were obtained from the same precipitate. Before realizing the wide variation of individual values, it was possible to draw curves of almost any shape and slope from the earlier plates. The use of a new lot of more compact electrodes seemed to have solved the difficulty, as shown by the reasonably good averaging of the values from plates 64 and 65 about a line near the uppermost one of Fig. 2. This line is parallel with, but displaced from, other lines obtained from any other given plate or set of plates prepared on the same day. A loss of unvolatilized Zr by a crumbling of the tip of a porous electrode appeared to offer a logical reason for the lower results obtained from porous electrodes as compared with compact ones. However, additional spectra (see data from plates 71, 78, 79 and 81), prepared to fix the "final" calibration curve more accurately, provided values as erratic as any previously obtained even though compact electrodes were used. Obviously, then, the texture of the electrodes was not the principle factor involved. An average of all of these widely spreading individual results provided a smooth concentration curve. However, the unpredictable variation and wide spread of the individual values, make such a curve worth very little for accurate quantitative work, since single determinations on an unknown sample can be in error by a factor of 10 when obtained from it.

DEPENDENCE OF Fe : Zr RATIO ON PREHEATING IN CARBON ARC

By a process of elimination, it was suspected that a very brief short circuiting of the electrodes containing the precipitated mixture of iron-zirconium oxide, plus two parts carbon powder immediately prior to arcing was the cause of the above erratic results. In practice, the arc was struck by very slowly separating the contacted electrodes, already carrying a short circuit current of 6 amp., for a brief period of time (averaging perhaps 10 seconds). This time was not accurately controlled as it was never imagined that slight variations in time—or, in fact, this brief preheat itself—was of any importance in the arcing operation.

The individual $\Delta \log T$ values projected to the right of the data referred to in Fig. 2 demonstrate a very definite effect of preheating on exposure time ratios. This experiment on the effect of preheating the sample in the arc was made on a mixture of the two precipitates containing 0.125 mg Zr and 25 mg Fe which were arced separately on plates 55, 64 and 63 and which yielded the erratic $\Delta \log T$ values plotted in Fig. 2. Six electrodes were filled with this composite sample and arced in identical manner after being

TABLE I. *Effect of short circuit heating in arc of* Fe–Zr *precipitated mixture+carbon. Density lines in step 6. Plate 86. Zr 3273.04*A. Fe *3280.26*A.

PREHEATED (BRIGHT RED) 12 AMP. 60 SEC.			NO PREHEAT			"NORMAL" (100°C) 6 AMP. 10 SEC.		
SPECT.	LINE	D	SPECT.	LINE	D	SPECT.	LINE	D
(5)	Fe	0.47	(3)	Fe	0.19	(1)	Fe	0.23
	Zr	0.14		Zr	0.13		Zr	0.15
(6)	Fe	0.39	(4)	Fe	0.24	(2)	Fe	0.35
	Zr	0.08		Zr	0.21		Zr	0.13
Av.	Fe	0.43		Fe	0.21		Fe	0.29
	Zr	0.11		Zr	0.17		Zr	0.14

subjected to three different degrees of preheating treatment in the arc. (1) *No preheat:* "live" electrodes merely quickly closed and opened, which resulted in spattering of approximately half of sample from electrode crater. (2) *"Normal" technique:* 6 amp. for 10 sec. (3) *Strong preheat:* 12 amp. for 60 sec., which produced bright red heat in the electrodes.

The individual values from duplicate spectra check each other more closely for the two extremes of preheating than do the ones from the "normal" (slightly) preheated samples. The spread of duplicate values on this plate for "normal" preheating is the same as that found on most previous plates, whereas the spread in $\Delta \log T$ between the two extremes of preheating is equal to the maximum spread obtained from all the previous spectra of that sample. Moreover, the two extremes of the individual values previously found are identical with those obtained from the strongly preheated and the not preheated samples, respectively. The fact that $\Delta \log T$ values from the slightly preheated samples lie between the two extremes, is additional evidence that preheating alters the sample, in some regular manner, to a condition which, when arced, emits Zr lines much weaker with respect to the Fe lines than otherwise. This change occurs in a few seconds at temperatures below 100°C, which explains the spread of $\Delta \log T$ from duplicate samples given the slight preheat. The erratic fluctuation of individual values over the wide range between the two limiting lines drawn in Fig. 2 is readily understood in view of the fact that the preheating time was not constant during that phase of the work. It must be emphasized that this slight unintentional preheating is of an entirely different order from any deliberate effective preheating of a sample in the electrodes prior to arcing as usually practiced. In fact, the amount of heat required to produce a greater portion of this measured effect is easily transmitted to the sample from the arc burner clamp already hot from arcing a preceding sample, which explains the curious observation throughout all this work, that the $\Delta \log T$ value was lower for the second spectrum of duplicate samples in a large majority of cases.

DEPRESSION OF Zr LINE INTENSITY BY PREHEATING PRECIPITATED MIXTURES IN ARC

The nature of the change produced in the sample by a slight preheating was sought by a study of the photographic density (D) of the Fe and Zr lines separately. The data shown in Table I shows that preheating has increased the intensity (as expressed by D) of the Fe lines by a factor of 2, but lowered that of the Zr lines by a factor of 1.5. Both lines thus contribute separately to the dependence of $\Delta \log T$ on heat treatment and their effects are additive. The lower intensity of the Fe lines in the sample not preheated is obviously due to the loss (actually collected on electrode clamp) of approximately one-half of the sample by spattering during the first few seconds of arcing. On this basis the intensity of the Zr line in the spectra of the larger unspattered preheated

TABLE II. *Effect of preheating precipitated mixtures in arc on tin lines. 0.14 percent* SnO_2 *in* Fe_2O_3. *Plate 86.* Sn *2839.99*A. Fe *2840.42*A.

PREHEATED			NOT PREHEATED			NORMAL		
SPECT.	LINE	D	SPECT.	LINE	D	SPECT.	LINE	D
(5)	Fe	0.42	(3)	Fe	0.15	(1)	Fe	0.17
	Sn	0.135		Sn	0.10		Sn	0.06
(6)	Fe	0.444	(4)	Fe	0.23	(2)	Fe	0.33
	Sn	0.17		Sn	0.11		Sn	0.115
Av.	Fe	0.43		Fe	0.19		Fe	0.25
	Sn	0.15		Sn	0.10		Sn	0.09
Spread		Fe=0.24 Sn=0.05						

Note: Sn is same in not preheated and normal; and 1.5 times higher in preheated, whereas Fe is 2 times higher.

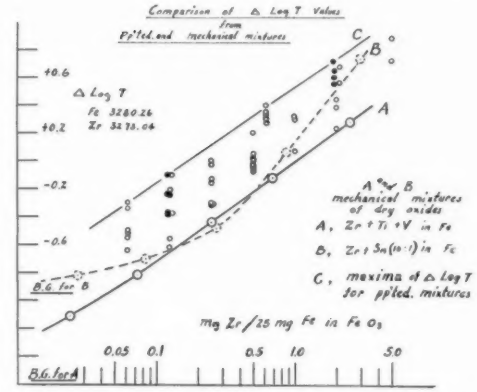

FIG. 3. Average curves obtained from mechanical oxide mixtures superimposed on precipitated mixture data of Fig. 2.

sample should have been three times greater than actually observed. It is interesting to note in Table II that tin has actually increased in intensity parallel with Fe in the preheated (unspattered) sample as shown by the same spectra. In contrast to tin, preheating changes Zr in the samples to a condition which emits Zr lines of only one-third the intensity when not preheated. The greatly reduced ability of the Zr to vaporize from the sample after the heat treatment and reach the arc gas indicates that the Zr in the precipitate has been converted to a more refractory compound.

SEGREGATION OF ZrO_2 FROM Zr–Fe OXIDE BY PREHEATING IN CARBON ARC

The temperature at which this change is produced is too low to form a zirconium carbide,

TABLE III. *Effect of preheating precipitated mixtures in arc (possible reactions).*

A. Electron exchange between Fe^{III} and Zr^{III},

$$Fe^{III}\,Zr^{III}\,O_3\cdot Fe_2O_3 \xrightarrow{\text{heat + carbon}} Fe^{II}\,Zr^{IV}\,O_3\cdot Fe_2O_3$$

Zircono-ilmenite

$$Fe^{II}\,Zr^{IV}\,O_3\cdot Fe_2O_3 \rightarrow FeO + ZrO_2 + Fe^{II}\,Fe_2^{III}\,O_4$$

Magnetite

B. or decomposition of an original $Fe^{II}\,Zr^{IV}\,O_3\cdot Fe_2O_3$ into $Fe^{II}\,Fe_2^{III}\,O_4 + ZrO_2$

Magnetite

Note: Corresponding natural Ti–Fe oxide is $Fe^{II}\,Ti^{IV}\,O_3\cdot Fe_2O_3$, which segregates TiO_2

Ilmenite — Rutile

but could be sufficient to cause a transition in the stability range of solid solutions and double oxides. The most apparent explanation of the effect of heat on the precipitated Fe–Zr oxide mixtures is given by reactions shown in Table III. The weight of the ignited Fe–Zr Cupferron precipitate checks exactly with the formula $FeZrO_3$ rather than with $Fe_2O_3+ZrO_2$. This is to be expected since some iron ions in the crystal lattice of Fe_2O_3 can be replaced by zirconium

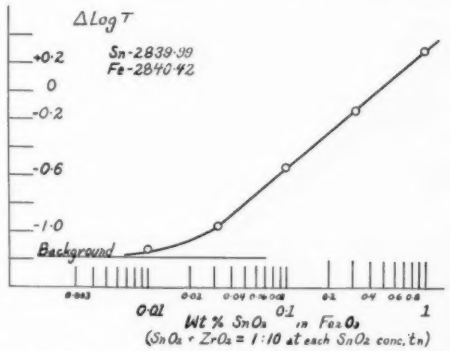

FIG. 4. Calibration curve for mechanical oxide mixtures of SnO_2 in Fe_2O_3. ZrO_2 is also present in each mixture in constant 10 : 1 ratio to SnO_2.

ions. By analogy with a corresponding compound of Ti and Fe, the precipitate most probably consists of a solid solution of Fe_2O_3 with a ferrous zirconate ($Fe^{II}Zr^{IV}O_3$). Whatever the original composition of the precipitated mixture before heating in the arc in the presence of carbon, two reactions are possible, both of which produce free ZrO_2. In reaction A, an electron exchange between the trivalent Fe and Zr ions of an $(Fe\cdot Zr)_2O_3$ molecule, corresponding with simultaneous reduction and oxidization of Fe and Zr, respectively, in a chemical sense, yields a ferrous zirconate. This compound is not known to occur naturally, as is the corresponding Ti compound, and it must be decomposed by a slight preheat with carbon, segregating free ZrO_2. Even if the Zr was originally present in the precipitate as a ferrous zirconate its decomposition into magnetite and ZrO_2 by the preheating is possible, as is shown by reaction B. In both cases, a higher concentration of Zr vapor in the arc column would result from arcing the mixture before its Zr had segregated as ZrO_2.

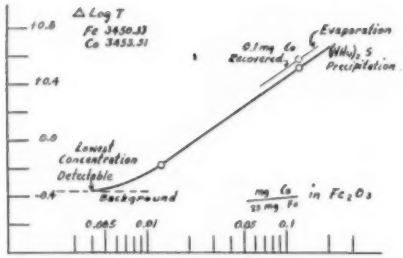

FIG. 5. Calibration curve for determining Co : Fe ratio in ignited iron sulfide precipitated from solution containing 25 mg Fe, 2 mg Zr plus $CaCl_2$ and NaCl equivalent to acidified Saratoga mineral water concentrated to 1/15th volume.

If the depressed intensity of the Zr line is actually due to the segregation of ZrO_2, then the exposure ratios obtained from mechanical mixtures of the dry oxides should approximate those obtained from the preheated precipitated mixtures. Concentration curves for two series of mechanical mixtures are shown in Fig. 3 along with the individual values of $\Delta \log T$ for the precipitated mixtures.

When adjusted to the same background, the curves for both series of dry mixtures are very similar up to approximately 2 percent ZrO_2. The curve for Zr in Fe_2O_3 (no Ti or V present) is steeper than the curve derived from mixtures containing Ti and V in addition to Zr, which is due to a more complete volatilization of Zr when present as the only refractory constituent of the sample. Obviously the minimum exposure ratios obtained from the variously preheated precipitated mixtures of Zr in Fe_2O_3 fall close to a curve representing the mechanical mixtures of the free oxides of iron and zirconium. This is a good indication of the correctness of the above explanation concerning the effect of preheating on the relative intensity of the Zr lines in spectra of the precipitated mixtures.

Attempts were made to detect segregated ZrO_2 in a preheated precipitated mixture by its x-ray diffraction pattern.* The intensity of the ZrO_2 lines was too low to detect in the 8 percent ZrO_2 mixture studied. However, a small but measurable contraction of the lattice constant, which the segregation of the larger Zr ions would be expected to produce, was observed. The amount of ZrN on the cathode after arcing was greater for the preheated electrodes and its appearance resembled that from the mechanical mixtures more closely than the unheated precipitated ones. The more pointed ZrN cap left by the unheated precipitated mixture also indicated more active participation of Zr in the arcing (and cathode enrichment) process than for the mechanical oxides.

The data presented above are the results of an attempt to devise an accurate quantitative spectrochemical method for determining zirconium in Saratoga mineral waters. They have been presented in some detail since the method, rather than the result, is of more specific interest to this Conference. However it is of interest to note that the Orenda spring contains 0.35 mg Zr/l, or 27 times more relative to Fe (8.5 : 1 = Fe : Zr) than the earth's silicate crust.

DETERMINATION OF Sn, Mn, Co AND Ni IN SARATOGA WATER

Tin was also detected in the Cupferron-iron precipitate of Saratoga water. It is enriched relative to iron by approximately the same factor as zirconium. In all the waters examined, the Sn : Zr ratio remains very constant regardless of the Zr : Fe ratio. A tentative determination of tin in one water is 0.84 percent SnO_2 in the total Cupferron precipitate which is equivalent to 0.032 mg/l or approximately 30 γ/l. This determination is based on the curve of Fig. 4 obtained from spectra of mechanical mixtures of SnO_2 in $Fe_2O_3+ZrO_2$ (ratio $SnO_2 : ZrO_2 = 1 : 10$). This determination furnishes a Sn : Fe ratio = 1 : 96, which is greater by a factor of 13 than

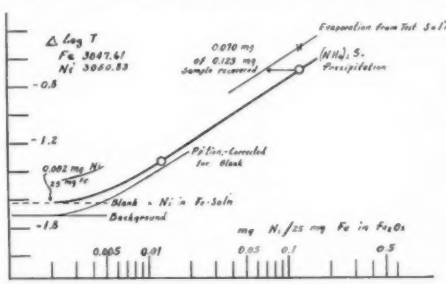

FIG. 6. Calibration curve for Ni in Fe_2O_3 precipitated from solution as described in Fig. 5.

* These x-ray powder photographs were kindly made by Mr. L. L. Wyman and Mr. E. T. Asp of the General Electric Research Laboratory in Schenectady.

that for the earth's lithosphere, which is 1250 : 1 according to V. M. Goldschmidt.[2]

In contrast with the enrichment of Zr and Sn in Saratoga water, the Mn, Co, Ni content is depleted relative to Fe. These elements were determined on the basis of curves obtained from spectra of ammonium sulfide precipitates of two test solutions containing 0.0125 and 0.125 mg each of Co, Ni and Mn plus 25 mg Fe, 2 mg Zr, and NaCl plus $CaCl_2$ in the same amounts as present in the concentrated water analyzed. As an independent control on the completeness of the sulfide precipitation of these elements, spectra were made of evaporated and ignited residues from identical test solutions, with the exception of the Na and Ca. The calibration curves so obtained are shown in Figs. 5, 6 and 7. The precipitation loss is considerable, as is indicated by the displacement of the sulfide precipitation and evaporation curves. For the 0.125-mg test solution, the percent recovery was Co 84 percent; Ni 55 percent; and Mn 13.2 percent. It was necessary to apply a slight correction to the curves for these elements, due to a detectable amount of Ni and Mn in the Fe used in the test solutions.

A typical water analyzed contained 3.03 mg Fe/l and 0.0027 mg Mn/l, while Co was not detected and was thus less than 0.0005 (probably 0.00011 mg/l). These analyses furnish the following ratios: Fe : Ni = 11,200, whereas ratio in av. lithosphere is 500 : 1; Fe : Mn = 1120,

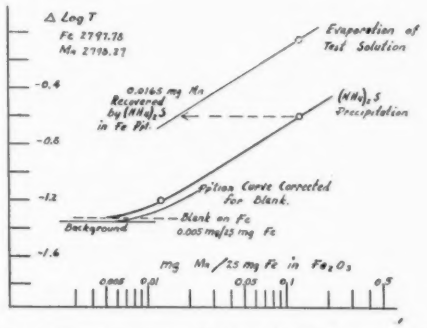

FIG. 7. Calibration curve for Mn in Fe_2O_3 precipitated from solution as described in Fig. 5.

whereas ratio in av. lithosphere is 50 : 1; Fe : Co = 27,500, whereas ratio in av. lithosphere is 1250 : 1.

Each of the elements Co, Ni and Mn are depleted in Saratoga water by a factor 25 relative to Fe as compared with the average of the earth's silicate crust. This is in striking contrast with the enrichment of Zr and Sn by a corresponding factor. The depletion of Ti and V is even greater. These displacements of the relative concentration of certain groups of elements in the course of the process by which these mineral waters were formed provided new experimental facts which suggest specific laboratory experiments designed to obtain a more complete knowledge of the geochemistry of mineral waters rich in bicarbonates and free CO_2.

The Clean-Up of Mercury Vapor in Discharges Through Hydrogen, Helium and Nitrogen*

O. S. Duffendack, R. A. Wolfe and Franz Lederer
University of Michigan, Ann Arbor, Michigan

At the Midwestern Spectroscopic Conference at the University of Chicago, March 31, 1940, two of us (O. S. D. and R. A. W.) reported on the determination of mercury vapor in hydrogen gas by spectrographic means. Because of the very rapid clean-up of mercury vapor by discharges through mixtures of mercury vapor and hydrogen, attempts to determine the amount of mercury vapor present in hydrogen by measurements on the emission spectra were abandoned and a method for this determination by measurements of the absorption of the 2537A resonance line of mercury was developed. This method has proved very satisfactory for the determination of the amount of mercury vapor in hydrogen for amounts down to one part Hg per hundred million by volume.

During the course of the experiments resulting in this development, a number of interesting phenomena were observed in connection with the clean-up of mercury by glow discharges in hydrogen-mercury mixtures and with the aid of Mr. Franz Lederer who carried out the experiments, these phenomena were further investigated and the experiments were extended to helium and nitrogen mixtures with mercury vapor as well.

Clean-Up of Mercury Vapor in Hydrogen

Hydrogen which had been in contact with liquid mercury at room temperature for some time was admitted to a glow discharge tube made of Pyrex glass and quartz and fitted with nickel cylindrical electrodes. The tube had been thoroughly cleaned and out-gassed before the hydrogen was admitted. The hydrogen was allowed to come to a pressure of 1 mm of Hg and then the tube was disconnected from the H_2-Hg source and a glow discharge was excited in it by means of a neon sign transformer. The first exposure shows a strong Hg 2537 line in the spectrum, but subsequent exposures show no trace of this or any other mercury line. The walls of the tube were heated somewhat during the first exposure which was for 90 sec. and began immediately after the tube had been cut off from the gas supply. Now the gas was pumped out of the tube and fresh gas admitted which had likewise been in contact with liquid mercury. This time the tube was not heated and none of the spectra, not even the first one taken, showed any trace of mercury. This procedure was repeated many times and great quantities of gas and mercury vapor were cleaned-up until finally a saturation was reached. Then the residual gas was pumped down to a pressure of 10^{-5} mm Hg and the tube was heated with a hand torch. During the heating of the tube a characteristic green fluorescence was observed on the walls and considerable gas was recovered. The spectrum of the recovered gas, taken while the tube was hot, contained strong mercury lines. During a period of two hours, while the tube was pumped while heated to about 450°C, it was possible again and again to recover enough gas from the walls to start a discharge. Finally no more gas was evolved.

A second series of experiments on the clean-up of mercury vapor in hydrogen was made with a tube that had previously been used for glow discharges in $He-Hg$ mixtures. After this use, the tube was pumped hard while heated to a temperature of 450°C. Not all of the helium was driven from the walls by this treatment before the H_2-Hg mixture was admitted. Now the rate of clean-up of H_2 and Hg was very slow. Table I gives the galvanometer deflections in microphotometric measurements on the λ2537 line. Next we removed with nitric acid a sputtered metallic film which had collected on the tube walls near the electrodes during its previous use. After baking the tube at 300°C for some hours to out-gas it, hydrogen saturated with mercury vapor at room temperature was again admitted and excited as before. The mercury cleaned-up rapidly again as in a new tube.

The rate of clean-up of mercury varied with

* Presented at the Eighth Summer Conference on Spectroscopy and Its Applications at Massachusetts Institute of Technology, July, 1940.

the tube current in an interesting way. In general, the rate increased with an increase in current, but, if a tube had been used before, the intensity of the mercury lines increased somewhat for some 1 or 2 minutes after the start of the discharge when the tube current exceeded 20 ma, as shown by the galvanometer deflections for the λ2537 line in Table II. This seemed to be caused by an evolution of mercury vapor by the electrodes for a few minutes after the start of the discharge and probably resulted from the heating of the electrodes. At lower currents, the electrodes used did not become hot enough to give off mercury at a greater rate than it was being cleaned-up. If the discharge was operated a few minutes before the connection to the mercury supply was cut off so that a steady temperature was reached during this time, the rate of clean-up of the mercury vapor was at the expected rate for the higher currents and no maximum in intensity of the mercury lines was observed.

The conclusions drawn from the experiments are the following:

(1) Mercury as well as hydrogen disappears from a tube containing a mixture of hydrogen and mercury vapor during the passage of electricity through the tube and surprisingly large amounts may be cleaned-up. The concentration of mercury vapor in hydrogen can be reduced to a subspectroscopic value in this way.

TABLE I. H_2 *at 1 mm pressure saturated with* Hg *vapor at 24°C. Current 10 ma.*

EXPOSURE	GALV. DEFLECTION CM
Fresh sample	23.9
After 2 min.	17.2
" 4 "	16.6
" 6 "	15.0
" 8 "	9.1
" 10 "	4.3
" 15 "	0.3

(2) While some of the clean-up is probably caused by adsorption by the tube walls and the electrodes, the major process is the formation of mercury hydride as proposed by Beutler and Rabinowitsch.[1] The hydride is not very stable and is decomposed by heating it to a temperature of about 150°C.

[1] H. Beutler and E. Rabinowitsch, Zeits. f. physik. Chemie **B8**, 231 (1930).

(3) The phenomenon of saturation and the reduction of the rate of clean-up by a layer of He on the tube walls indicates that the reaction in which mercury hydride is formed takes place on the tube walls and not in the gas phase in the volume of the tube.

CLEAN-UP OF MERCURY VAPOR IN HELIUM

A clean-up of mercury vapor from helium which had been in contact with liquid mercury at room temperature was observed to occur, but at a much slower rate than in H_2-Hg mixtures, as shown by the galvanometer deflections for λ2537 in Table III. Saturation is reached much more quickly in helium than in hydrogen; no clean-up was observed after a discharge had been operated in helium in contact with liquid mercury for a half-hour. When the tube was heated to a temperature of 300°C after the residual gas had been pumped out, the recovered vapor showed the whole arc spectrum of mercury but no helium lines. After this heat treatment, a clean-up of mercury could again be observed.

TABLE II. *Galvanometer deflections in microphotometer measurements on the λ2537 line.* H_2 *at 1 mm pressure after having been in contact with mercury at room temperature. Current 25 ma.*

EXPOSURE	GALV. DEFLECTIONS CM
Fresh sample	19.5
After 1 min. discharge	22.5
" 2 " "	20.9
" 3 " "	20.5
" 4 " "	18.9
" 5 " "	16.4
" 6 " "	15.5

In this case the small amount of clean-up of mercury observed seemed to be caused merely by an adsorption of mercury by the tube walls and electrodes. Much of the adsorption may result from the movement of mercury positive ions to the cathode and to the tube walls in the vicinity of the cathode. In the $He-Hg$ mixture a high concentration of mercury ions is to be expected as He^+ ions may be neutralized by the formation of Hg^+ ions by exchange phenomena on impact.

CLEAN-UP OF MERCURY VAPOR IN NITROGEN

Very little clean-up of mercury was observed in a clean, well-degassed tube into which nitrogen

gas which had been in contact with liquid mercury at room temperature had been introduced to a pressure of 1 mm Hg. Saturation was quickly reached. The clean-up can readily be accounted for by adsorption by the electrodes and tube walls. The lesser amount of mercury cleaned-up in nitrogen than in helium is difficult to explain. It may be caused by a difference in the concentration of Hg^+ ions produced in the two cases. When a tube had been used with hydrogen previous to its use with nitrogen and was not completely degassed, a noticeable clean-up of mercury was obtained during the time a glow discharge in the N_2-Hg mixture was maintained. This effect must be caused by the hydrogen adsorbed on the tube walls and lends support to the conclusion that much of the clean-up of mercury and hydrogen is caused by a reaction between mercury and hydrogen on the tube walls rather than in the volume of the gas.

TABLE III. *Galvanometer deflections for λ2537 in spectra of* He *that had been in contact with mercury at room temperature. Pressure of* He *1 mm. Current 25 ma.*

EXPOSURE	GALV. DEFLECTIONS CM
Fresh sample	24.8
After 1 min. discharge	23.3
" 5 " "	22.8
" 15 " "	22.6

These experiments illustrate the danger one encounters in making quantitative analyses of mixtures of gases by measurements on their emission spectra. Where one or more of the constituents cleans-up rapidly, considerable error may result. Two methods have been employed to eliminate or minimize such errors. One may make the analysis by measurements on the absorption spectra where this is possible as was done in the determination of mercury in hydrogen. No clean-up will occur during these measurements unless photochemical reactions are promoted. These may be minimized by using light of as small intensity as is feasible and by reducing the time of irradiation of the test specimen as much as possible. In most cases the photochemical reactions can be reduced to negligible amounts. The other method consists in the use of some carrier gas, as helium, into which only a small amount of the test specimen is introduced as was done in the method described by Duffendack and Wolfe[2] for mixtures of H_2, N_2, O_2, and CO_2.

[2] R. A. Wolfe and O. S. Duffendack, *Proceedings of the Sixth Summer Conference on Spectroscopy* (Wiley, New York, 1939), p. 66.

A Precision Method for the Measurement of the Wave-Lengths of Diffuse Lines*

W. W. A. JOHNSON AND DANIEL NORMAN
New England Spectrochemical Laboratories, Boston, Massachusetts

A NUMBER of methods have been suggested in the last few years for making objective measures of the wave-lengths of spectral lines. In most of them,[1,2] the criterion or parameter of maximum photographic density determines the wave-length of the line. In a few, the wave-length is the mean of the position of a pair of points of equal photographic density on either side of the maximum.[3] Difficulties have been encountered, however, in handling intrinsically diffuse lines, strongly self-reversed, and complex, and asymmetrical lines. The two systems, maximum density and equal density, are not equivalent in these cases. Harrison[4] has pointed out some of these difficulties in the *M.I.T. Wavelength Tables.*

Ross[5] and many others have shown that measures of wave-length from photographs by ocular setting of cross-hairs in the microscope of a comparator are an integration of a number of effects, the relative importance of which depends on density, contrast, background density, and the individual. The most influential criteria are: (a) the point of bisection of the visual edges of the line, (b) the point of maximum density, (c) the median point of photographic blackening. On simple symmetrical lines, all these estimates should, and do, give the same value for the line position. In measuring diffuse or asymmetrical lines, the predominance of a single factor is marked, and is a function of the observer, and very definitely affects the measured line positions.

The most common objective method employs method *A* principally: bisection of edges of the line. Other devices simply pick out the point of maximum density, method *B*. In the case of asymmetrical lines, method *B* leads to an erroneous value of the wave-length; method *A* leads to a value of unknown worth.

The theories of the Zeeman, Stark, and pressure effects indicate that, to a first approximation, the criterion of greatest significance as a measure of wave-length is the position of the center of intensity of the line—that is, the position of a vertical line dividing the spectral line into areas of equal intensity. This point must be determined by the usual technique of photographic photometry, employing a recording microphotometer. The center of gravity of the density image is not the same as that of the intensity image. Photoelectric systems almost invariably measure density criteria and not intensity criteria.

One of us has recently had occasion to measure diffuse asymmetric spectrum lines whose positions were exceedingly sensitive to the criteria employed. This has led to a re-examination of the criteria involved and the development of an objective method for measuring wave-lengths of spectral lines on microphotometer tracings of large magnification.

The spectrum of tin affords a convenient series of diffuse asymmetric, self-reversed lines suitable for testing the method. The tin lines, 3330, 3262, and 3175A, were photographed in the fourth order of a three-meter grating spectrograph, dispersion 1.3A per millimeter. The tin lines were as much as 1.5A across, while iron lines of the same maximum intensity were 0.2A to 0.3A. Microphotometer tracings of the plates were obtained with a recording photoelectric microphotometer at fifty-fold magnification. Variations of the microphotometer screw, expansion and contraction of the paper, etc., were compensated for by a series of light flashes photographed on the paper at constant intervals. The areas of equal intensity were determined by means of a mechanical tracing reducer incorporating the photometric standards of calibration. Full details of the method will be presented elsewhere. In brief, the method consists of selecting five horizontal lines equally spaced in intensity, and measuring the coincidence of the

* Presented at the Eighth Summer Conference on Spectroscopy and Its Applications at Massachusetts Institute of Technology, July, 1940.

[1] G. R. Harrison, J. Opt. Soc. Am. 25, 169 (1935).

[2] G. R. Harrison, Rev. Sci. Inst. 9, 15 (1938).

[3] See G. R. Harrison, *Proceedings of the Sixth Spectroscopy Conference* (John Wiley, New York, 1939), p. 117.

[4] G. R. Harrison, *M. I. T. Wavelength Tables* (Wiley, 1939), Introduction.

[5] F. E. Ross, *Physics of the Developed Photographic Image* (Van Nostrand, 1924), Chap. III *et al.*

trace, a vertical, and the five horizontals on both the ascending and descending branches of the spectral line trace. In practice, the individual measures may be set directly on an adding machine, and the sum of the ten individual measures recorded as the line measure. For analytical purposes, all measures were recorded, and the peak of each line measured, likewise. The time flashes on the tracing were also measured, using always the ones corresponding to whole revolutions of the microphotometer screw. The measures were then reduced to screw readings, and reductions to wave-length made in the usual way.

The probable errors from sets of three measures on different spectrograms are: for the center of gravity of intensity, 0.010A or 7.8 microns; for the maximum density setting, 0.016A or 12.2 microns. The differences, -13, $+9$, $+8$, microns for 3175, 3262 and 3330, respectively, do not appear to be systematic. Apparently the position of maximum density is a usable criterion of wave-length. Measurements of the bottom of the reversed portion of the line agree with the mean of the two peaks, in contradiction to the observation of Haschek,[6] who observed the dip generally to lie to the violet of the position given by the two peaks.

In making the reductions, we observed that the measures made at a point dividing the spectral line horizontally into two equal areas were consistently closer to the mean than any of the others by a factor of fifty percent. The average deviations of all measures was three microns (on the plate) and two microns for this central point. It is clear, therefore, that a wave-length-measuring device might well be so designed that it measures the position of lines at a density corresponding to about one-third the maximum intensity of the line.

[6] E. Haschek, Astrophys. J. **14**, 181 (1901).

A New Nonrecording Densitometer*

W. S. BAIRD
Baird Associates, Cambridge, Massachusetts

THE nonrecording densitometer to be described has been made reliable by incorporating a stable amplifier, acting as a null indicator, in a balanced photoelectric cell circuit. It possesses, in addition, a number of novel features arranged for the convenience of the operator.

This instrument is of the projection type, throwing a $\frac{1}{4}''$ diameter area of the plate, ten times magnified, on the viewing screen which contains the slit. The arrangement is as shown in Fig. 1. As can be seen, the viewing screen is directly in front of the operator, and at reading distance. The exit slit is 0.007″ wide, 0.750″ long, allowing spectral lines of width 25μ to be measured.

The light passing through the spectral line which is being measured is projected through the exit slit to a vacuum photo-cell. An identical photo-cell receives the light which has passed through the measuring train. A cam aperture serves as the measuring element. This aperture covers a specular density range from 0 to 1 and is divided into 100 equal parts. In order to measure densities from 1.0 to 3.0, fixed apertures are introduced in the measuring train, each reducing the light by a factor of ten, the cam aperture covering the interval.

The balancing of the light intensity of the two trains is indicated by one of the now familiar "magic eye" tubes. This tube is located alongside the projection screen, at reading distance.

The null balancing circuit is stable and quick acting. The electrical arrangement consists of the two photo-tubes and a single-stage amplifier, the output of which is fed to the "magic eye" tube. The only power source necessary is 110 volts a.c. The circuit has inherent stability because of its simplicity and because vacuum photo-tubes are used; the time constant of the "magic eye" tube is quite short, being 0.1 to 1 sec. at the low densities, and somewhat greater at the higher values. The response of the circuit is such that there is ample sensitivity even at the higher density levels.

Figure 2 shows the optical diagram of the instrument. In the measuring train, any one of three fixed apertures can be placed in the collimated beam proceeding from the light source. This then becomes the aperture stop of the system, and it is necessary to bring the light to a focus on a ground-glass diffusing screen. This screen then acts as a light source for a collimated beam uniformly illuminating the aperture of the measuring cam. Directly before the measuring cam is an adjustable slit, at all times narrower than a single division on the measuring scale. By adjusting this slit, the zero of the density scale can be set either for the case of air (100 percent transmission) in the projection train, or, as is frequently more convenient, to read clear plate transmission. The last lens in the train brings the beam to focus on the photo-cell.

The projection train consists of a condenser, a lens bringing the spectrum to a first focus, and the projection lens. Of course, this system has inherent errors due to the Swarzchild-Villiger effect (scattering at the lens surfaces). This effect could only be corrected completely by placing a slit directly over the spectral line being measured. However, it is felt that absolute density measurements are the extraordinary rather than the ordinary problem, especially in spectrochemical analysis. An adjustment for rotating the exit

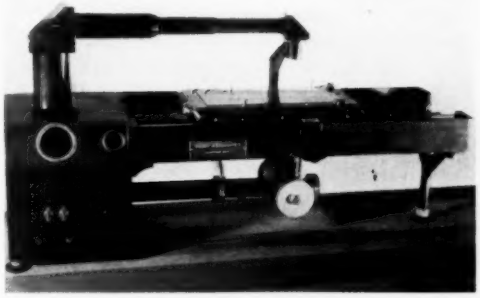

FIG. 1.

* Presented at the Eighth Summer Conference on Spectroscopy and Its Applications at Massachusetts Institute of Technology, July, 1940.

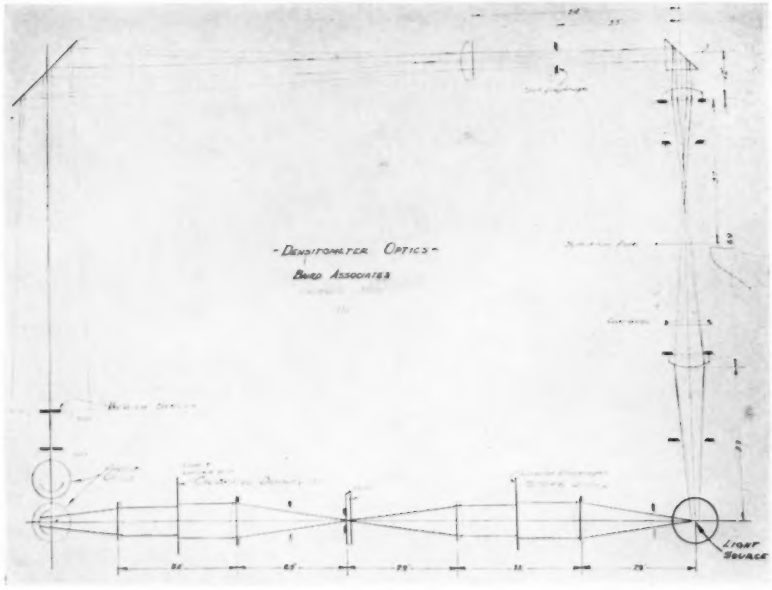

FIG. 2.

slit with respect to the spectrum has been provided. This facilitates the following of curved lines such as are encountered in full length prism spectra.

The instrument is sufficiently rugged not to be affected by vibrations which usually bother galvanometer type instruments. The transverse and cross carriages are arranged to move on ball slides, resulting in smooth easy travel. The transverse slide covers a range slightly less than 10 inches and is actuated through knobs, one of which is a direct drive, the other a 7 : 1 vernier. The cross slide has a travel of slightly less than 4 inches and is provided with a release for rapid motion, which, when locked, allows a fine adjustment to be made. The cross carriage, while designed specifically for 4″×10″ plates, will accommodate plates as long as 20″. Rough measurements of wave-length on plates can be made with a 20-cm scale and vernier reading of 0.1 mm. A micrometer reading to 0.0025 mm is provided with which it is possible to measure lines over a 13-mm range at any part of the plate.

One disadvantage inherent in this type of instrument is the fact that a reading must be made in two steps: First, the magnified image of the line is set on the slit; then the density is measured. This requires either the use of broad spectrum lines or a reasonable amount of care in setting. To ameliorate this, a fine adjustment has been incorporated which allows a line to be scanned by passing it back or forth over the slit. The maximum reading is then obtained easily.

The advantages may be listed as follows: (1) Is rugged, not sensitive to ordinary vibrations. (2) Uses standard 110-volt a.c. power source. (3) Utilizes a null balancing circuit and familiar "magic eye" tube. (4) Has a rapid response allowing measurements to be made quickly. (5) Reads specular density directly. (6) Has all adjustments conveniently arranged.

Figure 3 curve *A* shows readings taken on an

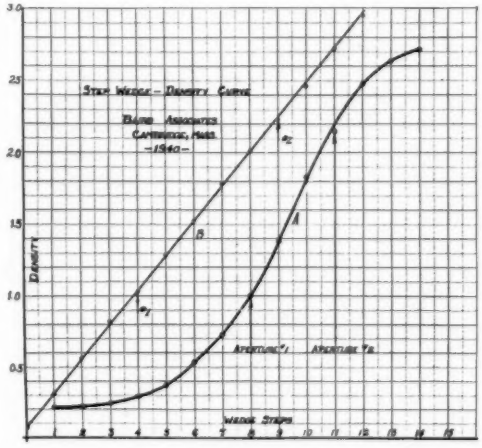

FIG. 3.

Eastman x-ray photographic wedge to show overlapping of scales and the range of the instrument. Curve *B* shows similar measurements taken on an Eastman wedge having equal density steps.

Proposed American Standard Z38.7.1 for Printing Equipment*

(Contact Printing Machines, Printing Frames, and Masks)

1. Contact Printing Machines

1.1 Printing equipment for a given nominal negative size shall accommodate all negative material within the standard dimensions for that nominal size and the exposure opening shall cover the full picture area for that nominal size.

1.2 The ratio of corner-to-center illumination shall not be less than 65 percent. The field shall be free from local irregularities that have an intensity difference of more than 15 percent per 1.0 inch (2.5 cm).

1.3 A test print shall show good contact using the test described with a halftone screen of 120 dots per 1.0 inch (2.5 cm). (See Proposed American Standard Methods of Testing Printing and Projection Equipment Z38.7.5, Section 1).

1.4 The temperature rise in one hour from intermittent exposures of ten seconds on and ten seconds off should not exceed 40C (72F). The maximum temperature should not exceed 65C (149F). Temperatures are to be measured as specified under testing methods.

1.5 The material for masking blades between the negative and paper should not exceed 0.005 inch (0.13 mm) in thickness, and masking blades to go below the negative should not exceed 0.020 inch (0.51 mm).

1.6 Masking blades should be square within ten minutes (0 degree 10 minutes).

2. Printing Frames

2.1 Printing equipment for a given nominal negative size shall accommodate all negative material within the standard dimensions for that nominal size and the exposure opening shall cover the full picture area for that nominal size.

2.2 A test print shall show good contact using the test described with a halftone screen of 120 dots per 1.0 inch (2.5 cm). (See 1.3.)

2.3 The material for masking blades, when present, should be square within ten minutes (0 degree 10 minutes) and not over 0.005 inch (0.13 mm) thick.

3. Masks

3.1 Any light transmitted through the mask must not fog the sensitive material under normal handling.

3.2 Mask sizes for film packs and roll film.

3.21 For sizes smaller than 2.25×3.25 inches, the mask opening should be $\frac{1}{16}$ inch (1.59 mm) smaller in both directions than the nominal negative size.

3.22 For 2.25×3.25 inches and larger sizes, the mask opening should be $\frac{1}{8}$ inch (3.18 mm) smaller in both directions than the nominal negative size.

3.3 The thickness of the mask should not prevent adequate contact using the test described for a halftone screen of 120 dots per 1.0 inch (2.5 mm).

3.4 Special size masks should be used for the few cameras, especially in the 2.25×3.25 and 3.25×4.25 inch sizes, which make negatives too small for the standard sizes of masks.

* Not Approved. Published for Trial and Criticism. The Optical Society of America is sponsor for the project.

Proposed American Standard Z38.7.2 for Projection Equipment*

(Film Strip Projectors, Viewing Devices for 35-mm Film and Reading Devices for Microfilm)

1. Film Strip Projectors Using Standard 35-mm Motion Picture Film and Exclusive of Microfilm Readers

1.1 *Film strip* means a strip of transparent, flexible material carrying photographic images for optical, but not for cinematic, projection.

1.2 Pictures shall be single or double frame on safety stock standard motion picture film. Perforations shall conform to the American Standard Dimensional Standards for Motion Picture Apparatus Z22–1930 or the latest revision approved by the American Standards Association.

1.3 The spacing of double-frame pictures shall be eight perforations and of single-frame pictures four perforations, on centers.

1.4 When both vertical and horizontal pictures are on the same film, they shall be arranged so that the film strip is rotated counter-clockwise ninety degrees to change from a vertical to a horizontal picture. The film is to be viewed from the lamp side and looking toward the screen.

1.5 The ratio of corner-to-center illumination of the screen shall not be less than 65 percent and any two adjacent areas of the nine areas specified for the testing method for lumen output shall not vary more than 25 percent. No areas of marked different visual intensity shall appear on the screen. (See Proposed American Standard Methods of Testing Printing and Projection Equipment Z38.7.5, Section 3.)

1.6 The temperature of the film strip shall not exceed 100C (212F), when measured by the testing method given.

1.7 A leader of not less than six inches (15 cm) and a trailer of not less than three inches (7.5 cm) should be provided on each film strip.

1.8 The mechanism should relieve the pressure of the aperture plates prior to and during movement of the film when the pictures are changed.

1.9 The film track should be relieved in the path of the picture area.

2. Viewing Devices for 35-mm Film

2.1 Such devices should permit easy manipulation with a minimum damage to the photographic materials viewed. Evenness of illumination and temperature rise should conform to the standards given for Film Strip Projectors insofar as practicable. Local variations in illumination should not be obvious to the unaided eye. Lenses should be free from aberrations obvious to the unaided eye.

3. Reading Devices for Microfilm

3.1 Such devices should permit easy manipulation with minimum damage to the photographic materials viewed. Evenness of illumination and temperature should conform to the standards given for Film Strip Projectors (see Section 1) insofar as practicable. Local irregularities of illumination should not be obvious to the unaided eye. The image should be free from aberrations obvious to the unaided eye.

---

* Not Approved. Published for Trial and Criticism. The Optical Society of America is sponsor for the project.

Proposed American Standard Z38.7.3 for Lantern Slide Projectors*

(exclusive of Microfilm Readers)

1. Standard Lantern Slide

1.1 The standard lantern slide after binding with a cover glass and mask shall have a horizontal length of 4 inches (101.6 mm) and a vertical width of $3\frac{1}{4}$ inches (82.6 mm). These dimensions are not to be exceeded by more than 1/64 inch (0.4 mm) and should not be shorter by more than $\frac{1}{32}$ inch (0.8 mm).

1.2 The thickness including binding tape, mask, slide, and cover glass shall not exceed 9/64 inch (3.57 mm).

1.3 The maximum amount of the slide used for projection shall not exceed $2\frac{3}{4}\times 3$ inches (70×76.2 mm).

2. Miniature Standard Lantern Slide

2.1 The miniature standard lantern slide after binding with a cover glass shall be 2×2 inches $+0, -\frac{1}{32}$ inch (50.8×50.8 mm $+0, -0.8$ mm) in size.

2.2 The thickness including slide, mask, cover slide and binding tape shall not exceed $\frac{1}{8}$ inch (3.2 mm).

2.3 The maximum amount of the slide used for projection shall not exceed:

23×34 mm ($\frac{29}{32}\times 1\frac{11}{32}$ in.) for slides from double frame 24×36 mm negative.
26.2×38.1 mm ($1\frac{1}{32}\times 1\frac{1}{2}$ in.) for slides from a 28×40 mm negative.
17.5×23 mm ($\frac{11}{16}\times\frac{29}{32}$ in.) for single-frame 18×24 mm negatives.

2.4 Other types of holders for film (metal carriers, etc.) shall conform to the above dimensions.

3. Thumb Mark

3.1 A thumb mark is to be placed at the lower left-hand corner when the slide is viewed as it is to appear on the screen.

4. Screen Illumination

4.1 The ratio of corner-to-center illumination of the screen, when the lens designated by the manufacturer for the projector is used, shall not be less than 65 percent and any two adjacent areas of the nine areas measured in the testing method for Lumen Output shall not be different by more than 25 percent. No areas of marked different visual intensity shall appear on the screen.

5. Range of Focal Lengths

5.1 The following range of focal lengths should be available for standard-size lanterns ($3\frac{1}{4}\times 4$ in.):

152 mm (6 in.); 203 mm (8 in.); 254 mm (10 in.); 305 mm (12 in.); 356 mm (14 in.); 406 mm (16 in.); 457 mm (18 in.); 508 mm (20 in.); 559 mm (22 in.); 610 mm (24 in.); and 660 mm (26 in.).

5.2 The following range of focal lengths should be available for miniature standard lanterns (2×2 in.):

76 mm (3 in.); 101.6 mm (4 in.); 127 mm (5 in.); and 178 mm (7 in.).

6. Intermediate Standard Size

6.1 It is recommended that the slide after binding with a cover glass shall be $2\frac{1}{2}\times 2\frac{1}{2}$ inches (63.5×63.5 mm) within $\frac{1}{32}$ inch (0.8 mm) with a thickness not to exceed $\frac{1}{8}$ inch (3.2 mm). The area used for projection should not exceed $2\frac{1}{16}\times 2\frac{1}{16}$ inches (52.4 mm).

7. Stray Light

7.1 The design of the projector should prevent any direct light from reaching the room and should minimize the stray light reaching the room.

8. Slide Temperature

8.1 The temperature of the lantern slide should not exceed 110C (230F) when measured with the testing method given.

* Not Approved. Published for Trial and Criticism. The Optical Society of America is sponsor for the project.

Proposed American Standard Z38.7.4 for Opaque Projectors for Written or Printed Matter and Pictures*

1. The projected aperture should be 152×152 mm (6×6 in.) square or larger.

2. The ratio of corner-to-center illumination on the specimen to be projected should not be less than 33 percent and the illuminated aperture shall be free from local irregularities having a difference of more than 75 percent per 1 inch (2.5 cm).

3. Sufficient range should be provided to focus the image on a screen from 3 to 10.7 meters (10 to 35 feet) from the projector when the projector is equipped with a lens of 18 inches or shorter focal length.

4. The following range of focal lengths should be available for opaque projectors:

14 in. (356 mm); 16 in. (406 mm); 18 in. (457 mm).

5. The rise of temperature of a piece of white paper placed at the aperture on an insulating block shall not exceed 35C (63F) above room temperature.

---

* Not Approved. Published for Trial and Criticism. The Optical Society of America is sponsor for the project.

Proposed American Standard Z38.7.5 Methods of Testing Printing and Projection Equipment*

1. Test for Uniformity of Contact between Negative and Positive Printing Equipment

1.1 A contact print of a 120-dot screen with equal light and dark areas is made with an exposure to produce an average reflectance in the print of 50 percent in the region of good contact. Contact is judged satisfactory when there are no regions greater than $\frac{3}{8}$ inch (9.5 mm) which depart from a uniform gray.

2. Measurement of Film or Slide Temperature

2.1 A thermocouple of No. 38 or 39 Brown & Sharpe gage wire shall be held in contact with the test film at the center of the maximum aperture standard for the given nominal size being tested and the rise in degrees Centigrade above room temperature determined with an instrument accurate to ±2C. The test film shall be of uniform density of two or greater. The thermocouple should be cemented to the test film or held by being bound with it (as in a lantern slide) on the side of the test film away from the light source.

3. Measurement of Lumen Output

3.1 To measure lumen output of a projector, focus a clear glass slide, masked to the maximum aperture given in the standards for the size being tested, on the screen and magnified to arbitrary dimensions h and w. The screen image is divided into nine equal areas as shown in the figure. The illumination I_n at the center of the areas is measured, with the lamp operated at its rated voltage, after removing the glass or other slide from the aperture. The measuring equipment is to have a precision of ±4 percent. If a photoelectric cell is used, it is to have an attached filter to correct its sensitivity to that of human visibility to the different wave-lengths of light.

$$\text{Screen lumens} = (hw/9) \sum_{n=1}^{n=9} I_n.$$

I_n is measured in foot candles; h and w in feet.

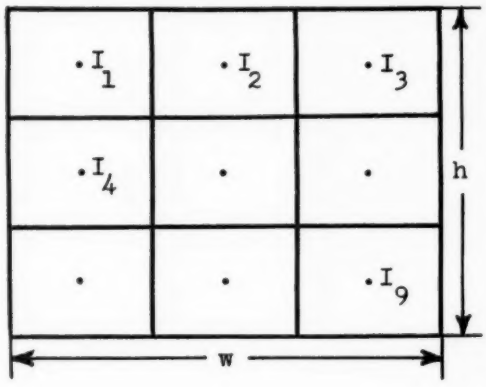

* Not Approved. Published for Trial and Criticism. The Optical Society of America is sponsor for the project.

LETTER TO THE EDITOR

The Effect of Pneumatic Pressure on Photographic Sensitivity

CHOONG SHIN-PIAW
Institute of Radium, Shanghai, China
(November 7, 1940)

Since F. E. Poindexter[1] reported on the effect of mechanical pressure[2] on photographic sensitivity, the problem has been studied extensively by Ny Tsi-Ze[3] and his associates. It was thus established that the desensitizing effect, produced by applying mechanical pressure during exposure, increased generally with the wave-length of light and also with the pressure applied, and that no appreciable effect was produced if the pressure was applied either before or after exposing.

It is proposed, in this note, to study systematically the effect of other kinds of pressure on photographic sensitivity. The pressure employed in these experiments was furnished by a tank of compressed nitrogen, the highest attainable pressure of which was about 150 kg/cm². The photographic chamber consisted essentially of a short brass tube with a thick quartz window on one end and a circular film holder on the other. Three kinds of films were used, namely Eastman Ortho-X film, Eastman Super-Speed Portrait film and Agfa Isochrome film. The latter two kinds have been used by previous workers[3,4] for studying the effect of mechanical pressure. The films used were developed in the Eastman high contrast developer (formula D-19) under practically identical conditions. The violet (4040–4300A) and the yellow (5720–5920A) lights obtained by inserting suitable light filters before an electric lamp were used in the experiments.

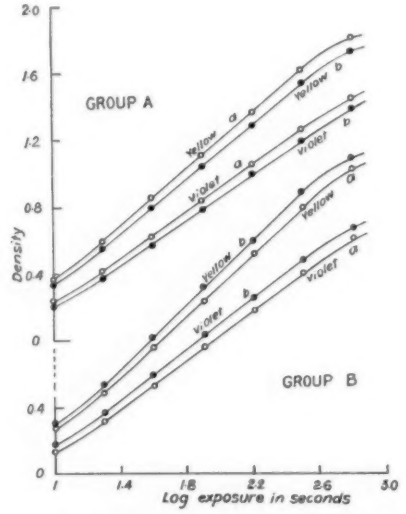

FIG. 1. Group *A* shows the desensitizing effect on Eastman Ortho-X film produced by the application of 140 kg/cm² of pneumatic pressure during exposure. Group *B* shows the sensitizing effect on the same film by applying the same pressure before exposure.

All the films showed lower sensitivity when they were subjected to pneumatic pressure during exposure. The desensitizing effect, as interpreted by the mean value of the variation of density from the portion of normal exposure on the characteristic curve, was found, within the experimental error, to be independent of the wave-length of light, but to increase with the pressure applied. The effect produced by a pressure of 140 kg/cm² was about 0.02 on the Portrait film and a value three to four times greater on the Isochrome and Ortho-X films. On the other hand, the application of pneumatic pressure before exposing increased the sensitivity of the films. The sensitizing effect was somewhat more prominent on the Portrait film than on the other two. The effect was found to be, in general, independent of the wave-length and the magnitude of the pressure previously applied. No appreciable modification of sensitivity was observed when pressure was applied after the exposure.

The effect for different lights on Eastman Ortho-X film is represented in Fig. 1. The curves marked "*a*" represent films exposed at normal atmospheric pressure. The curves in group *A* marked "*b*" represent films to which a pressure of 140 kg/cm² was applied during exposure, and those in group *B*, films to which the same pressure has been applied before the exposure.

It is rather remarkable that the desensitizing effect caused by pneumatic pressure is independent of wave-length, in contradistinction to the effect caused by mechanical pressure where the yellow light is generally much greater than the violet. The fact that Agfa Isochrome film shows a desensitizing effect caused by pneumatic pressure much greater than Eastman Portrait film is likewise remarkable, as the reverse is true in the case of mechanical pressure. There are obviously certain distinct differences between the effect produced by pneumatic and mechanical pressures on photographic sensitivity.

[1] F. E. Poindexter, J. Opt. Soc. Am. **21**, 59 (1931).
[2] The effect caused by mechanical pressure will be specified in this note.
[3] Ny Tsi-Ze and Tsien Ling-Chao, Comptes rendus **194**, 1644 (1932); Sci. et Ind. Phot., Series 2, **4**, 1 (1933); Chinese J. of Phys. **1**, 66 (1934); Ny Tsi-Ze, IX^e Congrès international de Photographie (1936), p. 83; Ny Tsi-Ze and Lu Ta-Yuan, J. Opt. Soc. Am. **26**, 26 (1936).
[4] A. J. Reardon, J. Opt. Soc. Am. **29**, 427 (1939).